Honouring Geological Information in Seismic Amplitude-Versus-Slowness Inversion
A Bayesian Formulation for Integrating Seismic Data and Prior Geological Information

Sharma, Siddharth

Citation (APA)
Sharma, S. (2019). *Honouring Geological Information in Seismic Amplitude-Versus-Slowness Inversion: A Bayesian Formulation for Integrating Seismic Data and Prior Geological Information.* [Dissertation (TU Delft), Delft University of Technology]. https://doi.org/10.4233/uuid:763e8f40-d920-4b22-a105-b392553fe2f4

Important note
To cite this publication, please use the final published version (if applicable).
Please check the document version above.

Honouring Geological Information in Seismic Amplitude-Versus-Slowness Inversion

A Bayesian Formulation for Integrating Seismic Data and Prior

Geological Information

Proefschrift

Ter verkrijging van de graad van doctor
aan de Technische Universiteit Delft
op gezag van de Rector Magnificus Prof. dr.ir. T.H.J.J van der Hagen
voorzitter van het college voor promoties,
in het openbaar te verdedigen op donderdag 17 oktober 2019 om 12:30 uur

door

Siddharth SHARMA

Master of Science in Exploration Geophysics,
Institut de Physique du Globe de Paris, Paris, France,
geboren te Shahajahanpur, Uttar Pradesh, India.

Contents

Contents

Contents

Summary

Seismic waves from active experiments carry information regarding the subsurface in the form of reflected data that is recorded at the surface. This recorded data is subjected to sophisticated processing methods to estimate relevant parameters describing the geology of the subsurface. Traditionally the recorded data is used to create an image of the subsurface in terms of reflectivities, using seismic migration, which back-projects the data recorded at the surface into the earth. The resulting image can be interpreted in terms of structures and depositional patterns. There is another route that is followed to quantify the elastic properties of the subsurface by means of inversion of the recorded data. The essence of seismic inversion is to obtain the elastic properties of the earth's subsurface from a finite set of noisy measurements, by forward modelling based on assumed properties and feed-back that projects the data mismatch onto model parameter space. Full-waveform inversion (FWI) is a special form of inversion that is gaining considerable attention in the last decade, which can be attributed to the advancement in the computational power available. However, several challenges remain for multi-parameter FWI to be successfully implemented on real size data problems in industry or academia at a scale fine enough to be useful in reservoir characterization.

The full wave-equation based scheme used in this thesis is a full elastic wave-equation based pre-stack amplitude vs. offset (AVO) inversion, or rather amplitude versus ray-parameter (AVP) inversion, in which the 1.5D full elastic wave-equation is solved locally, in conjunction with inversion for density and the elastic parameters compressibility and shear-compliance, or their inverse: bulk modulus and shear modulus. This relatively new method, developed in the last decade, is called wave-equation-based amplitude vs ray-parameter inversion, or WEB-AVP inversion. The essence of wave-equation based inversion is that the physics of the wave equation is a constraint that is applied during the inversion. The non-linearity of the relationship between the data and the properties to invert for in the inversion based on the wave-equation assures that a broadband result is obtained, extending below and above the spatial equivalent of the temporal bandwidth of the seismic data. Like any other FWI scheme, the WEB-AVP method suffers from the problem of non-uniqueness of the solution and many innovative methods have been proposed to address these issues. In this thesis, geological information available before the inversion is carried out is considered as a prior information to address the issue of non-uniqueness of the solution.

Prior geological information is usually based on well data, regional trends and seismic interpretation, and is typically defined in terms of layer models. On the other hand, wave-equation based inversion is essentially based on properties on a grid.

Summary

One of the challenges of bringing prior geological information into the inversion, is translating the layer-based prior distributions to grid-based prior distributions. This gives rise to highly non-Gaussian, multi-modal distributions, even when the layer-based properties and thicknesses are normally distributed.

Rather than bringing this highly non-Gaussian prior as non-linear constraint into the inversion, we apply Bayes' rule and update the non-Gaussian prior distribution by the likelihood function resulting from the unconstrained inversion. Since the wave-equation based, and therefore non-linear, inversion is performed as an iterative process of linearised inversions, the likelihood function resulting from these linearised inversions can be calculated from the full Hessian of the objective function and the residual energy after the full inversion, or after every iteration in the inversion.

The posterior multi-variate distribution function in the gridded property space will also be non-Gaussian and multi-modal. The current procedure for using prior geological information is to use the unconstrained seismic inversion result as a starting point and search for the nearest maximum in the posterior distribution function. However, we could also look for more local solutions and assign probabilities to them. Both the prior distribution and the likelihood function can be described analytically, which greatly facilitates the search for a local maximum and determination of the standard deviation of the solution obtained. If one would wish, the result could be translated back to the layer model on which the prior information was defined, but there are much better techniques for geological interpretation of the grid-based posterior solution. Also, a single interpretation of geology in terms of a layer model will not justify the high dimensionality of geological information. To address this issue we propose a methodology to quantify different layer model scenarios describing various aspects of geological information in terms of probabilities, by quantifying these scenarios with the help of the unconstrained WEB-AVP inversion results. This new method is referred to in this thesis as scenario testing.

The methodology presented in this thesis provides an effective framework for incorporating prior geological information in WEB-AVP inversion. It is shown that prior geological information can be used to provide more informative starting models for WEB-AVP inversion and has the ability to improve the resolution of the inversion results. The methodology has provided an improvement over the WEB-AVP inversion results for synthetic data as well as for field data.

Samenvatting

Seismische golven bevatten informatie over de aarde waardoor ze propageren. De gereflecteerde golven van actieve experimenten worden doorgaans geregistreerd aan het aardoppervlak. Op deze geregistreerde metingen worden allerlei geavanceerde dataprocessing technieken toegepast om de relevante informatie te verkrijgen die de geologie van de aarde beschrijft. Historisch gezien wordt de geregistreerde informatie gebruikt om een afbeelding van de aarde te maken, met behulp van een proces dat seismische migratie heet, waarin de geregistreerde golven terug de aarde in worden geprojecteerd. De verkregen afbeelding kan geïnterpreteerd worden in termen van geologische structuren en depositionele patronen.

Er wordt een andere route gevolgd voor het kwantificeren van de elastische eigenschappen van de gesteenten. Dit proces heet inversie van de seismische data. De essentie van seismische inversie is dat de eigenschappen van de gesteenten worden bepaald door het berekenen van de seismische responsie voor een geschatte verdeling van de gesteente eigenschappen. Verschillen tussen de gemeten en de berekende responsies worden terug geprojecteerd op de gesteente eigenschappen in een terugkoppelingslus, tot overeenstemming is bereikt. Volledige golfvorm inversie is een speciale vorm van inversie die de laatste 10 jaar veel belangstelling heeft gekregen. Dit kan verklaard worden door de sterk vergrote rekencapaciteit van moderne computers. Echter voor het oplossen van echte problemen in de industrie op een fijne schaal, of voor grote wetenschappelijke toepassingen, is er nog een lange weg te gaan voordat deze techniek succesvol kan worden toegepast in reservoir karakterisatie.

De volledige golf-vorminversie (FWI) die in dit proefschrift gebruikt wordt is een volledig elastische, op de golfvergelijking gebaseerde, amplitude vs. bron-ontvanger afstand (AVO) inversie. In plaats van bron-ontvanger afstand wordt eigenlijk de horizontale traagheid van de stralen gebruikt (AVP inversie). In deze inversie wordt de 1.5D volledig elastische golfvergelijking lokaal opgelost, tegelijk met het bepalen van de dichtheid en de elastische parameters compressibiliteit en afschuifcompliantie, of de inversen daarvan: de compressibiliteitsmodulus en de afschuifmodulus. Deze nieuwe methode wordt op de golfvergelijking gebaseerde amplitude vs. horizontale traagheid inversie, of WEB-AVP genoemd. Een belangrijk aspect van WEB-AVP is dat de fysica die aan de golfvergelijking ten grondslag ligt wordt gebruikt voor het beperken van de oplossingsruimte voor de inversie. De niet-lineariteit van de relatie tussen de gemeten data en de eigenschappen waarvoor we inverteren maakt dat we een spatieel breedbandig resultaat verkrijgen dat zich uitstrekt zowel boven als onder het spatiele equivalent van de temporele bandbreedte van de data. Zoals ieder andere FWI-methode heeft WEB-AVP ook last van meerduidigheid van de oplossing en er zijn al veel innovatieve methoden

Samenvatting

voorgesteld om dit probleem op te lossen. In dit proefschrift wordt a priori geologische informatie gebruikt om het probleem van de meerduidigheid op te lossen.

A-priori geologische informatie is meestal gebaseerd op metingen in geboorde putten, op regionale trends en op seismische interpretatie. Deze informatie wordt altijd gebruikt om een lagen-model te definiëren. De op de golfvergelijking gebaseerde inversie daarentegen gebruikt de elastische parameters op een rooster van equidistante punten. Een van de grote uitdagingen voor het gebruiken van a priori geologische informatie is het vertalen van de op lagen gebaseerde a priori kansdichtheid verdelingsfuncties, naar kansdichtheid verdelingsfuncties voor de parameters die op roosterpunten zijn gedefinieerd. Deze vertaling leidt tot sterk niet-Gaussische multimodale verdelingsfuncties, ook als de onderliggende verdelingsfuncties voor de lagenparameters wel Gaussisch zijn.

In plaats van de zeer niet-Gaussische verdelingsfuncties te gebruiken als beperking van de oplossingsruimte in de inversie, passen we de regel van Bayes' toe en passen de niet-Gaussische a priori verdelingsfuncties aan met behulp van de zogenaamde likelihoodfunctie die het resultaat is van inversie zonder beperking. Aangezien de op de golfvergelijking gebaseerde en daardoor niet-lineaire inversie wordt uitgevoerd als een iteratief proces van gelineariseerde inversies, kunnen de likelihoodfuncties die bij deze lineaire inversies horen berekend worden uit de Hessiaan van de functie die geminimaliseerd wordt en de residuen na minimalisatie. Dit kan worden herhaald na iedere lineaire inversie in het iteratieve proces.

De a posteriori multivariabele verdelingsfuncties voor de op roosterpunten gedefinieerde parameters is ook sterk niet-Gaussisch en multimodaal. De huidige procedure voor het gebruik van a priori geologische informatie is om het resultaat van onbeperkte inversie als startpunt te gebruiken voor het zoeken naar het dichtstbijzijnde maximum van de a posteriori verdelingsfunctie. We zouden echter ook verder kunnen kijken en meer oplossingen kunnen vinden, waar dan waarschijnlijkheden aan toegekend kunnen worden. Zowel de a priori verdelingsfuncties als de likelihoodfunctie kunnen volledig analytisch beschreven worden, wat het zoeken naar lokale maxima een stuk makkelijker maakt en ook het toekennen van standaarddeviaties aan de oplossingen mogelijk maakt. Als we zouden willen zouden we het resultaat van inversie, zoals gedefinieerd op de roosterpunten, terug kunnen vertalen naar een lagenmodel, maar er zijn veel betere manieren om het op roosterpunten gebaseerde resultaat geologisch te interpreteren. Daar komt nog bij dat een enkel lagenmodel nooit de complexiteit van de echte geologie kan benaderen. Om dit te ondervangen hebben we een methodologie beschreven om meerdere scenario's voor lagenmodellen te proberen. Met behulp van het inversieresultaat zonder a priori informatie kunnen we nu waarschijnlijkheden toekennen aan de verschillende scenario's. Dit concept noemen we scenariotesten.

De methoden die in deze thesis beschreven worden geven een adequate basis om geologische voorkennis te kunnen gebruiken in WEB-AVP inversie. Er wordt gedemonstreerd dat hiermee zowel

Samenvatting

betere startmodellen voor de inversie geconstrueerd kunnen worden, evenals het de uitkomst van deze inversie kan verbeteren. Dit alles is met succes toegepast op numeriek gesimuleerde metingen en op echte veldmetingen.

Samenvatting

Chapter 1
Introduction

Chapter 1

Since the advent of commercial production of oil and gas on a large scale, the industry has striven towards building more efficient methods to explore and produce hydrocarbons. This motivation led to development of innovative ideas to recover hydrocarbon from the most challenging reservoirs. The oil and gas value chain comprises many steps regarding exploration and production (E&P) sometimes called upstream, midstream and downstream, the latter dealing with storing, marketing, transporting and refining of crude petroleum and processing of raw natural gas. At the exploration stage, the search for hydrocarbons in the subsurface is carried out by geophysical prospecting methods mainly using seismic data acquired using sophisticated technology. This seismic data is interpreted in terms of geological structures present in the subsurface, which are the indicators of prospective hydrocarbon reservoirs. After identifying a potential viable field, decision makers come together to decide on the location and the number of wells to be drilled. Once wells have been drilled, the appraisal and production phases follow and commercial production of crude oil and natural gas starts.

The steps mentioned above are aided by geophysical methods, mainly the acquisition of seismic data and its interpretation to gain more knowledge of the characteristics of the reservoir. The process of exploring for oil and gas reserves in the subsurface and eventually planning wells and starting production involves seismic data to a great extent. These are acquired by sending sound waves into the subsurface and recording the reflected waves at the surface (Figure 1.1). The recorded data is processed to make qualitative and quantitative images of the subsurface that represent an estimate of the structural aspects of the geology in the subsurface. These images are subject to interpretation by experts, to obtain a geological understanding of the subsurface in terms of rock formation, environments of deposition and geological structures such as traps, seals, folding, faults etc. The interpretation should provide a qualitative estimate of the presence or absence of potential oil and gas reserves. The interpretation of seismic data thus helps decision makers on the subsequent well planning and drilling. Once a potential target is located, a detailed analysis is needed to understand the subsurface better using more sophisticated inversion methods such as full waveform inversion, which provide quantitative estimates of properties, instead of only providing structural information. This process of estimating reservoir properties using seismic data, structural interpretation and well logs is known as seismic reservoir characterisation.

1.1 Seismic Reservoir Characterisation

Reservoir characterisation is the process of creating quantitative representations of the reservoir using data from a variety of sources and disciplines. Reservoir characterisation is inherently a data integration process where all information collected at various scales in the reservoir characterisation process is integrated into a single, comprehensive and consistent representation of the reservoir (Franchi, 2002). Today, the field of reservoir characterisation routinely involves the disciplines of geology, geophysics, petrophysics, petroleum engineering, geochemistry, biostratigraphy,

Introduction

geostatistics, and computer science. Production can be enhanced strongly by conducting a proper reservoir characterization of the field. This improvement can be credited to better understanding of the geological complexities of the field, which might come from better geological evaluations based on 3D seismic imaging technology. The seismic imaging has the power to image fine scale stratigraphic and structural features that were previously unnoticed but can be obtained after applying seismic attributes extraction methods (Chopra and Marfurt, 2007).

Horizontal drilling is now widely used to improve hydrocarbon recovery over a larger area of a reservoir, either in highly compartmentalized reservoirs or in blanket-type deposits. Thus, the characterization of reservoirs has evolved from a simple engineering evaluation to one developed by multidisciplinary teams of geologists, geophysicists, petrophysicists, and petroleum engineers. The integration of data of different sources and scales is one of the most challenging tasks in reservoir characterization and can computationally be very expensive. In this thesis we are dealing with the integration of geological data and seismic data to build comprehensive scenarios that are relevant to all the disciplines involved
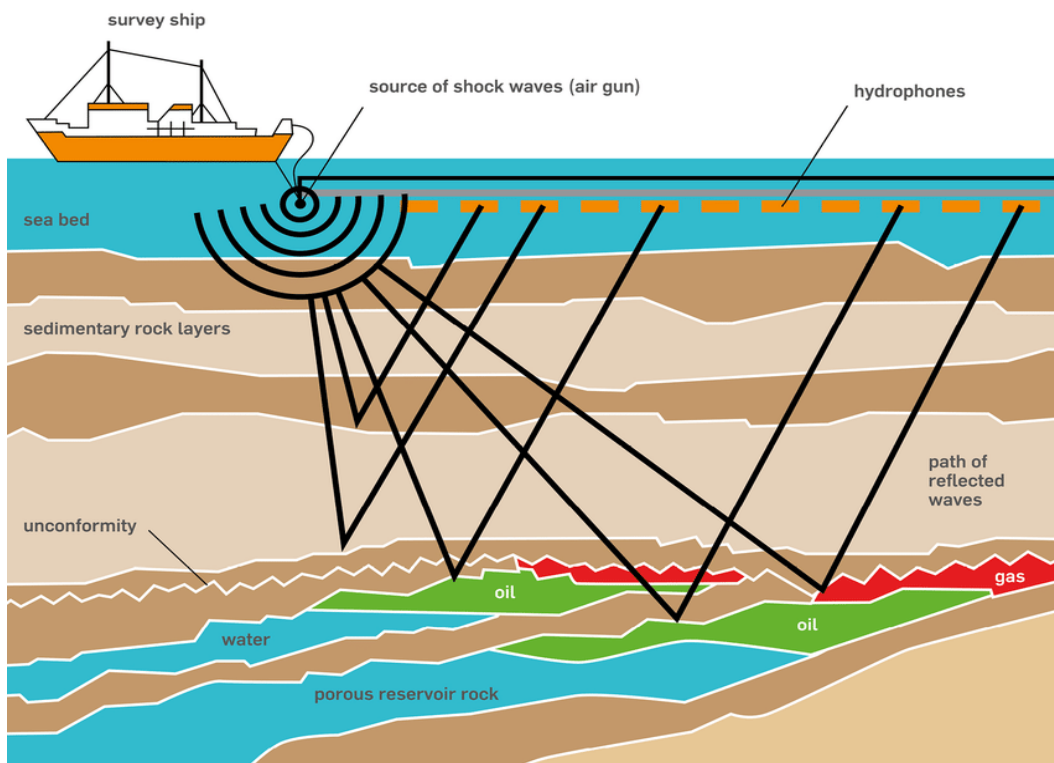

Figure 1.1: Offshore Seismic Survey, from Kukreja et al., (2017). A source pulse is sent inside the earth using man-made sources such as airguns. The incident pulse is reflected in the subsurface recorded by hydrophones towed behind vessel. The reflection data contains physical information regarding the subsurface.

in the project. Seismic data is used in various applications in the exploration phase to provide qualitative structural images through migration (Bednar, 1999; Robinson, 1982; Claerbout, 1971; Stolt, 1978; Schneider, 1978; Schuster et al., 2004) as well as quantitative images of elastic properties through inversion (Tarantola, 1984; 1987; 2005; Bunks et al., 1995; Pratt, 1999; Gisolf et al., 2017; Mora, 1987). Usually the seismic data is inverted for acoustic or elastic parameters such as velocity and density, which explain the wave propagation aspects in the subsurface. The product of seismic inversion have to be integrated with well logs in order to provide reservoir parameters such as lithology, porosity, saturation and permeability (Doyen, 2007; Mavko et al., 2009; Dvorkin et al., 2014; Avseth et al., 2005; Sen and Stoffa, 1998; Larsen et al., 2006; Buland and Omre, 2003; Rimstad et al., 2012; Gunning and Glinsky, 2007). Recently, researchers have started exploiting the idea of joint inversion, where seismic data is inverted directly to estimate reservoir parameters with the help of rock physics models linking elastic properties to reservoir properties (González et al., 2008; Bosch et al., 2010; Grana and Rossa, 2010; Azevedo et al., 2015; Connolly and Hughes, 2016; Fjeldstad and Grana, 2017).

1.2 Imaging versus Inversion

When dealing with seismic data, two approaches are common in practice. The first approach, commonly known as imaging, deals with the interpretation of geology in the subsurface in terms of structural images of reflectivities. The second approach called inversion, deals with providing quantitative information of the rock properties of the formation of interest in the subsurface.

Imaging, commonly referred as seismic migration, is the process of back-propagating the recorded wave-fields into the subsurface while the simulated source is forward-propagated, followed by the application of an imaging condition where these two wave-fields meet in the subsurface. If these wave-fields are time co-incident at geological boundaries they yield an image amplitudes, but if there are no reflecting boundaries, the back-propagated and forward-propagated fields are not time-coincident and no image amplitudes are produced. This process is repeated for all the sources and every subsurface location and, by summing the results for different sources, a structural image can be obtained. The process is schematically shown in Figure 1.2 (a). Here it is assumed that a wave-field from the source propagates downwards until it reaches a geological boundary, and after being reflected the wave-field propagates upwards to the acquisition surface. This method assumes that the incident and the reflected waves always propagate in opposite directions. If this is not the case, e.g. through multiple reflection, the application of an imaging condition can introduce artefacts.

Inversion uses a different approach because it makes use of forward modelling of synthetic data on the basis of a model representing the best current knowledge of the medium properties. It then compares these results with the actually measured data and the residual energy is used to define an update to the medium properties. This process is repeated until a satisfactory match between the measured and the

synthetic data is obtained. Inversion has the very obvious advantage that it produces elastic properties directly, and not image amplitudes that are difficult to relate to rock properties. It has the obvious disadvantage that in its simplest formulation as shown in Figure 1.2 (b), inversion is an extremely big, ill-posed problem, which is also computationally very expensive.
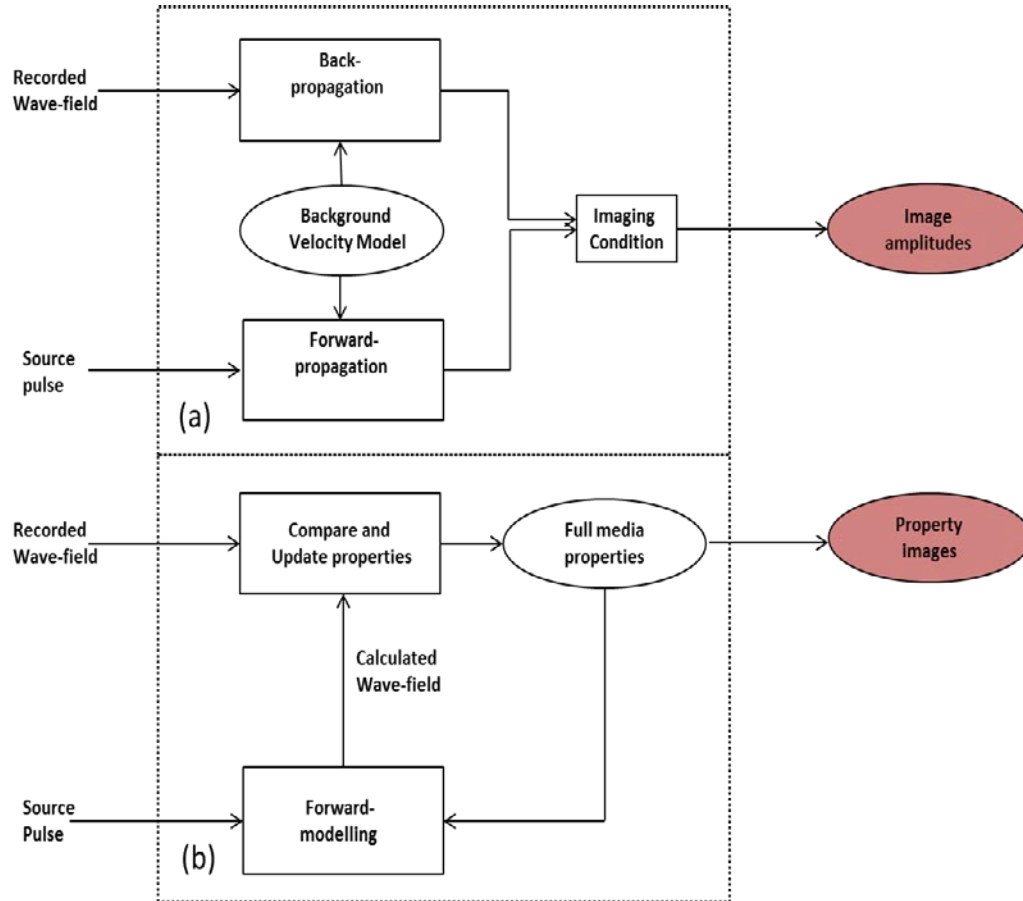
Figure 1.2:a) General flowchart of imaging by wave-field extrapolation and application of imaging condition. The output is in the form of image amplitudes. b) General flowchart of the inversion formulation of imaging. The output is in the form of cubes of media properties. From Gisolf et. al.(2017).

1.3 Inverse Problems

Inverse problems can be defined as problems of estimating or inferring parameters from observational data (Tarantola, 1984;1987). The related theory is called inverse theory. A theoretical relationship between the parameters to be estimated and the observed data is a prerequisite in inverse problems. The problem of the computation of synthetic data, given the values of the parameters, is called the forward problem. Imaging of the Earth's subsurface using seismic data is a typical example of an inverse problem. The data used is the reflected wave-fields recorded at the surface, whereas the forward model is based on methods used such as ray-tracing, or solving the wave-equations.
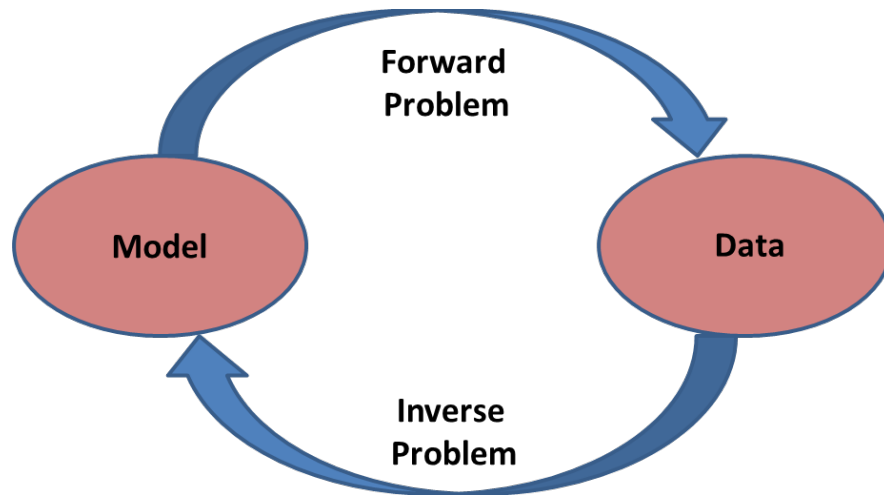
Figure 1.3: Schematic representation of forward and inverse problems. A forward problem is defined as a prediction of the data based on a model that represents the physical and mathematical relationships. An inverse problem is defined as a prediction of the parameters of the model using the observed data.

1.3.1 Forward Problem

The forward modelling engine is one of the two key components for inverse problems. It links the observations to parameters using mathematical and physical laws. In seismic imaging problems, the most commonly used models are ray-tracing, or wave-equations based methods that can be numerically solved using finite difference methods, finite element methods, integral methods etc. In rock physics inversion of seismic data, a physical relationship between the elastic and petrophysical properties is established using a rock physics template (Grana and Rossa, 2010).

1.3.2 Shortcomings

Inverse problems that use only data can often be plagued by issues such as non-uniqueness, ill-posedness, and instability (Virieux and Operto, 2009). These problems can be overcome by using a-priori information on the parameters, provided that this information is available and correct. The most fundamental and straightforward way to introduce prior information is to utilize the so-called Bayesian approach to inversion.

1.4 Full Waveform Inversion

Full Waveform Inversion (FWI) has been gaining attention among researchers in the last decades because of its ability to provide a direct estimate of the subsurface properties from raw data (Tarantola, 1984; 1987; 2005; Bunks et al., 1995; Pratt, 1999; Gisolf et al., 2017; Mora, 1987; Prieux et al., 2009; Brossier et al., 2009; Plessix, 2006; Pratt, 1990; Pratt et al., 1998; Fichtner et al., 2008; Gisolf et al., 2014). It differs from classical seismic inversion techniques in that it accounts for the full

physics of wave propagation (Virieux and Operto, 2009; Plessix and Perkins, 2010) and that it inverts all the data containing multiple scattering, converted waves etc., to estimate elastic parameters. In case of acoustic FWI, pressure data is considered and acoustic wave equation is used as forward modelling engine. In case of elastic FWI, elastic wave equation is used as forward modelling engine and converted waves are also taken into consideration. FWI, in practice, suffers from many practical and numerical issues that hamper the commercial use of the method. The major issues are :

- Starting model: Because of the high dimensionality of the problem, FWI's objective function is usually optimized using local gradient methods. For convergence of the local gradient method a good starting model is essential. Depending on the starting model, one may end up in a local minimum. If one could use global optimization methods, the local minima problem would be overcome, but these methods are either very expensive, or non-existent.

- The non-uniqueness of the solution: FWI is an under-determined problem in terms of data, which leads to many different solutions that all are able to explain the data. To overcome this problem various regularization methods are being used that turn the under-determined problem into a well-determined problem, e.g. by allowing only admissible solutions to the problem.

- Uncertainty: A deterministic solution looking for the minimum in the objective function only provides a single solution. What we need is uncertainty bounds for this solution.

There is a plethora of literature addressing these issue, which uses other data sources such as well logs, guiding horizons, or seismic attributes (Hansen et al., 2008, Douma and Naeini, 2014, Nivlet, 2004). These other sources of information can be used as prior information in Bayes' rule, to solve the inverse problem.

1.5 Bayes Rule

A mathematical model describing the generation of observed data $\mathbf{d}$ will contain parameters $\mathbf{m}$ that have to be estimated (Bayes, 1763). In geophysical problems, for example, these parameters could describe thicknesses and acoustic/elastic properties of geological layers in the subsurface. Let the joint probability distribution $P(\mathbf{d},\mathbf{m})$ describe the states of information on $\mathbf{d}$ and $\mathbf{m}$. From the probability theory it is known that $P(\mathbf{d},\mathbf{m})$ can be written as $P(\mathbf{d},\mathbf{m}) = P(\mathbf{d}|\mathbf{m})P(\mathbf{m})$, or as $P(\mathbf{d},\mathbf{m}) = P(\mathbf{m}|\mathbf{d})P(\mathbf{d})$, where $P(\mathbf{m}|\mathbf{d})$ and $P(\mathbf{d}|\mathbf{m})$ are conditional probabilities. When $\mathbf{d}$ is observed, the state of information on $\mathbf{m}$ should be represented by $P(\mathbf{m}|\mathbf{d})$, which can be evaluated directly from the above equation as:

$$P(\mathbf{m}|\mathbf{d}) = \frac{P(\mathbf{d}|\mathbf{m})P(\mathbf{m})}{P(\mathbf{d})} \ . \qquad (1.1)$$

This represents the well-known Bayes' theorem. The function $P(\mathbf{d}|\mathbf{m})$ is called likelihood function which is a conditional distribution of $\mathbf{d}$ for a given model $\mathbf{m}$. It contains the theoretical relations between parameters and synthetic data and is in fact the distribution of the noise that explains the difference between the modelled synthetic and the measured data $\mathbf{d}$. $P(\mathbf{m})$ is called prior probability distribution that describes the state of prior information on the model parameters. It reflects the information on $\mathbf{m}$ when disregarding the data and thus it should contain the a priori knowledge on the parameters. The $P(\mathbf{m}|\mathbf{d})$ is called the posterior distribution. It contains all the information available on $\mathbf{m}$ when the observed data is taken into account and therefore is, in fact, the solution to the inverse problem. The denominator $P(\mathbf{d})$ does not depend on a model realisation $\mathbf{m}$ and could be considered as a constant factor in the inverse problem only serving the purpose of normalising eq.(1.1) to a proper probability density function. However, it will turn out there is more to be gleaned from $P(\mathbf{d})$. Bayes' rule is especially appealing because it provides a means to update the degree of belief in previous knowledge when new data becomes available.

1.6 Geological Knowledge as Prior information

Geological information has been used in many ways and usually is used as a priori information to address applied and theoretical problems such as information about the subsurface architecture (Mukerji et al., 2001; Schön, 2015), or the assessment of geohazards (Rosenbaum and Culshaw, 2003). Wood and Curtis (2004) provide an overview of applications of geological knowledge in geophysical problems. Here we propose to construct geological scenarios from well logs, the environment of deposition and outcrops, and to use these scenarios as prior information in seismic inversion. Scenario testing is also addressed in this thesis, where a scenario derived from information available before the inversion is carried out and is integrated into FWI to address the above mentioned issues. We use a statistical model that generates blocky realisations from the probability density function of the layer parameters of a stratified medium. The modelled layer-based distributions are used to build prior distributions in a gridded model space, where the spatial grid is defining the model space in which the inversion is carried out. The translation from layer-based model prior information to grid-based prior information is carried out by creating an ensemble of blocky model realisations and applying statistical analysis on the ensemble.

In the case that one considers different prior model scenarios one can distinguish the prior probability distribution defined on the gridded model space for the different layer-based scenarios by adding the

scenario S as a label to the prior probability distribution: $P_s(\mathbf{m}_{grid})$. This distribution is used as prior information in Bayes rule (Figure 1.4), leading to

$$P_S(\mathbf{m}_{grid}|\mathbf{d}) = \frac{P(\mathbf{d}|\mathbf{m}_{grid})P_S(\mathbf{m}_{grid})}{P(\mathbf{d})} \quad . \tag{1.2}$$

This makes $P(\mathbf{d})$ a functional of the scenario S. The scenario testing presented in Chapter 5 is based on this functional relationship.

1.6.1 Layer-Based Model vs Grid-Based Model

A sedimentary geologist's notion of the subsurface is by nature a layered system, where different lithologies or facies have been stacked on top of each other during deposition (Figure 1.4). Layer interfaces can be defined as the boundaries between different lithologies (facies) or as stratigraphic time boundaries. These often coincide, but not always. Examples where facies boundaries and time boundaries do not coincide are erosional surfaces cutting obliquely across the stratigraphy. The scale of these layered media is dictated by the time scale one is considering. The units can be as thin as 1 m, such as thin coal seams, or massive sand packages of many tens of meters in thickness. The subsurface can thus be characterised by a stack of these individual units. For reservoir geophysical purposes the individual units are characterized by their thickness and property values. The units can be mixtures of different lithologies, or facies, such as an interbedded sand/shale sequence, thus assigning to them a single deterministic property value will not do justice to the variability within the unit that could be seen in a well. To incorporate the variability of a geological unit in terms of its elastic parameters within the unit, we describe these properties as Gaussian random variables with given means and standard deviations. For the purpose of FWI, the subsurface has to be discretised as an equidistant grid, on which the properties are defined. The grid spacing is dependent on the shortest wavelength in the data. This is needed for application of the elastic wave equation. Because the inversion considered here uses an integral representation of the elastic wave equation, we sample the shortest wavelength five times, in order to keep the numerical integrations accurate. However, the prior geological information is defined as a parametric layer model. In order to be able to use the prior geological information in the inversion for gridded properties, one needs to translate the layer-based prior model to a grid-based prior model. The translation of the layer-based prior model distribution to the grid-based model space looks mathematically complex, but is straightforward. Given truncated Gaussian distributions for the layer thicknesses, theoretically a grid point could belong to any layer and, therefore, the prior probability density function for a grid-point property is a weighted sum of all individual layer property distributions. The weights are found by drawing an ensemble of layer-model realisations and creating blocky property traces in depth for all these realisations. The weights are found simply by counting how many times a given grid-point is found in a given layer. The

application of geological prior information has a wide scope and can be utilized to address some of the shortcomings of AVP inversion.
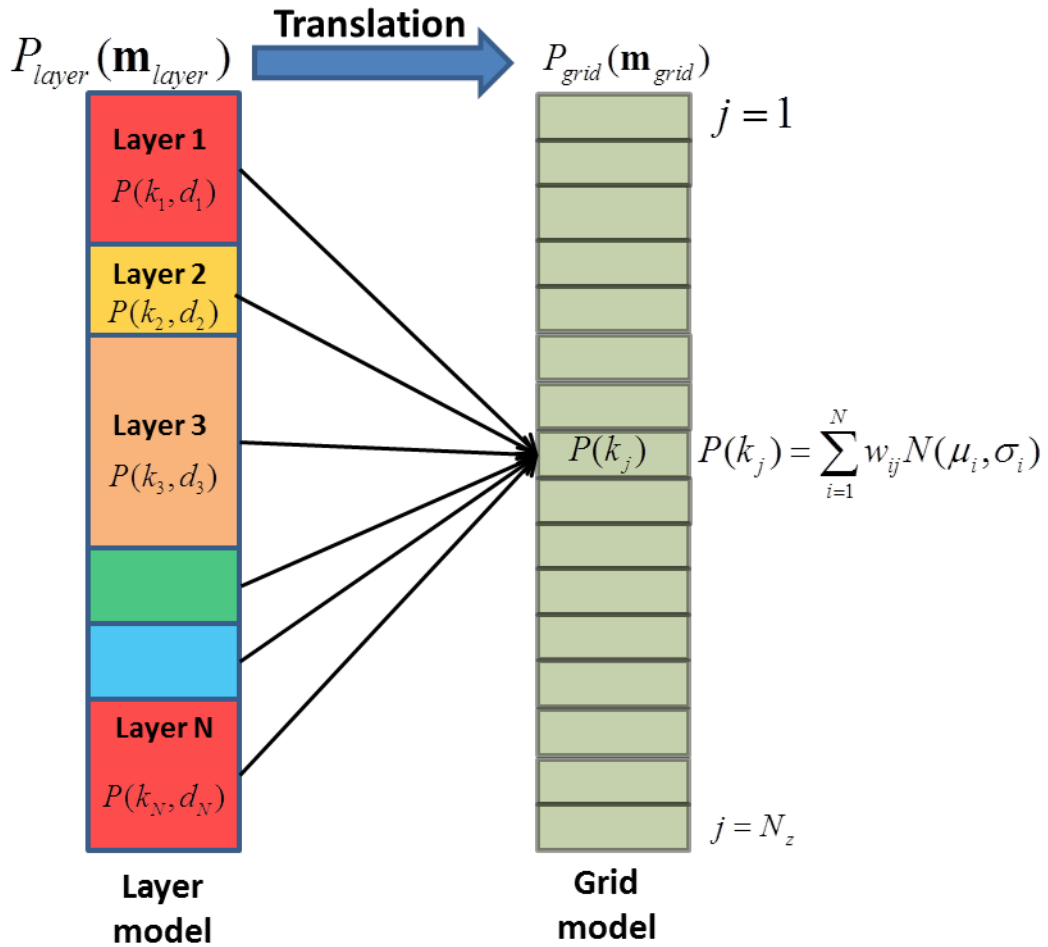
Figure 1.4: Translation of the probability density functions of a layered model $P_{layer}(\mathbf{m}_{layer})$, where different colours represent different facies or lithologies, to an equidistant gridded model $P_{grid}(\mathbf{m}_{grid})$, where $P(k_j)$ represents the probability distribution for property k at grid point j. Every grid point has a probability of being in any layer, leading to the Gaussian mixture model.

1.6.2 Starting Model

After having constructed a prior model scenario there is a number of options for starting models for seismic inversion. The first is the low frequency background model for the inversion, which is a highly smoothed version of the properties seen in wells. The purpose of such a background model is mainly to explain the travel times in the data by using a very smooth propagation velocity model, however very little actual property information is contained in such a starting model. Secondly a realisation of the prior model is constructed by using all mean values of the prior layer model distribution and take a blocky trace representation of that realisation. This starting model contains much extra property information compared to the first option. A third, milder option is to use the mean for every grid point

of the ensemble of blocky traces, drawn from the prior model distribution for the purpose of getting the weights for the Gaussian mixture model. There is less detailed property information in this prior model, because the grid-based mean is a weighted mix of different layer properties. Finally, we can use an ensemble of random starting models drawn from either the layer-based prior distribution, or the grid-based prior distributions. This is a very expensive option because the inversion would have to be carried out for every member of the starting model ensemble. Given the nature of the FWI inversion applied in this thesis, we do not think there is much to be gained from such a procedure. Whichever option is chosen, a starting model will always bring in some form of prior information that helps to mitigate the shortcomings of seismic inversion.

1.6.3 Non-Uniqueness

Unconstrained seismic AVP inversion usually has a large null-space. Depending on the compactness of the prior distributions of a proposed scenario, this null space can be significantly reduced. The prior information will bring regularisation constraints in the inversion process and helps in steering the minimisation process towards a number of discrete solutions. The solutions are defined as estimates of the maxima of posterior probability density functions (MAP estimates).

1.6.4 Uncertainty

The whole purpose of the Bayesian approach is to reduce the uncertainty by adding new information to an existing knowledge base. The Prior distributions will reflect uncertainties of the subsurface parameters as obtained from non-seismic sources. By bringing in the seismic inversion results, the prior information is updated with the help of the likelihood function, leading to the posterior distribution functions. These always will have narrower distributions around the maxima than the priors.

1.7 Thesis Objectives and Outline

The objective of this thesis is to use quantitative prior information, based on geology and other non-seismic measurements of the subsurface, for seismic inversion in order to obtain results that are better than both the prior knowledge itself and the stand-alone seismic inversion result. We follow a Bayesian paradigm updating the FWI result in the light of prior information coming from different sources such as well logs, structural information and regional geology. Although it may be confusing, mathematically there is no difference between saying that the likelihood function updates the prior, and saying that the prior updates the likelihood function. In order to be able to use Bayes' rule, all geological prior information has to be transformed into the probabilistic domain. For properties like elastic parameters this is rather straightforward, using the observed variability of the logged elastic parameters. However, for the layer thicknesses this is not straightforward, because only a single thickness realisation is seen in a single well i.e. deterministic, not probabilistic. Here the geological

Chapter 1

concept and possible environments of deposition come into play, leading to different prior scenarios that can be tested against the seismic data (Chapter 5).

The thesis can be subdivided into two parts: in the first part the theoretical framework of the methodology is established while in the second part the methodology is demonstrated using the synthetic Book Cliffs model as well as on a real field data example.

Chapter 2: This chapter gives an overview of the seismic inversion methodology that is applied in this thesis (Gisolf and van den Berg, 2010a, 2010b; Gisolf et al., 2017). The methodology is called Wave Equation Based Angle Versus ray-Parameter (WEB-AVP) Inversion. We have adopted this inversion technique, because it allows very efficient interaction with the prior information that we want to introduce. The mathematical basis for the likelihood function obtained from the inversion is also introduced in this chapter.

Chapter 3: The methodology for scenario building is introduced in this chapter. The mathematical formulation of prior distributions, posterior distributions and the optimization of the objective function to arrive at the MAP estimate are also introduced in this chapter. Some preliminary results on a three-layer wedge model are shown and discussed in this chapter.

Chapter 4: Here we demonstrate the methodology developed in the previous chapters on the Book Cliffs model. The prior distributions are constructed by designating three locations along the 2D model as well logs and deriving all the statistical properties from these. Seismic horizons picked from the synthetic seismic data are also used to build the prior model. The prior distributions are used to test the starting model, to address the non-uniqueness issue and to reduce uncertainty of the final predictions.

Chapter 5: Given the available prior data it may not be possible to define a unique prior model and a single prior scenario will not do justice to the variability in subsurface. We address this issue by building different prior scenarios. Again with the help of Bayes' rule it will be shown how to assign probabilities to the scenarios given the observed data (unconstrained seismic inversion result).

Chapter 6: We shall demonstrate the methodology developed in the previous chapters on a field data set, provided by OMV (Vienna , Austria).

Chapter 7: In this chapter the conclusions will be summarised and some recommendations for future work will be discussed.

Chapter 2
Reservoir-Oriented Non-Linear Full-Waveform Inversion

Exploration geophysics aims at delivering high resolution images of the subsurface with the aid of recorded seismic data. Inversion of seismic data to elastic parameters has been one of the most important aspects of exploration geophysics. Seismic inversion, for commercial as well as academic applications, comes in two flavours. The first approach is the sequential one, where seismic data is inverted to obtain reflectivity images of the subsurface, which, in turn are inverted to acoustic and shear impedances. The second approach aims at directly obtaining more relevant (elastic/acoustic) subsurface parameters and accounts for all aspects of wave propagation over the target interval. This is called full-waveform inversion because it follows the full wave-field modelling of the wave propagation. In this chapter, the methodology for full-waveform inversion, as used in this thesis, is presented which is based on the full elastic wave equation and inverts for elastic parameters of the subsurface (compressibility κ, shear compliance M and, density ρ).

Chapter 2

2.1 Introduction

Seismic waves, by travelling through the earth, carry information regarding the earth's elastic parameters. The data actually recorded, is the data that travelled from the source at the earth's surface, through the subsurface, and finally back to the receivers at the surface. This reflection data, recorded at the surface, is subjected to sophisticated processing methods to obtain images of the earth's subsurface. In practice the processing of seismic data obtained should solve an inverse problem to obtain an estimate of the parameters describing the earth's subsurface (Duijndam, 1988a ; 1988b). In geophysics two different approaches are followed to solve seismic inverse problem. In the first approach, one usually aims at obtaining the reflectivity image of the earth's subsurface, which is usually called migration or imaging of the earth's subsurface. The seismic data is processed to remove multiples, and a downward projection algorithm is used, followed by application of the imaging condition, to obtain a band-limited reflectivity image that explains the structural aspects of the geology in the subsurface. The second approach aims at providing images of the relevant rock properties (such as velocity, density), thereby providing quantitative information on the earth's subsurface. This approach can either use a linearised wave-propagation model, where only primary reflections are considered, or use the full wave-equation to describe the propagation, transmission, and reflection in the subsurface despite viscoelastic wave equation should be used to fully explain the propagation, approximations are generally made all the way down to acoustic wave equation. There are many strategies to solve these problems, differing in terms of forward modelling, parametrisation and optimisation, including hybrid methods, called joint inversion methods, in which one aims at obtaining both velocity and reflectivity information in a single process.

Full-waveform inversion (FWI) is a challenging data fitting process where synthetic data is generated using forward modelling based on the wave-equation, which is matched to observed data. FWI is a very promising tool in geophysics, because of its theoretical ability to provide high-resolution quantitative property images over the target section. The seismic modelling embedded in the inversion algorithm honours the full physics of wave propagation (Virieux and Operto, 2009). This makes the technique potentially an effective instrument for improving the characterisation of complex sedimentary settings (Plessix and Perkins, 2010).

2.2 Non Linear Wave–Equation Based Inversion

Target-oriented non-linear wave-equation based inversion (WEB-AVP) is a special form of FWI, at the reservoir scale, over a limited target interval, which is appealing in terms of run-time and memory usage. Wave-equation based inversion accounts for the total wave-field over the target interval, i.e. the seismic forward modelling for the inversion algorithm honours the full physics of wave propagation. The non-linearity of the relationship between the wave-field and the properties inverted for, yields a broadband solution, extending below and above the spatial equivalent of the temporal bandwidth of

the seismic data. The inversion used in this study is a wave-equation based pre-stack AVO, or rather amplitude versus ray-parameter (AVP) inversion, in which the 1.5D full elastic wave-equation is solved locally, in conjunction with inversion for the elastic parameters compressibility κ and shear compliance M, or their inverse: bulk modulus K and shear modulus μ. If data quality permits, even density ρ can be inverted for. The inversion algorithm we use in this thesis is developed by Gisolf and van den Berg (2010a; 2010b) and has been applied in various studies for the purpose of reservoir-oriented seismic inversion for synthetic data (Tetyukhina et al., 2014; Feng et al., 2017). The method has proven to provide improved quantitative images of the subsurface for real field data (Gisolf et al., 2014; Feng et al., 2017; Gisolf et al., 2017; Haffinger et al., 2015; Feng et al., 2018a). For a full description of the elastic WEB-AVP inversion we refer to earlier papers (Gisolf and van den Berg, 2010a; Gisolf et al., 2014; Gisolf et al., 2017). The WEB-AVP inversion differs from conventional FWI in many aspects such as parametrisation, forward modelling, input data, and optimisation scheme. WEB-AVP is target-oriented inversion, meaning it works on a small subset (the target interval containing the reservoir) of the acquired data. This significantly reduces the computational cost for the forward modelling. WEB-AVP uses the full bandwidth of the data, unlike the conventional large-scale FWI, and thereby ensures a broadband solution. In addition, it solves the full elastic wave equation, while conventional FWI usually is limited to the acoustic version of the wave equation, as it mainly aims at explaining the kinematics of the seismic P-wave data.

2.2.1 Parametrisation

In the non-linear WEB-AVP inversion scheme, the outputs are the contrasts in shear compliance $M = 1/\mu$ (μ is the shear modulus), compressibility $\kappa = 1/K$ (K is the bulk modulus) and bulk density (ρ). The properties actually inverted for are the normalised relative contrasts of the absolute properties against very smooth background properties (κ_0, M_0, ρ_0):

$$\chi_\kappa = \frac{\kappa(z) - \kappa_0(z)}{\kappa_0(z)}, \tag{2.1}$$

$$\chi_M = \frac{M(z) - M_0(z)}{M_0(z)}, \tag{2.2}$$

$$\chi_\rho = \frac{\rho(z) - \rho_0(z)}{\rho_0(z)}. \tag{2.3}$$

These very smooth backgrounds are also a priori information taken from the wells. The P and S velocities can be expressed as a function of the elastic moduli (κ and M) as:

$$V_p = \sqrt{\frac{1}{\rho}\left(\frac{1}{\kappa} + \frac{1}{3M}\right)},$$ (2.4)

$$V_s = \sqrt{\frac{1}{\rho M}}.$$ (2.5)

The elastic compliances (κ and M) are occurring naturally in the integral representation of the elastic wave equation and in several geological scenarios are found to relate more closely to useful reservoir parameters than the impedances obtained from conventional reflectivity-based AVO inversion. They also allow for better lithological or facies-based classifications (Feng et al., 2018a, Feng et al., 2018b).

2.2.2 Background Medium

The background medium is a very important aspect of the WEB-AVP inversion as the incident wave-field and Green's function are calculated in this medium. It has to be smooth, because the incident fields and Green's functions are calculated with the WKB (Wentzel–Kramers–Brillouin) (Bremmer,1951) approximation, which is only valid in smooth media. It should be a smooth heterogeneous background medium that is non-reflective over the data bandwidth. On the other hand, one would like to have as much information as possible in the background, because it represents the starting model for the inversion, and to keep the contrasts χ as low as possible in order to reduce the non-linearity of the problem. However, at the current state-of-art, we need to keep the backgrounds non-reflective over the bandwidth of data. Usually, low-wavenumber backgrounds are derived from well-logs and interpolated between wells-logs. That is another reason why the background should have only a low wave-number content.

2.2.3 Forward Modelling

The forward modelling in the WEB-AVP inversion is based on the scattering approach to calculating wave-propagation in inhomogeneous elastic media, which makes use of the integral formulation of the wave equation. For the purpose of matching it to the observed data we use the data equation, which is a subset of the full integral equation, or the object equation. For the purpose of providing insight into the WEB-AVP methodology we show the data equation and object equation for the simple single parameter acoustic case:

$$P_{data}(\mathbf{x_r},\mathbf{x_s},\omega) = \int_{\mathbf{x}\in D} G(\mathbf{x_r},\mathbf{x},\omega)\chi(\mathbf{x})P_{tot}(\mathbf{x},\mathbf{x_s},\omega)d\mathbf{x},$$ (2.6)

Where $\mathbf{x_r}$ and $\mathbf{x_s}$ are the receiver location and source location, respectively, ω is the frequency and where the integral over $\mathbf{x}$ is an integral over the whole object domain.

Reservoir-Oriented Non-Linear Full-Waveform Inversion

Equation 2.6 predicts the data recorded at the surface P_{data} in terms of wave-field transmitted by a source that propagates to every point in the subsurface. The wave-field is transmitted back from the points where the contrast χ is non zero to the surface through the smooth background medium. The contrast functions χ are given as:

$$\chi(\mathbf{x}) = 1 - \left[\frac{c_0(\mathbf{x})}{c(\mathbf{x})} \right]^2 . \tag{2.7}$$

where $c(\mathbf{x})$ is an unknown subsurface acoustic wave velocity model and $c_0(\mathbf{x})$ is the known background medium.

On the other hand, the object domain equation predicts the total wave-field at each grid point in the subsurface.

$$P_{tot}(\mathbf{x}, \mathbf{x_s}, \omega) = P_{inc}(\mathbf{x}, \mathbf{x_s}, \omega) + \int_{\mathbf{x}' \in D} G(\mathbf{x}, \mathbf{x}', \omega) \chi(\mathbf{x}') P_{tot}(\mathbf{x}', \mathbf{x}_s, \omega) d\mathbf{x}' . \tag{2.8}$$

Equation 2.8 can be used to estimate the total wave-field with all its complex propagation, given the contrast function χ is known. Equation 2.8 can be substituted in equation 2.6 to get the recorded seismic data in terms of subsurface properties.

For the elastic case, the formalism is same as equation 2.6 and 2.8 except for pressure field we have stress tensor. In the 1.5D elastic case we have four object equations, related to two elements of the stress tensor τ_{zz}, τ_{zx} and two for the particle velocity v_z and v_x, the remaining stress tensors τ_{xx}, τ_{yy} can be expressed in terms of other four. Without further derivation we present the system of object equations for the elastic case here (Haffinger, 2013; Gisolf and Verschuur, 2010):

$$\tau_{zz} = \tau_{zz,0} + L_{11}\tau_{zz} + L_{12}\tau_{zx} + L_{13}v_z + L_{14}v_x \tag{2.9}$$

$$\tau_{zx} = \tau_{zx,0} + L_{21}\tau_{zz} + L_{22}\tau_{zx} + L_{23}v_z + L_{24}v_x \tag{2.10}$$

$$v_z = v_{z,0} + L_{31}\tau_{zz} + L_{32}\tau_{zx} + L_{33}v_z + L_{34}v_x \tag{2.11}$$

$$v_x = v_{x,0} + L_{41}\tau_{zz} + L_{42}\tau_{zx} + L_{43}v_z + L_{44}v_x . \tag{2.12}$$

The integral operator L_{ij} in the abovementioned equations contains the Green's function from any point in the domain to any other point. The 16 L_{ij} operators consist of combinations of the 24 Green's functions that relate the six different source elements to the four different field quantities. The four incident fields and all Green's functions are defined in the smooth inhomogeneous background

medium. The total field as well as the incident field are in the frequency radon domain. Next to the object equations, we have the data equation that relates the measured data in data domain, to the total fields and contrasts in object domain. For the data equation related to *PP* data in the linear Radon time domain we have:

$$\mathbf{\Phi} = \mathbf{K}^{(\Phi)}\mathbf{\chi}, \tag{2.13}$$

where the vector $\mathbf{\Phi}$ contains the N_t time samples of the measured data, and where the vector $\mathbf{\chi}$ is of length $3N_z$, containing the depth samples of all three contrasts given in equations 2.1, 2.1, 2.3 respectively. The kernel matrix $\mathbf{K}$ contains $N_t \times 3N_z$ elements consist of total fields in the object domain.

2.2.4 Optimisation Scheme

For the purpose of this thesis it is important to know that the inversion is an iterative process where linearised inversion of the recorded data is alternated with re-calculation of the total wave-field in the object domain (Figure 2.1). The inversion kernel and the re-calculation of the total wave-field are based on the full elastic wave-equation and are carried out in a way that every re-calculation brings in a higher order of multiple scattering in the modelled data. An optimisation is needed to ensure non-divergence of the field updates.

In the context of iterative inversion scheme equation 2.6 and 2.8 are solved alternatively for the elastic case. The process is augmented by using the Born approximation, where the incident wave-field propagating in the background medium are subjected to a simple linear inversion to estimate the approximate subsurface properties. These approximate subsurface properties are then used to update the total field in the domain using equation 2.8 and this process is repeated until the subsurface properties and the updated total field do not change anymore.
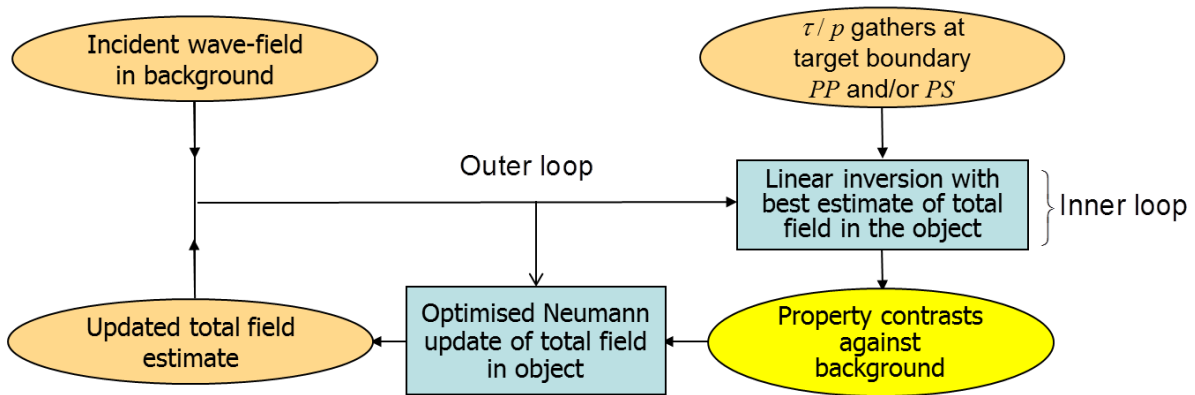

Figure 2.1 Iterative inversion scheme for WEB-AVP Inversion. It consists of two loops, an inner loop that inverts for the elastic parameters for a given wave-field in the object domain, and an outer loop

Reservoir-Oriented Non-Linear Full-Waveform Inversion

that updates the estimated wave-fields by adding a higher order of scattering after every inner loop iteration.

Inner Loop: In the inner loop, the subsurface properties or the contrast functions are estimated by means of a simple linear inversion. The linearisation in the iterative inversions consists of the fact that the inversion kernel, which is dependent on the total field in the object, and therefore on the properties, is kept fixed during an inner loop (Figure 2.1) inversion pass through the data. This otherwise linear inversion can be made non-linear again by application of a regularisation that would, for example, promote blockiness (i.e. piecewise model) of the properties. During this process the seismic data are modelled based on the given subsurface properties and synthetic data is compared to the measured data. The total field obtained from object equation is kept fixed and the objective is to minimise the difference between the synthetic data and measured data to obtain the subsurface properties. The modified version of conjugate gradient scheme (Shewchuk , 1994) is used for the purpose of minimisation of the resulting non-linear objective function. The measured data is usually corrupted by noise and regularisation methods have to be used to stabilise the inversion process. For the results presented in this thesis, the multiplicative regularisation (van den Berg et al., 2003 and Abubakar et al., 2004) is used that has an edge preserving effect, thus promoting blockiness in the final solutions.

Outer loop: During the inner loop the total field are kept fixed and only the property contrasts are updated. However, when the property contrasts are updated during the inner loop, the total field should also be updated. The updates of the total field are carried out in the outer loop by iteratively building up the total field as a sum of the background fields and a number of basis functions.

$$p_{tot}^{(N)}(\mathbf{x},\mathbf{x_s},\omega) = p_0(\mathbf{x},\mathbf{x_s},\omega) + \sum_{n=1}^{N}\alpha_n^{(N)}(\mathbf{x_s},\omega)\phi_n(\mathbf{x},\mathbf{x_s},\omega), \qquad (2.14)$$

where α_n^N are frequency dependent weighting factors and depends on the number *N* of basis functions taken into account. If they all equal to one, equation 2.14 becomes a Neumann series which is known to be unstable for large contrast or high frequency. α_n^N are estimated by means of least square minimisation and each time a new basis function is added to the total field, *N* is increased by one and a complete set of optimised α_n^N is calculated. Because of the instability issues, a Krylov subspace method (Kleinman et al., 1991) is used where total field can be estimated by using equation 2.14 with basis functions given by:

$$\phi_n(\mathbf{x},\mathbf{x_s},\omega) = \int_{\mathbf{x}'\in D} G(\mathbf{x},\mathbf{x}',\omega)\partial W_n d\mathbf{x}', \qquad (2.15)$$

and the incremental contrast sources ∂W_n are given by:

$$\partial W_1 = \chi^{(1)} p_{tot}^{(0)} \; , \qquad \partial W_n = \chi^{(n)} p_{tot}^{(n-1)} - \chi^{(n-1)} p_{tot}^{(n-2)} \; , \qquad n > 1 \quad , \qquad (2.16)$$

where W_1 describes the first order interaction between the points in the subsurface, higher order interactions are subsequently included in the contrast sources W_n in the nth iteration. One needs to realise that the contrast sources are only a mathematical concept and that they are not physical sources. In every outer loop iteration the full suite of basis functions and weighting factors in equation 2.14 are estimated.

2.2.5 Input for reservoir-oriented inversion

The seismic data is usually acquired along the earth's surface and the inversion scheme outlined in the previous section can only be applied in a target-oriented way (Figure 2.2), where the surface data has to be brought back to the top of the target window that contains the reservoir together with the top seal and the bottom layers, typically comprising a 500 m vertical interval. The WEB-AVP inversion works on seismic data in the τ / p domain. There are several routes that can be taken to bring the surface recorded data on the top of the target window.
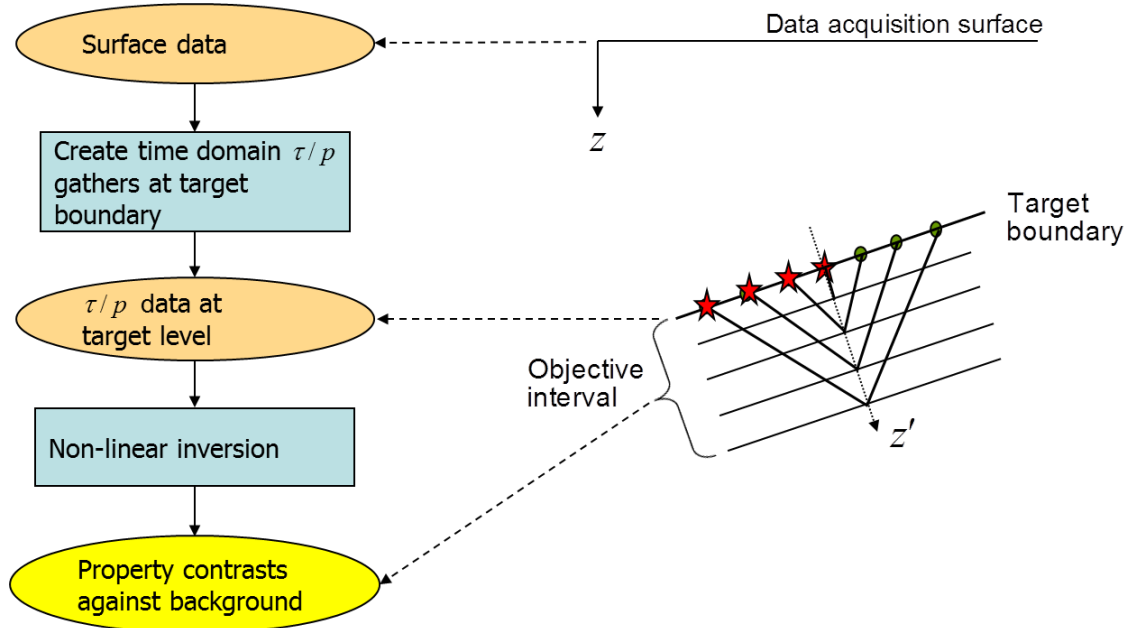

Figure 2.2: General Set-up for target oriented WEB-AVP inversion. The surface recorded data is redatumed to a target boundary at, or near, the top of the objective sequence. The redatumed data is tranformed in τ / p domain. The redatuming can be carried out by JMI-res or demigration. This redatumed data is used as an input to WEB-AVP inversion.

Redatuming via JMI: In this process the seismic data recorded along the earth's surface is backpropagated to a target depth in the subsurface to create a virtual dataset. Traditionally, such back-propagation is done using a primaries-only assumption in the overburden (Berryhill, 1984). Recently, a full wavefield approach has been developed based on Joint Migration Inversion (JMI) (Berkhout, 2014b; Staal, 2015) to redatum the data to a target depth. During this process the one-way down-and upgoing elastic wavefields are estimated at the target depth below the overburden and afterwards these redatumed wavefields are transformed into local impulse responses at the top of the target boundary via so-called proximity transformation (Garg and Verschuur, 2016). These obtained local impulse responses can be used as an input for WEB-AVP inversion. The JMIs properly handles the complex overburden internal multiples and transmission effects and the combination of JMI with local elastic reservoir inversion has been referred to as JMI-res

Demigration: Industry spends a large amount of resources in processing the data with an aim to obtain high-quality migrated angle gathers. The seismic migration (Berkhout, 1982) involves backprojection of seismic sources and receivers into the subsurface where the resulting responses are cross-correlated to produce image amplitudes using a given background velocity model. The demigration is a process of removing the effects of migration and restoring the travel-time data from image amplitudes. Demigration can be used to create a travel-time data at the target boundary using migrated angle gathers. These travel-time data can also be used as an input for WEB-AVP inversion. The field data example in this thesis is handled via this route.

2.3 Synthetic Example

To demonstrate the inversion methodology we carried out a synthetic experiment on the well-known three layer wedge model, where the middle layer is pinching out. This synthetic data was obtained using Kennett invariant imbedding method (Kennett, 2009). In the 1.5D domain this method also gives an exact solution, provided the layer thicknesses are thin enough. A wavelet with a peak frequency of 60 Hz was used for synthetic modelling, and data with a maximum angle of 40 degrees were generated. The synthetic seismic data was generated in the τ / p domain, whereby every location was modelled and inverted independently in the 1.5D domain. The zero-offset section is shown in Figure 2.3.
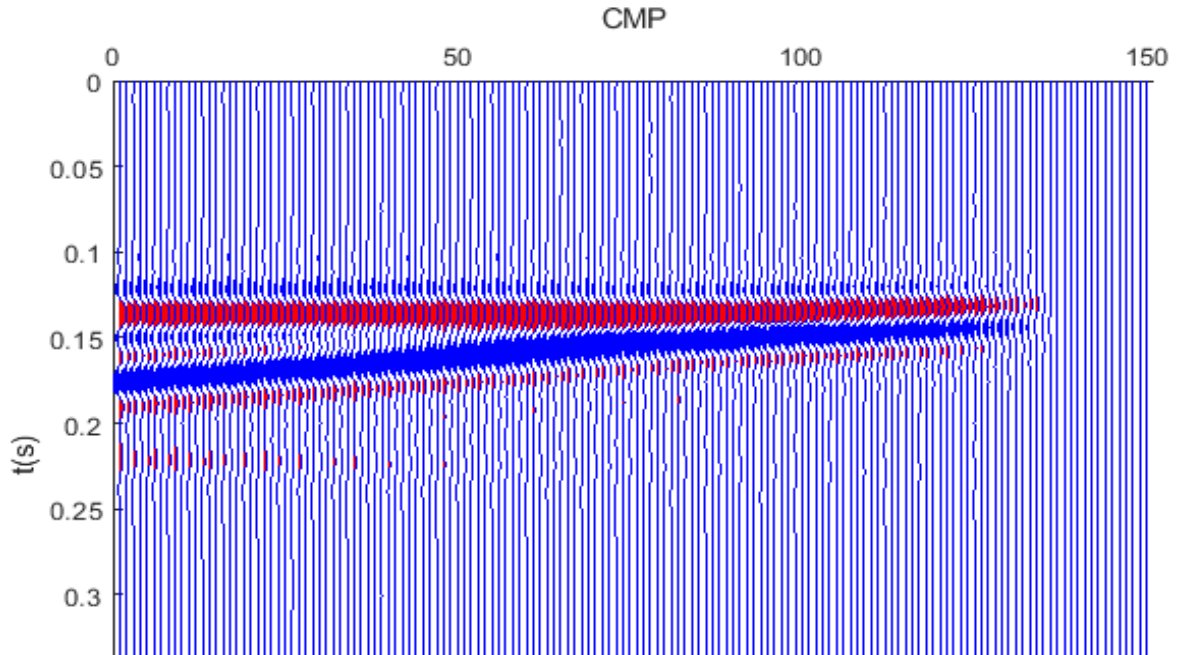
Figure 2.3: Zero-offset section for the Wedge Model, exhibiting the tuning effect as the thickness of layer becomes lower than the seismic resolution. This data is used as input to WEB-AVP inversion.

2.3.1 Results and Discussion

The WEB-AVP inversion provides good results for the Wedge Model (the results for density ρ are not shown), where the bandwidth is extended all the way down to zero frequency content (D.C) (Figure 2.4). On the high wave-number side the resolution has increased significantly. We are not using any starting model except the background model for carrying out the inversion. However, the inversion has a regularisation that promotes blockiness of the result, which was, in this case, the correct assumption to make.
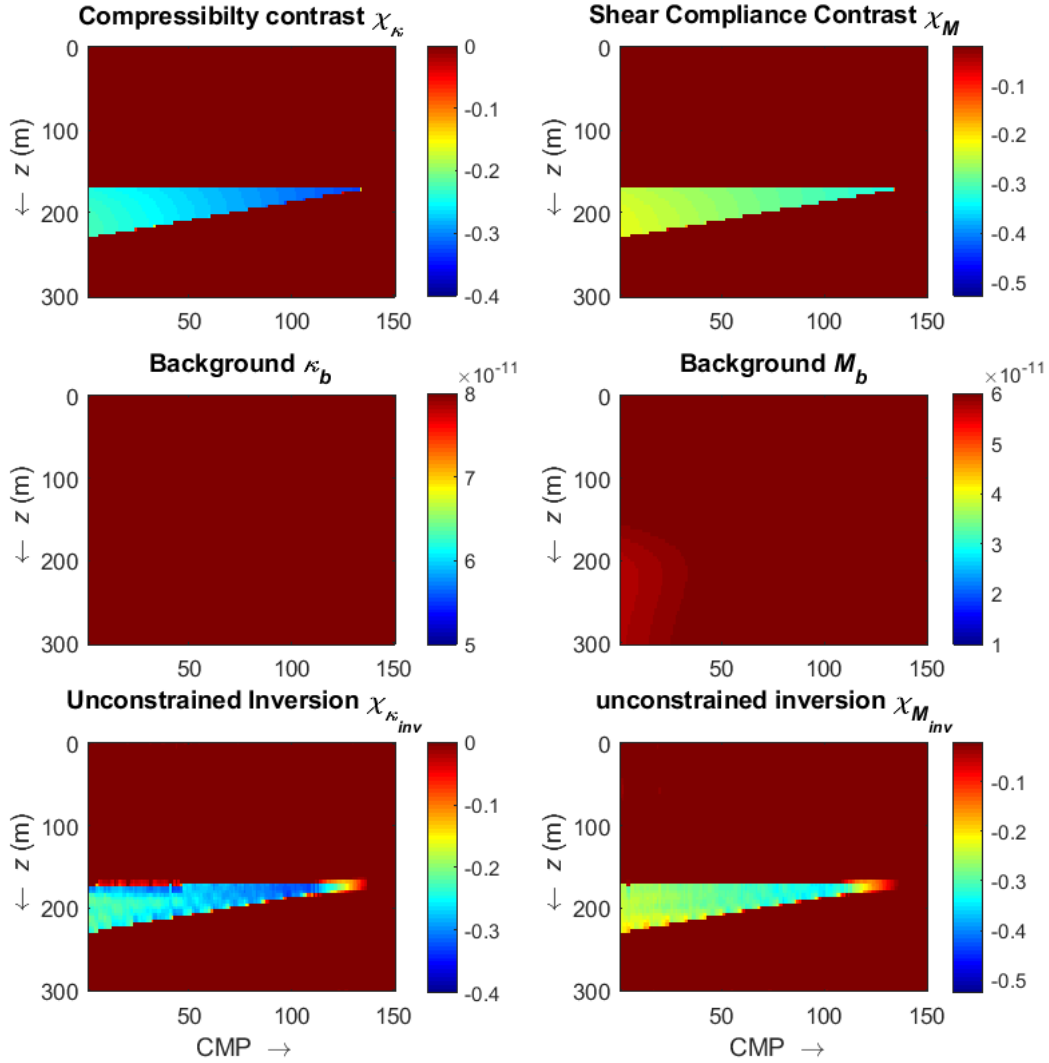
Figure 2.4 Compressibility (κ) and shear compliance (M) contrast inversion result for the Wedge Model experiment. (Top row) True compressibility and shear compliance contrast. (Middle row) background model for compressibility and shear compliance. (Bottom row) The WEB-AVP inversion result for compressibility and shear compliance contrast. WEB-AVP inversion provides quantitative and promising results except where the layer thickness becomes smaller than the seismic resolution.

2.4 Conclusions

WEB-AVP inversion is a very powerful and promising method for inverting seismic data to the elastic properties: compressibility κ, shear compliance M. This method is different from conventional AVP inversions with respect to the parametrisation and the use of the full physics of wave propagation over the target interval. The iterative routine of adding a higher order of scattering with every iteration keeps the inversion linear and computationally efficient. The scheme provided good quantitative results on the Wedge Model.

Chapter 2

Chapter 3
Bayesian Formulation for incorporating Prior Information in Inversion

In this chapter we present a method to include prior geological information in the target-oriented non-linear WEB-AVP inversion discussed in the previous chapter. We use a wave-equation based Amplitude-Versus-Slowness inversion, which solves for different rock properties (shear compliance M, compressibility κ and density ρ), instead of the P and S impedances obtained from the traditional reflectivity based methods. Prior information on these properties comes from a layer-based model obtained by geological interpretation of the well logs and other prior knowledge available: typically a geological concept of the environment of deposition and a structural seismic interpretation in the form of some horizons to guide the prior model in-between wells. Using this information in a target-oriented AVP inversion requires a link between the depth grid on which the wave-equation is solved and the layer-based geological prior information. The highly non-linear character of this transformation provides an interesting challenge to the reservoir geophysicist. In this chapter we present a Bayesian approach to updating this layer-based prior model, with the help of the grid-based unconstrained seismic inversion result, to a grid-based posterior property distribution, from which means and standard deviations for all grid-points can be obtained.

Chapter 3

3.1 Introduction

Reservoir-oriented WEB-AVP inversion is a very promising new tool in reservoir geophysics because of its ability to provide high-resolution quantitative property images over the target section. Wave-equation-based inversions account for the total wave-field in the object domain. The seismic modelling embedded in the inversion algorithm honours the full physics of wave propagation (Virieux and Operto, 2009). This makes the technique an effective instrument for improving the characterisation of complex sedimentary settings (Plessix and Perkins, 2010). The essence of wave-equation-based inversion is that the physics of the wave equation is the only constraint applied during the inversion. The non-linearity of the relationship between the data and the properties to invert for in the inversion based on the wave-equation assures that a broadband result is obtained, extending below and above the spatial equivalent of the temporal bandwidth of the seismic data (Sharma et al., 2018). The inversion used in this study is a full elastic wave-equation based pre-stack Amplitude-versus-offset (AVO) inversion, or rather Amplitude-versus-Ray-Parameter (AVP) inversion, in which the 1.5D full elastic wave-equation is solved locally, in conjunction with an inversion for density and the elastic parameters compressibility and shear-compliance, or their inverse: bulk modulus and shear modulus (Gisolf and van den Berg, 2010a; 2010b; Gisolf et al., 2017). As WEB-AVP is a local optimization algorithm it is sensitive to the choice of starting models (Datta and Sen, 2016; Sams and Carter, 2017). There is a plethora of literature on building starting models for inversion, which uses other data sources such as well logs, guiding horizons or seismic attributes (Hansen et al., 2008, Douma and Naeini, 2014, Nivlet, 2004). Several studies have shown innovative ideas to address the problem of local minima. There are multi-scale techniques (Bunks et al., 1995; Sirgue and Pratt, 2004), where the inversion is carried out by hopping from one frequency band to a higher one, with the result of the previous frequency band functioning as the starting model for the next frequency band. Multi-scale methods are applied in various studies such as the ones by Dessa and Pascal (2003), Fichtner et al., (2013) and Brossier et al., (2009). Another class of methods deals with modifying the objective function to reduce the multi-modality of the objective function such as the Laplace domain FWI formulation by (Shin and Min, 2006), or the Laplace Fourier domain inversion proposed by Kim et al., (2013). Differential semblance optimization (Symes and Carazzone, 1991; Shen and Symes, 2008) constrains the objective function by an extra measure of semblance, whereas wave-equation migration velocity analysis (WEMVA) uses reflectivity images as a constraint in the objective function. Some studies used neural networks to build starting models such as in Hampson et al. (2001) and Hansen et al. (2008). Alternatively, Chunduru et al. (1997), Varela et al. (1998) Xia et al. (1998), Datta and Sen, (2016) proposed global optimization to build a starting model using very fast simulated annealing (VFSA). In this method they proposed to invert for a sparse model with a number of interfaces and velocities rather than the full velocity model. This inverted model contains sharp

Bayesian Formulation for incorporating Prior Information in Inversion

velocity changes around the boundaries that are smoothed and used as starting model for the conventional Full-Waveform-Inversion (FWI) scheme.

Bayesian approaches are the preferred methods when it comes to data integration and they have been very common in geophysical literature. In seismic inversion, Bayesian methods have been successfully applied for linearised seismic models, such as linearised amplitude variation with offset (AVO) inversion. Buland and Omre (2003) provide a seismic inversion algorithm based on the convolution (linear operator) of the wavelet and a linearised approximation of Zoeppritz equations (Aki and Richards, 1980). This method was also extended to time-lapse seismic inversion (Buland and El Ouair, 2006), Dix inversion (Buland et al., 2011), and CSEM inversion (Buland and Kolbjørnsen, 2012). The flexibility of the Bayesian approach also allows including a spatial model as in Buland et al. (2003) and Hansen et al. (2006). Other statistical approaches have been presented by Mukerji et al. (2001), Mazzotti and Zamboni (2003), Eidsvik et al. (2004), Bornard et al. (2005), Coléou et al. (2005), Bachrach (2006), Gunning and Glinsky (2007), Spikes et al. (2007), González et al. (2008), Bosch et al. (2009) and Johansen et al. (2013). The Gaussian assumption is not necessarily required to achieve an analytical solution. Indeed, Grana and Della Rossa (2010) and Rimstad and Omre (2010) extend the Bayesian approach to Gaussian-mixture and generalized-Gaussian models, respectively. However, the numerical evaluation of the posterior increases the computational cost, and the sampling algorithms are generally computationally demanding. The Bayesian approaches relies heavily on the specified prior information, which could be uninformative priors such as Jeffreys' priors (Jeffreys, 1939), or weakly informative priors, such as pure Gaussian priors, of which the distributions are easy to sample from, and which make the posterior distribution evaluation simple as well. We are introducing more complex geological scenarios with significantly more information than a single Gaussian prior model. These geological scenarios are layer-based by nature and exhibit two levels of information, one describing the variability of the properties within the layer and one describing the distribution of the layer thicknesses, including the presence, or absence, of a layer.

The wave-equation-based inversion used in the present study is more robust against local minima than the general FWI methods mentioned above, but if the starting model is too far off the iterative solution may still not converge. Even if convergence is obtained, there may be a large null-space and prior information will help steer the solution towards the inside of the null space. The prior information can be used to find a better starting model, but also to apply a Bayesian update to the unconstrained inversion result. In this chapter we present a new method of building prior distributions for the gridded properties, from prior distributions pertaining to a layer-based model. The layer-based model is built from well logs interpreted in terms of limited number of layers or zones and is, therefore, much sparser in nature in terms of information as compared to information present in well logs. From the layer-based prior distributions blocky property realisations can be drawn that provide the statistics for the a priori probability for a specific grid-point to be in a specific layer. The mean of all realisations of

the ensemble can be used as starting model for the inversion. Furthermore, the prior distribution can be used to update seismic inversion results in the Bayesian sense.

3.2 Methodology

Bayes' theorem states that combining the prior probability density function $P(\mathbf{m})$ in the model space $\mathbf{m}$, with the likelihood function $P(\mathbf{d}|\mathbf{m})$, which is the probability density function of the data $\mathbf{d}$, given a model $\mathbf{m}$, we get the posterior probability density function, which is the probability density of the model $\mathbf{m}$ given the data $\mathbf{d}$:

$$P(\mathbf{m}|\mathbf{d}) = \frac{P(\mathbf{d}|\mathbf{m})P(\mathbf{m})}{P(\mathbf{d})}, \tag{3.1}$$

Where $P(\mathbf{d})$ is the probability distribution of the data, acting as a normalisation factor to make $P(\mathbf{m}|\mathbf{d})$ a valid probability density function:

$$P(\mathbf{d}) = \int_{\mathbf{m}\in\mathbf{M}} P(\mathbf{d}|\mathbf{m})P(\mathbf{m})d\mathbf{m}, \tag{3.2}$$

which is the integral of the likelihood function multiplied by the prior distribution, over the whole model space $\mathbf{M}$.

The equation is hard to evaluate analytically in most cases because of the large dimensionality of the model space $\mathbf{M}$, usually approximated by using sampling methods such as Markov Chain Monte Carlo methods (MCMC). In the context of this study we are not concerned with evaluating this integral as we are mostly interested in finding the point estimate or maximum a posterior (MAP) estimate. If one is interested in sampling from the posterior distribution, the probability of data becomes very important because it turns the posterior distribution into a properly normalised probability density function. In the following sections we will discuss all these different probability density functions.

3.2.1 Prior Modelling

A sedimentary geologist's notion of the subsurface is by nature a layered system, where different lithologies or facies have been stacked on top of each other during deposition. Layer interfaces can be defined as the interfaces between different lithologies (facies boundaries) or by stratigraphic time boundaries. These often coincide, but not always. Examples where facies boundaries and time boundaries do not coincide are erosional surfaces cutting across the stratigraphy. The scale of these layered media is dictated by the time scale one is considering. The units can be as thin as 1 m, such as thin coal seams, or massive sand packages of hundreds of meters thickness. A stratified subsurface can

Bayesian Formulation for incorporating Prior Information in Inversion

be characterised by a stack of these individual units. For reservoir geophysical purposes the individual units are characterized by their thickness and property values (shear compliance M, compressibility κ, density ρ). The units can be mixtures of different lithologies, or facies, such as interbedded sand/shale sequences, so assigning to them a single deterministic property value will not do justice to the variability within the unit that can be seen in the well. To incorporate the variability of a geological unit in terms of its elastic parameters, we describe these properties as Gaussian random variables with means and standard deviations. The data from which layer models can be constructed is provided by wells and structural seismic interpretation. To allow for thickening or thinning of the layers away from well control, we also define the layer thicknesses as Gaussian random variables. The tail of the Gaussian function that is extending over negative thicknesses is re-set to zero thickness, leaving a truncated Gaussian function with a delta-function at zero thickness. The area under the delta function expresses the probability of that layer being absent. The means of the layer thickness distributions can easily be taken from the wells, but for the standard deviations of the layer thicknesses we have to introduce a geological depositional model that may allow some layers to vary laterally in thickness, or be absent altogether, whereas other layers could be assumed to have rather limited thickness distributions. The prior geological layer model for a given location is parameterised by the number of layers (N_L) and every individual layer is assigned four Gaussian random variables: three for the properties (shear compliance M, compressibility κ and density ρ) and one for the thickness (D).

Thus, a geological layer, or unit, is parameterised by three properties and a thickness value [κ, M, ρ, D]. The geological model is defined as a stack of N_L of such units. For any property p we can define a blocky trace representation in depth for any realisation of the set of layer parameters:

$$p(z) = \sum_{i=1}^{N_L} p_i(z) \left[U(z - Z_{i-1}) - U(z - Z_i) \right], \tag{3.3}$$

with:

$$Z_i = \sum_{j=1}^{i} D_j \tag{3.4}$$

and where $U(z)$ is a Heaviside function, z are the grid locations and Z_i are the interfaces between the units. The $p_i(z)$ are all Gaussian random variables on all grid-points z, defined by mean μ_i and standard deviation σ_i of the distributions. The D_j are truncated Gaussians, as discussed above.

For the purpose of the wave-equation based AVP inversion, the subsurface has to be discretised as an equidistant grid on which the properties (in our case M, κ,) are defined. The grid spacing is dictated by the shortest wavelength, a requirement for applying the elastic wave equation. Because the inversion uses an integral representation of the elastic wave equation, we sample the shortest

wavelength five times, in order to keep the numerical integrations accurate. However, the prior geological information is defined as a parametric layer model. In order to be able to use the prior geological information in the inversion for gridded properties, we need to translate the layer-based prior model to a grid-based prior model. The translation of the layer-based prior model distribution to the grid-based model space looks mathematically complex, but is straightforward. Given truncated Gaussian distributions for the layer thicknesses, theoretically, a grid point could belong to any layer and, therefore, the prior probability density functions for a grid-point property is a weighted sum of all individual layer property distributions (Figure 3.1). The weights are found by drawing an ensemble of layer-model realisations and creating blocky property traces along depth for all these realisations (Figure 3.1b). The weights are now found simply by counting how many times a given grid-point is found in a given layer. The histograms for these statistics are shown in the middle row in Figure 3.1. Considering the number of layers in the model (N_L) and the number of grid-points in the domain (N_z), numerically all this would be very difficult to handle, but so far we have been able to describe the gridded prior distribution function completely analytically as a set of N_z distributions, all consisting of a weighted sum of N_L Gaussians.

Gaussian mixture models are used extensively in many clustering applications. A Gaussian mixture describes the multi-modality of the distribution as the weighted sum of individual Gaussian distributions. The Gaussian mixtures are given by:

$$P(x) = \sum_{i=1}^{N_L} w_i N(x, \mu_i, \sigma_i),$$

(3.5)

where

$$\sum_{i=1}^{N_L} w_i = 1,$$

(3.6)

and where N is the well-known Gaussian distribution function:

$$N(x, \mu_i, \sigma_i) = \frac{1}{\sigma_i \sqrt{2\pi}} e^{-\frac{(x-\mu_i)^2}{2\sigma_i^2}}.$$

(3.7)

The w_i are the individual weights for the individual Gaussian distributions $N(x, \mu_i, \sigma_i)$ representing the probability that a specific grid-point is sitting in the ith layer.

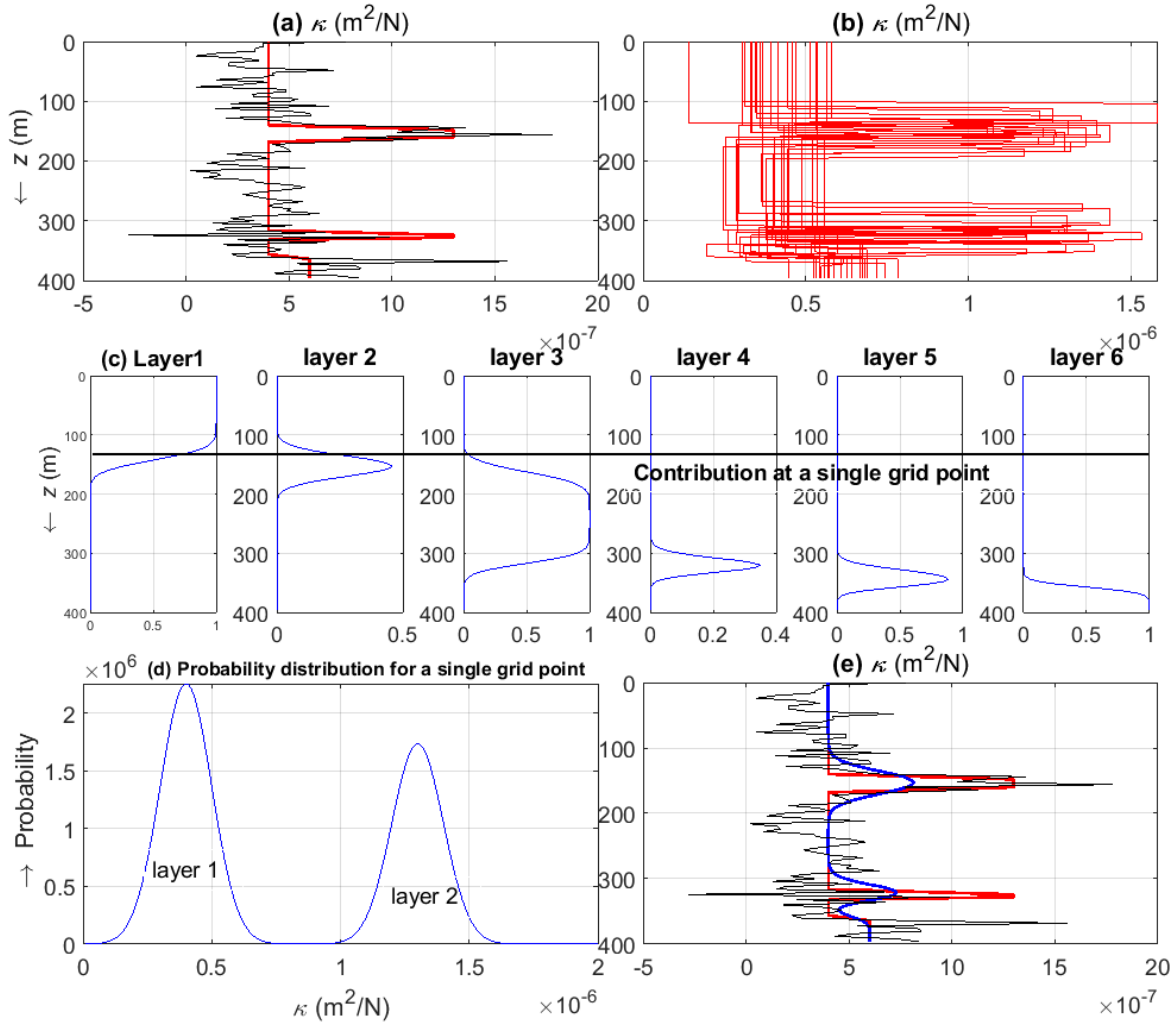# Bayesian Formulation for incorporating Prior Information in Inversion

Figure 3.1: Schematic representation of translation of the probability density functions of a layered model to a gridded model. (a) A well-log (black) is interpreted in terms of layers (red) that has been assigned a Gaussian probability distribution for each layer. (b) The layer-based model is used to create an ensemble of realisations. (c) The realisations are used to estimate the weight matrix by counting the number of times a layer appeared at a single grid point giving rise to multimodal distribution shown in (d) for a single grid point. (e) The well log (black) with layer-based interpretation (red) is shown with translated grid-based (blue) model estimated by taking the mean of the multimodal distribution for every grid point.

In Figure 3.1c the weights are shown for the prior model. We can see how the weights are distributed along the whole trace dictated by the thickness variations for the units.

The joint probability density of all the grid points together can be defined as the multiplication of all the distributions for the individual grid points, assuming they are all statistically independent. Although this may not seem to be strictly true, bearing in mind that within a layer the properties are distributed according to a random process that is visible in well logs. A Gaussian distribution is

assigned to the layer with mean and standard deviation estimated from the variability seen in the well log. After translation every grid point is assigned a unique distribution in terms of layer distributions. Adding to that there are no correlations between layers in our prior models, making the assumption of statistical independence of all grid points plausible. In addition, it gives a very tractable set of equations and leads to good results, as will be shown later in this chapter. The probability distribution for property p at a single grid point at z_j is now given by:

$$P_j(p) = \sum_{i=1}^{N_L} w_{ji} N(p, \mu_i, \sigma_i),$$
(3.8)

with the normal distribution N already defined by equation (3.7).

The joint probability distribution for the whole model vector at a specific location, for any property p, is now given by:

$$P(\mathbf{p}) \propto \prod_{j=1}^{N_z} P_j(p_j),$$
(3.9)

where $\mathbf{p}$ is the property model vector for property p for all N_z grid-points.

3.2.2 The Likelihood Function

The wave-equation-based inversion iteratively solves for the model parameter $\mathbf{m}$, consisting of all three different properties p for all grid-points, in a least squares sense, using the following equation:

$$\mathbf{d} = \mathbf{Km},$$
(3.10)

where $\mathbf{d}$ is the data to be inverted written as one long vector with a length equal to the number of time samples in the data times the number of ray-parameters. The vector $\mathbf{m}$ is a vector of length $3N_z$ containing all κ, M and ρ values for all grid-points, and $\mathbf{K}$ is the kernel during the current outer-loop iteration (see Figure 2.1). This equation may be augmented with a constraint to promote blockiness in the $\mathbf{m}$ vector. The solution of the inverse problem posed by equation 3.10 is referred here as the maximum-likelihood-estimator $\mathbf{m}_{mle}$. There will also be the minimum value E_{min} of the objective function after minimisation, which contains the unexplained part of the data.

After every outer loop iteration (Figure 2.1) there is a final set of properties, a data residual and the inversion kernel of the last iteration, at every location along the target boundary. From these ingredients a Hessian and, subsequently, a Gaussian probability density function in the gridded model space can be constructed that is going to be used as likelihood function in the Bayesian way of bringing in geological prior information. Note, however, that the inversion itself is unconstrained by prior knowledge, apart from a blockiness promoting regularisation in the, otherwise, linearised

inversions (Figure 2.1). The linearisation consists of the fact that during the inversion (inner loop) the dependency of the kernel $\mathbf{K}$ on the total field in the object domain is frozen.

The Likelihood function is usually assumed to be a Gaussian of the noise that explains the difference between the measured data and the predicted data, when the model vector $\mathbf{m}$ is given:

$$P\left(\mathbf{d}\,|\,\mathbf{m}\right) \propto e^{-\frac{1}{2}\left|\mathbf{d}\text{-}\mathbf{d}(\mathbf{m})\right|^2 / \sigma_N^2} \quad , \tag{3.11}$$

where $\mathbf{d}$ is the data to be inverted, $\mathbf{d(m)}$ is the modelled data for model vector $\mathbf{m}$ and σ_N^2 is the Gaussian noise in the data. After this unconstrained inversion one can write:

$$\begin{aligned} \mathbf{d} &= \mathbf{Km}_{mle} + \mathbf{n} \\ \mathbf{d}\left(\mathbf{m}\right) &= \mathbf{Km} + \mathbf{n} \end{aligned} \quad , \tag{3.12}$$

where $\mathbf{n}$ is the noise with zero mean and variance σ_N^2. Substituting equation (3.12) into equation (3.11) and absorbing the noise-power dependent factor into an unspecified proportionality factor, one can write the likelihood function as

$$P\left(\mathbf{d}\,|\,\mathbf{m}\right) \propto e^{-\frac{1}{2}(\mathbf{m}\text{-}\mathbf{m}_{mle})^T \mathbf{C}_m^{-1}(\mathbf{m}\text{-}\mathbf{m}_{mle})} \quad , \tag{3.13}$$

where $\mathbf{m}_{mle}$ was the output vector of the inversion and $\mathbf{C}_m$ is now the covariance matrix in the model space given by:

$$\mathbf{C}_m^{-1} = \frac{\mathbf{K}^T \mathbf{K}}{E_{\min}} \quad , \tag{3.14}$$

where E_{min} is now our estimate of the noise in the data. The diagonal elements of C_m^{-1} provides an estimate of variance at the depth level whereas off-diagonal elements provides an understanding of the correlation between the different depth samples. As the correlation between different layers is not considered in the prior model. While creating realisation from the prior model every single depth level is considered independent of the other depth samples. Due to this reason we make an approximation of considering only diagonal elements of C_m^{-1} in the likelihood function.

3.2.3 Posterior Distribution

The posterior distribution in grid-based parameter space is the product of the prior in the gridded parameter space and the likelihood function constructed from the unconstrained inversion results.

The unnormalised posterior probability density function is, therefore, found simply by multiplication of equations (3.9) and (3.13)

$$P\left(\mathbf{m}\,|\,\mathbf{d}\right) \propto e^{-\frac{1}{2}(\mathbf{m}\text{-}\mathbf{m}_{mle})^{T} C_{m}^{-1}(\mathbf{m}\text{-}\mathbf{m}_{mle})} \prod_{j=1}^{Nz} P_{j}\left(\mathbf{m}_{j}\right), \tag{3.15}$$

where $\mathbf{m}_{j}$ is a three element sub-vector of the vector $\mathbf{m}$, containing the properties associated with grid-point j : κ_{j}, M_{j} and ρ_{j}.

The Posterior distribution needs to be maximised in order to find the maximum a posterior estimate, which is the same as minimising the negative logarithm of the posterior distribution. We use the non-linear conjugate gradient method (Shewchuk, 1994) for minimising the objective function F_{Post}, which is the negative logarithm of the Posterior (equation 3.15)

$$F_{Post}\left(\mathbf{m}\right) = \tfrac{1}{2}\left(\mathbf{m} - \mathbf{m}_{mle}\right)^{T} \mathbf{V}^{-1}\left(\mathbf{m} - \mathbf{m}_{mle}\right) - \sum_{j=1}^{Nz} \ln P_{j}\left(\mathbf{m}_{j}\right), \tag{3.16}$$

where $\mathbf{V}$ is a diagonal matrix containing the diagonal elements of the Hessian $\mathbf{C}_{m}$. The advantage of equation 3.16 is that it is now easy to calculate analytically the gradient in model space, which is needed to find the minimum of $F_{Post}(\mathbf{m})$ and the second derivative of $F_{Post}(\mathbf{m})$ in that minimum, from which the local standard deviation of the property prediction can be determined. These equations can be found in the Appendix A.

The update from the Maximum Likelihood Estimator (MLE) to a Maximum a Posteriori (MAP) estimator can be applied in every outer loop iteration in Figure 2.1.

3.3 Synthetic Example

In order to validate the methodology and assess its limitations, we carried out a simple synthetic experiment with the well-known Wedge Model shown in Figure 2.4. The model is a three layered system. The specification of the model is shown in Table 3.1.

Table 3.1: Table 3.1: Wedge Model specifications.

Layers	Thickness (m)		Compressibility (κ)		Shear compliance (M)	
	Mean	STD	Mean	STD	Mean	STD
Layer 1	172	0.01	9.917e-11	1e-12	6.61e-11	1e-12
Layer 2	20	15	6.1e-11	1e-12	4.25e-11	1e-12
Layer 3	100	20	9.917e-11	1e-12	6.61e-11	1e-12

Bayesian Formulation for incorporating Prior Information in Inversion

To validate the method on the Wedge Model two experiments with different scenarios are carried out.

3.3.1 Scenario 1

The model specification for Scenario 1 is given in Table 3.2. The model consists of three layers, but the same property distribution populating all three layers. This model has the least amount of information that can be modelled as prior distributions, and therefore it is called zero prior information scenario. The likelihood function is derived from the result of an unconstrained WEB-AVP inversion. The prior model is constructed using the model parameters as given in Table 3.2.

Table 3.2: Wedge Model specification for prior model for Scenario 1.

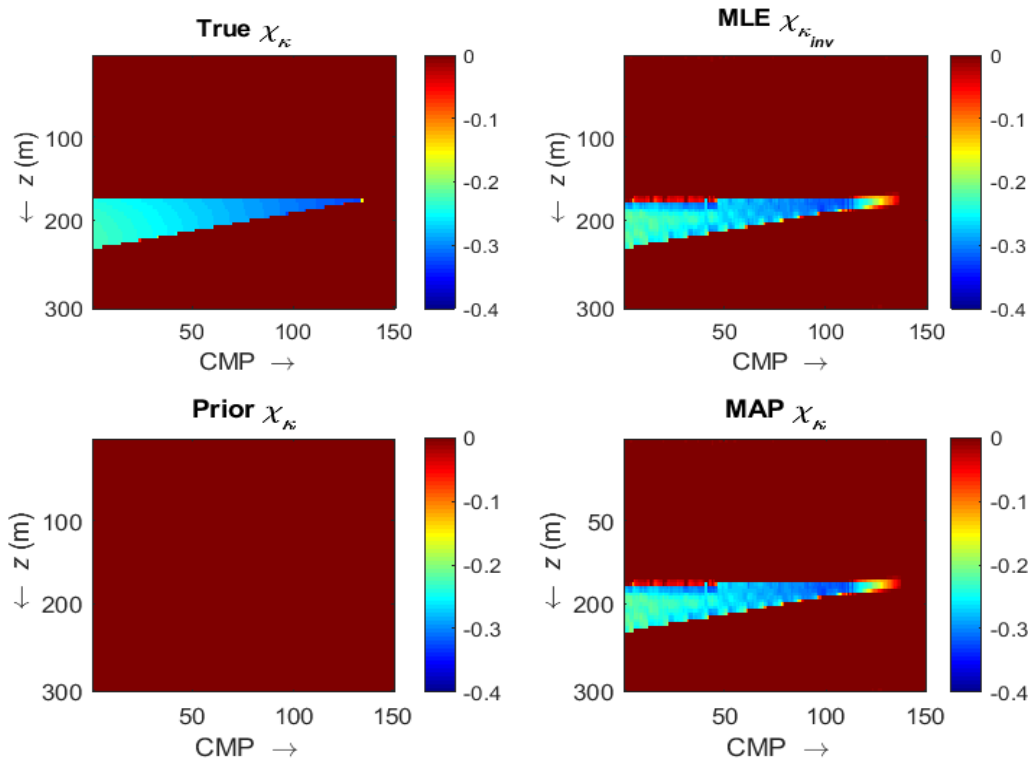| Layers	Thickness (m)		Compressibility (κ)		Shear compliance (M)	
	Mean	STD	Mean	STD	Mean	STD
Layer 1	300	100	9.917e-11	1e-11	6.61e-11	1e-11
Layer 2	300	100	9.917e-11	1e-11	6.61e-11	1e-11
Layer 3	300	100	9.917e-11	1e-11	6.61e-11	1e-11

Figure 3.2: Posterior MAP estimate for the compressibility contrast (κ) for Scenario 1. As scenario 1 does not contain any information except the background model one expects the MAP to be similar to MLE, which is very evident from the MAP and MLE estimates.

The a priori and maximum a posteriori (MAP) estimate are shown in Figure 3.2 and Figure 3.3, together with the maximum likelihood estimate (MLE) from seismic inversion. As can be seen from the mean realisation of the prior model, it is not very informative, as it contains only 1 distinguishable layer. These parameters are plugged into equation 3.13 and, using the conjugate gradient method one maximises the posterior distribution (or minimises the negative of the logarithm of the posterior distribution, see Appendix A). Considering that the prior distribution is not very informative one expect the MAP estimate to be close to maximum likelihood estimate (MLE), which is evidently the case from Figure 3.2 and Figure 3.3.
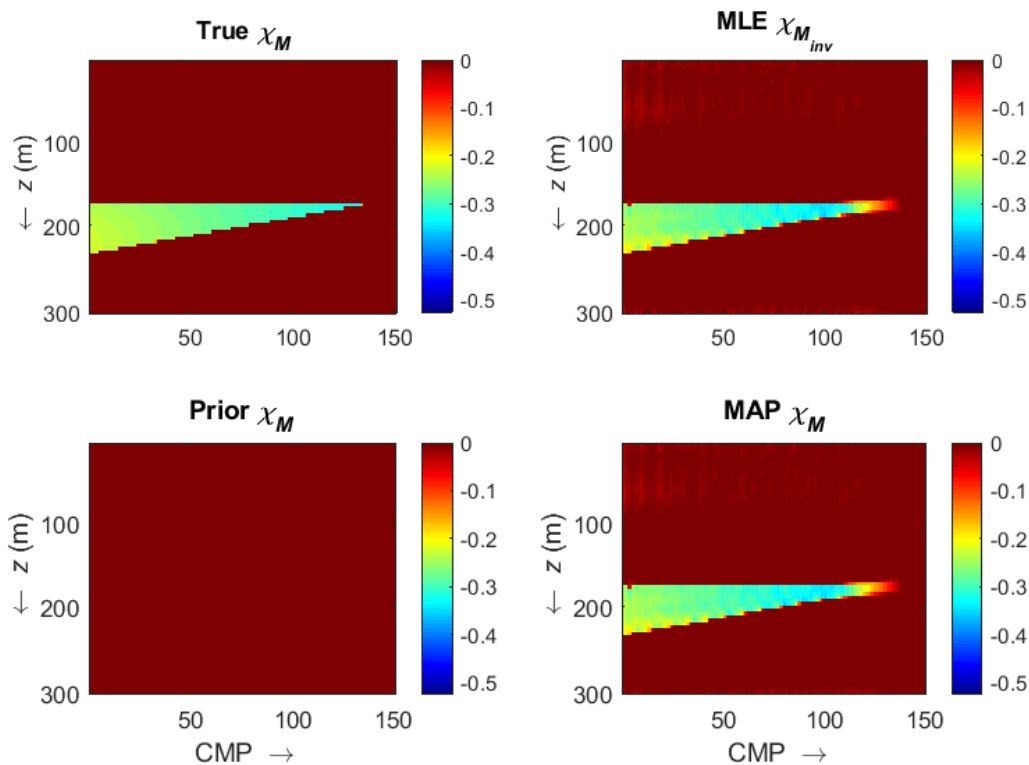

Figure 3.3: Posterior MAP estimate for the shear compliance contrast (M) for Scenario 1. As scenario 1 does not contain any information except the background model one expects the MAP to be similar to MLE, which is very evident from the MAP and MLE estimates.

3.3.2 Scenario 2

The model consists of three layers, each with its own thickness and property distributions. This model has the exact amount of information that can be modelled as prior distribution and is considered a full prior information scenario. The likelihood function is obtained by running the WEB-AVP inversion. The prior probability density functions are constructed using the model parameter as given in Table 3.3.

Bayesian Formulation for incorporating Prior Information in Inversion

Table 3.3: Wedge Model specifications for prior model for Scenario 2.

Layers	Thickness (m)		Compressibility (κ)		Shear compliance (M)	
	Mean	STD	Mean	STD	Mean	STD
Layer 1	172	0.01	9.917e-11	1e-12	6.61e-11	1e-12
Layer 2	20	15	6.1e-11	1e-12	4.25e-11	1e-12
Layer 3	100	20	9.917e-11	1e-12	6.61e-11	1e-12

The a priori and maximum a posteriori (MAP) estimates are shown in Figure 3.4 and Figure 3.5. The likelihood function resulted from the unconstrained seismic inversion. As can be seen from the mean realisation of the prior model, it is a good representation of the true model. These parameters are plugged into equation 3.13 and using the conjugate gradient method one maximises the posterior distribution (or minimises the negative of the logarithm of the posterior distribution, see Appendix A). Considering that the prior distribution represents the true model, we expect the MAP estimate to move from maximum likelihood estimator to the mean of the prior estimate, that is the good representation of true model as evident from Figure 3.4 and Figure 3.5.

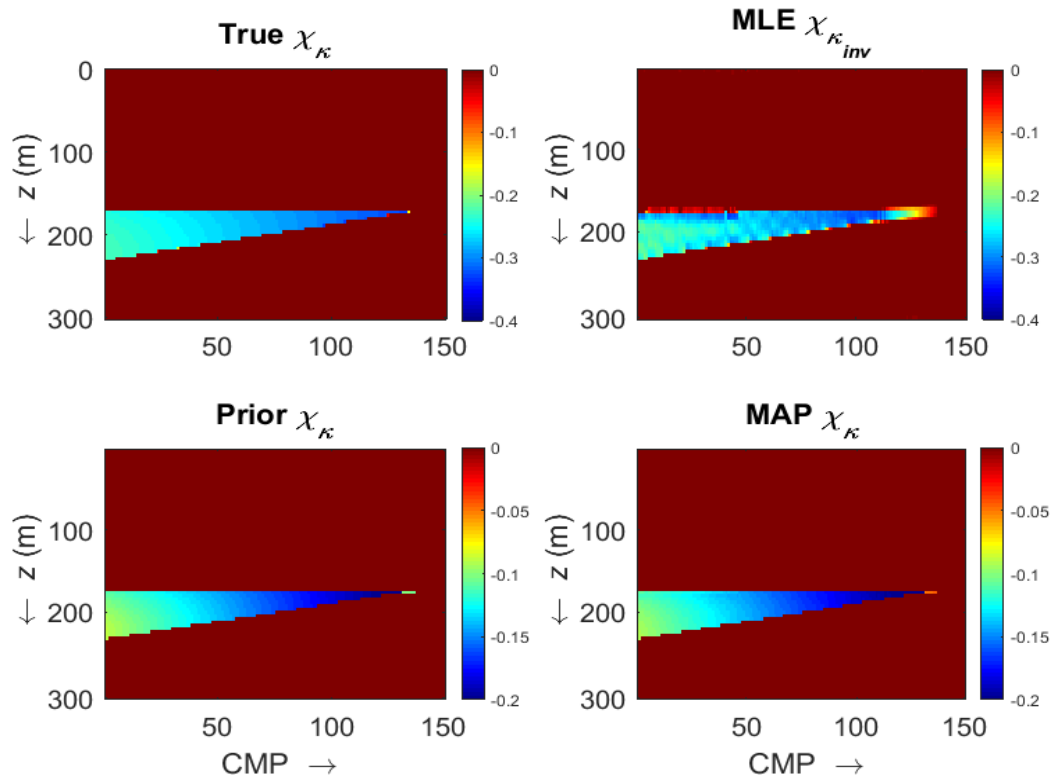*Figure 3.4: Posterior MAP estimates for the compressibility contrast (κ) for Scenario 2. As scenario 2 is a good representation of the true model one expect the MAP estimate to move from the MLE towards the mean of the prior model, as shown in this figure.*
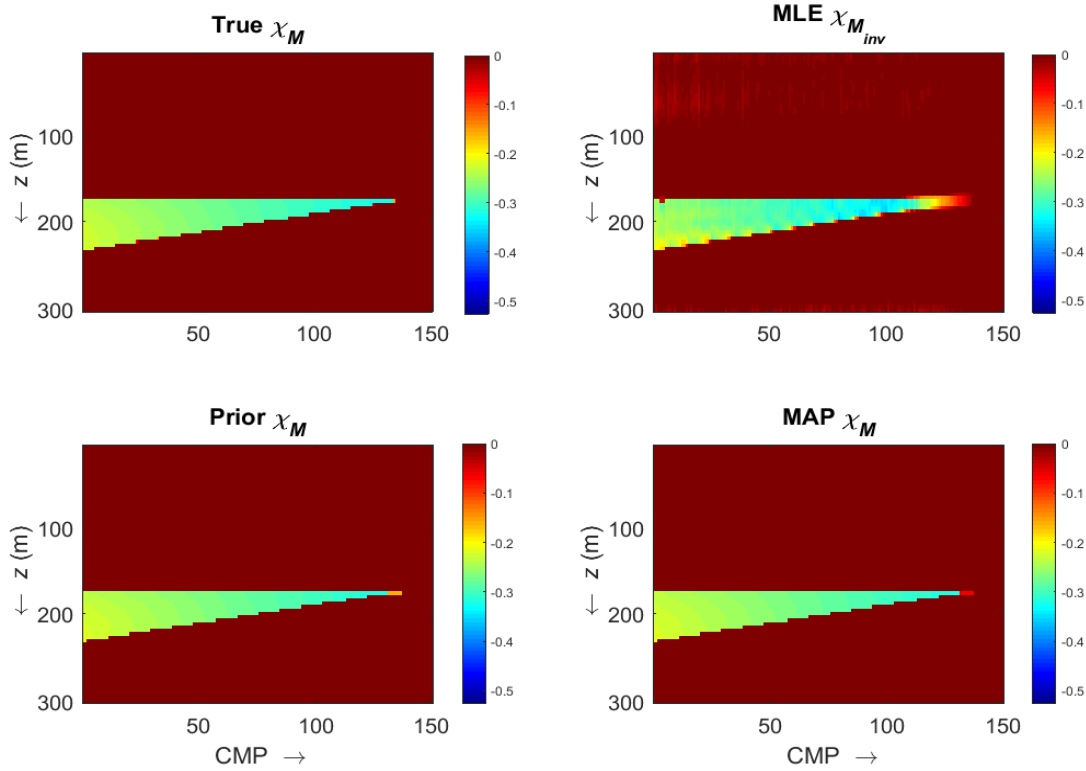
Figure 3.5: Posterior MAP estimates for the shear compliance contrast (M) for Scenario 2. As scenario 2 is a good representation of the true model one expect the MAP estimate to move from the MLE towards the mean of the prior model, as shown in this figure.

3.4 Discussion

In the previous section a Bayesian methodology is presented that incorporates geological prior information in terms of a layer model into the WEB-AVP inversion. We demonstrated the methodology on a simple three layer wedge model with two different scenarios: Scenario 1 containing zero prior information and representing the background model, while Scenario 2 is a good representation of the true model, or full prior information, which is therefore very informative. The experiments carried out have confirmed that by using the prior information the WEB-AVP inversion estimate is $\mathbf{m}_{mle}$ updated to $\mathbf{m}_{map}$ which is biased towards the seismic data for Scenario 1 because prior information does not add any extra information. Using Scenario 2 that represents the true model very well, the $\mathbf{m}_{mle}$ is updated to the mean of the prior model distributions.

3.5 Conclusions

In the present study it is shown how to translate geological prior information for layer models into prior information for a gridded model, such as used in non-linear wave-equation-based inversions. This leads to multi-modal prior distributions, consisting of mixtures of original geological layers (units) distributions. This Gaussian mixture distribution for each grid point indicates the likely layers

Bayesian Formulation for incorporating Prior Information in Inversion

to which this grid point can belong. We can use this prior knowledge in the inversion to update the unconstrained inversion result. It is also shown how to construct a likelihood function from the unconstrained inversion result. The likelihood function, multiplied by the prior probability distribution, gives a posterior distribution that can be written in an analytic form. Then the maximum nearest to the unconstrained inversion result is picked from this posterior distribution. The results validate the approach and also give insight into how to incorporate the geological knowledge provided by geologists into WEB-AVP inversion.

Chapter 3

Chapter 4

Application to the Book Cliffs Model

In the previous chapters, we have developed a Bayesian formulation to include prior geological information in the wave-equation-based angle-versus-slowness (WEB-AVP) inversion. The geological knowledge used to build prior distributions is obtained from the well logs, structural interpretation of the seismic data and regional geology. Previously, we have demonstrated the methodology for a very simple three-layer wedge model, which provided some conclusions on the feasibility of the method. In this chapter we shall demonstrate the methodology on a very detailed synthetic model based on the outcrop from the Book Cliffs, Utah, USA.

Chapter 4

4.1 Introduction

In Chapter 1 and Chapter 2 it is shown that wave-equation-based angle-versus-slowness (WEB-AVP) inversion is a very promising scheme for estimating elastic parameters from seismic data. The methodology uses the integral formulation of the wave equation as its forward modelling engine which honours the full physics of the wave propagation. It provides an innovative way of incorporating multiple scattering and converted waves in the modelling engine while keeping the computational requirements at an acceptable level. The algorithm is implemented as an iterative sequence of almost linear inversions. The method has been demonstrated on synthetic and field data examples in previous studies. But like any other inversion method it suffers from the non-uniqueness of the solution due to the presence of null spaces in the model space. To address this issue we incorporate geological information as *a-priori* knowledge for the inversion.

In Chapter 3, a Bayesian formulation of a new methodology that includes geological information in the WEB-AVP inversion is presented. The method relies on geological information obtained from well logs and seismic interpretation, which are used to build prior models with probability density functions as layer models. These layer-based model scenarios are translated to grid-based prior distributions in the grid-based model space. The translated prior distributions in the grid-based model space are used in a Bayesian formulation to update the estimate obtained from the unconstrained WEB-AVP inversion. The posterior distribution is maximised to find the nearest maximum (maximum a posterior MAP estimate), starting from the unconstrained inversion estimate (maximum likelihood estimate, MLE). The method also provides an estimate of the local uncertainty around the MAP estimate. The method has been demonstrated on a simple three-layer wedge model as a feasibility test. In this chapter, the newly developed method is applied to the synthetic, outcrop-based model from the Book Cliffs (Utah, USA).

4.2 Book Cliffs Model

In a previous study carried out by Tetyukhina et al., (2014) a relatively detailed geological model was built based on the Book Cliffs outcrops, as described by O'Byrne & Flint (1993); Pattison (1995); Taylor & Lovell (1995); Hodgetts & Howell (2000). Eight depositional environments, or lithotypes, were distinguished and the WEB-AVP inversion method has been applied in order to retrieve the medium parameters such as bulk rock density and compressibility (Tetyukhina et al., 2014). However, from a reservoir-geological perspective, the geological model presented in Tetyukhina et al. (2014) is considered relatively coarse. A more detailed model is needed in order to do justice to the inherent variations within the lithotypes. Feng et. al. (2017) presented a downscaled model having twelve different lithotypes that contains more details as compared to previous model. By analysing the forward-modelled seismic data based on a more detailed geological and petrophysical model, interpreters can understand which geological information can be extracted, and which ones cannot,

42

Application to the Book Cliffs Model

depending on the layer thickness and the wavelength of the seismic data. Such an improved model can also serve as a benchmark for an elastic wave-equation based inversion scheme, by allowing an analysis of the resolution and accuracy of the method.
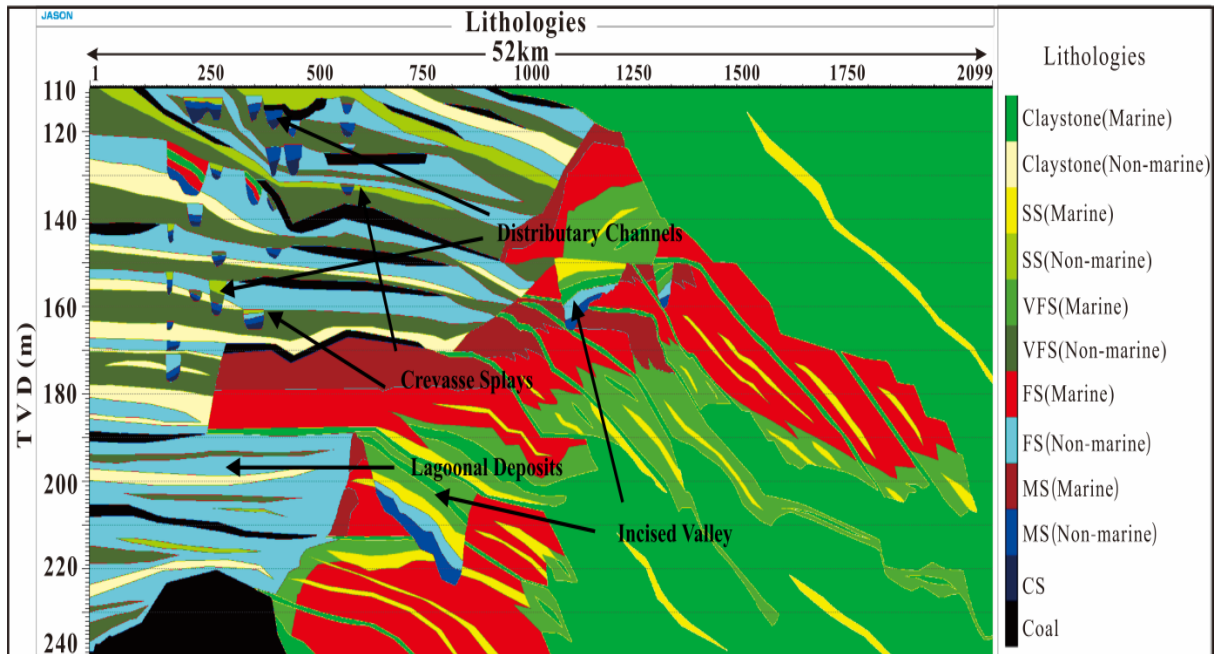

Figure 4.1: The geologically refined 2-D lithology model based on Book Cliffs (Utah, USA) consists of 12 different lithologies as compared to the previous version having 8 different lithologies. Different colours represent different lithologies (CS: Coarse-grained sandstones; MS: Medium-grained sandstones; FS: Fine-grained sandstones; VFS: Very fine-grained sandstones; SS: Siltstones). The numbers on the horizontal axis indicate the CMP locations. (Feng et al. 2017)
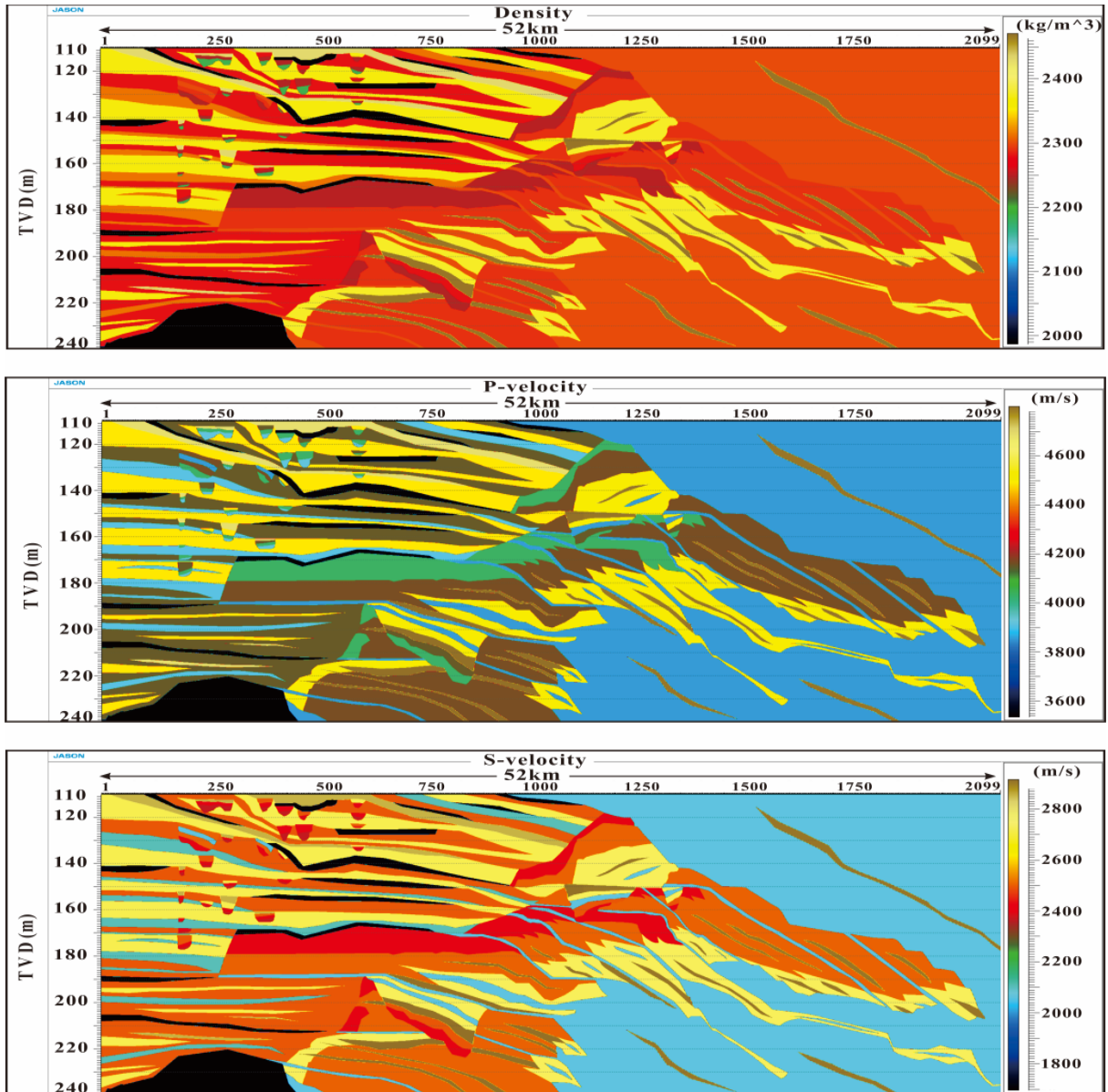
Figure 4.2: The physical properties of the new geological model in terms of bulk rock density ρ, compressional velocity V_P and shear velocity V_S. The horizontal width is 52 km approximately and has 2099 CMPs in total. Feng et. al. (2017)

4.3 Seismic Modelling

We use a different method to model the synthetic data to be inverted, from the modelling that is used in the WEB-AVP inversion. Since the inversion will be based on the full elastic wave-equation, for generating the data a different forward modelling algorithm is chosen that should also be exact, but is very different in nature from the one used in the inversion. For the forward modelling of the data to be inverted the Kennett invariant embedding method (Kennett, 2009) is used, which should also give exact results when applied with sufficiently small depth increments. The synthetic data was generated in the τ / p domain over this model, for 10 different ray-parameters, or horizontal slownesses. The

highest ray-parameter was such that on the outermost trace the maximum angle of incidence is 42 degrees. For the modelling a zero-phase band-pass wavelet was used with a maximum frequency of 60 Hz (Figure 4.3).
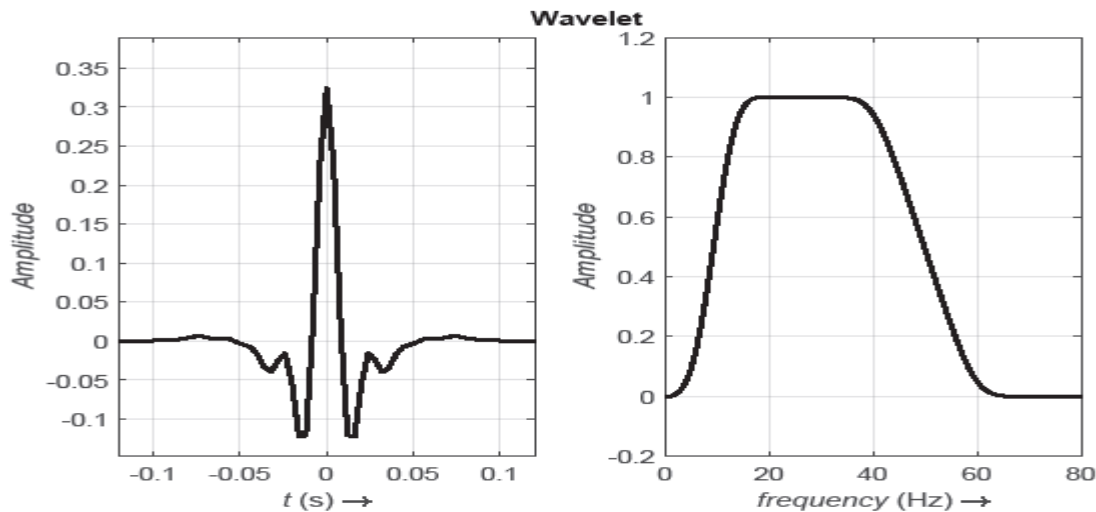

Figure 4.3: The zero-phase wavelet together with its amplitude spectrum used in the forward modelling with trapezium corner frequencies of 6-12-40-60 Hz. Edges of the wavelet have been tapered.

4.4 Geological Prior Information From Well Logs

The well logs provide an estimate of the Earth properties at a very fine scale. However, for the prior information obtained from wells to be useful away from the wells, we need to interpret the logs in terms of units that can be correlated over larger distances. The blocking of well logs is a well-established method in the oil and gas industry (Agunwoke et al., 2004; D'windt, 2007, Al-Adani et al., 2012). From the point of view of bringing in prior information, the blocking process should not be an automated algorithm, but should be a process that brings together geologists, petrophysicists, geophysicists and reservoir engineers, for all of whom these blocks should make sense in their various disciplines. Well-log information is very sparse in the lateral direction, even in mature fields and therefore, in order to predict the properties in between the wells the seismic data can be used. Seismic data provide a relatively coarse sampling in the vertical direction but an extensive areal sampling in the lateral direction. For the purpose of interpolation of layer model between well logs, horizon interpreted from seismic are used. For implementing the method on the Book Cliffs model we chose three different locations along the model, 10km and 8.75 km apart, that were designated as wells (Figure 4.4) where detailed prior information is available. At all three locations a number of layers were identified that seemed relevant from a geological and a geophysical perspective. In the current example the best correlatable units are the coal seams that stand out in all three properties. With some extra layers to fill up the spaces between the coal seams we arrive at a model with well 1 (W1), well 2

Chapter 4

(W2) and well 3 (W3) having seven layers. Normally from the well logs the observed variability within individual layers provides an estimate of the property variations with mean value (μ) and standard deviation (σ) for each layer, while the standard deviation of the thickness distribution of each layer is subject to a geologist's insights. However, in the present example the synthetic logs do not show variabilities within a layer that would give an indication about variabilities away from the wells. Therefore, in this case, also the standard deviations of the properties were to some extent subject to choice. The layer interpretation of the logs of these three pseudo-wells is shown in Figure 4.5.

At the well location the prior model building is a straightforward task. The layer boundaries are picked on the basis of geological, petrophysical and geophysical information, while the means of the layer thickness distributions are the thicknesses seen in the wells. The means and standard deviations of the properties of the layers are calculated from the observed means and variability of the properties within a layer. Only the standard deviations for the layer thickness distributions are subject to a general geological interpretation of the environment of deposition. They can be used to express more or less faith in a specific prior scenario. The mean realisation of the layered model for Well 1 and the mean of an ensemble of blocky trace realisations in depth, drawn from the layer model distributions, are shown later on.
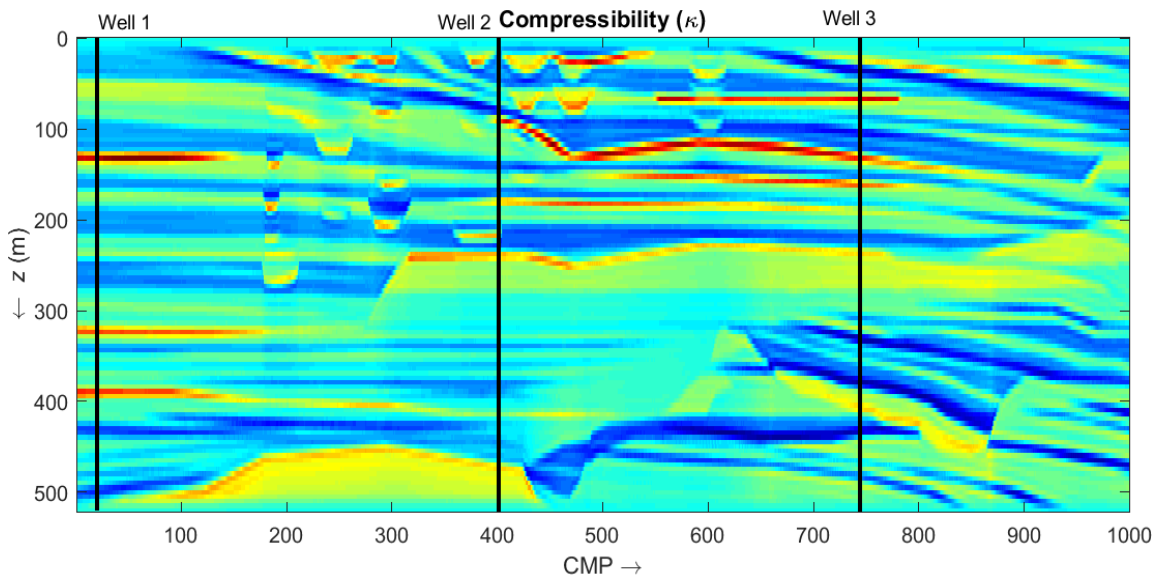
Figure 4.4: : The Book Cliffs Model with three wells at CMP 3, 400, 750 which are 10km and 8.5km apart. The property shown is the compressibility κ.

For the purpose of interpolating the layer model away from, or in-between the wells, we make use of horizons picked from seismic. Normally we would use a fully migrated stack for the interpretation, but in this synthetic example with the data directly modelled in the τ / p domain, it is easier to interpret the zero-angle section. The zero-angle PP data section over the model range between W1 and W3 is

shown in Figure 4.6, where also the elastic properties at the three wells location are shown. As can be seen from Figure 4.6, there are very few depositional interfaces that can be correlated between all three wells. The only consistent depositional features are the coal seams, two between W2 and W3 and one between W1 and W2. For this reason we decided to use horizons associated with the coal seams only. The zero-angle data, with horizons picked between wells 2 and 3, is shown in Figure 4.6, where we see horizons 4 and 5, correlatable from well 2 to well 3, and where we see horizon 3 that pinches out in the middle of the section.
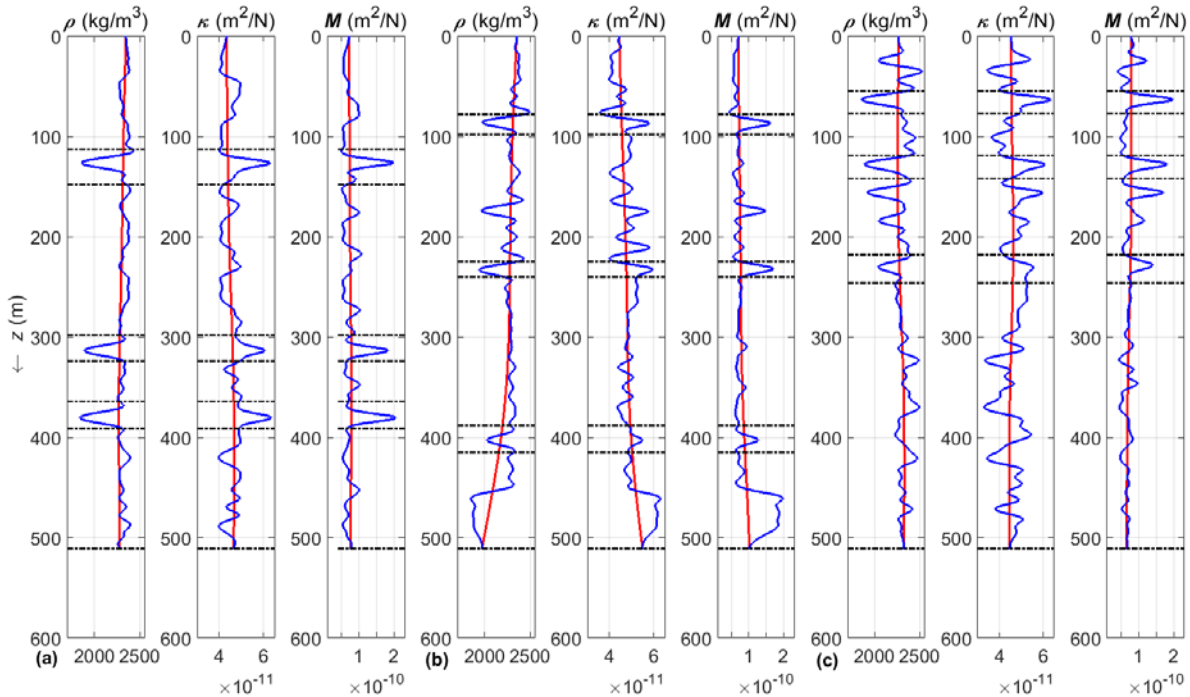

Figure 4.5: The interpreted well logs for κ, M, ρ (a) W1 with seven layers, (b) W2 with seven layers (c) W3 with seven layers. The red curves are the backgrounds obtained by severe smoothing of the real curves.

The layers associated with horizons 1 and 2 can be seen in W2 and W3 as the soft coal seams that are continuous between the wells, whereas the layer corresponding to horizon 3 can be seen in W3 but pinches out between W2 and W3. There is only one layer that can be correlated between W1 and W2, and we picked a horizon associated with that layer and let it pinch out between W2 and W3, whereas the other two coal layers are pinching out between W1 and W2. The mean and standard deviation for the three properties and thicknesses for W1 , W2 and W3 are given in Table 4.1, Table 4.2, Table 4.3, respectively.

Chapter 4

Table 4.1: Interpreted seven-layer model for W1 with the mean and standard deviation for the different properties. H1, H2 and H3 are horizons corresponding to thin coal seams.

Well 1 (W1)	Kappa (κ) (m^2/N)		M (M) (m^2/N)		Density (ρ) (kg/m^3)		Thickness (m)	
Layer	Mean	STD	Mean	STD	Mean	STD	Mean	STD
1	4.3e-11	3.3 e-10	1.6 e-11	3.8 e-10	2346	100	124	100
2 (H1)	6.1 e-11	1 e-11	4.4 e-11	1 e-11	1880	20	10	10
3	4.4 e-11	3.6 e-10	1.8 e-11	4.4 e-10	2328	100	180	100
4 (H2)	6.1 e-11	1 e-11	4.4 e-11	1 e-11	1880	20	10	10
5	4.7 e-11	2.5 e-10	1.8 e-11	5.9 e-10	2294	100	58	100
6 (H3)	6.1 e-11	1 e-11	4.4 e-11	1 e-11	1880	20	10	3
7	4.6 e-11	4.5 e-11	1.8 e-11	5.9 e-10	2298	100	128	100

Table 4.2: Interpreted seven-layer model for W2 with the mean and standard deviation for the different properties. H4, H5 and H3 are horizons corresponding to thin coal seams.

Well 2 (W2)	Kappa (κ) (m^2/N)		M (M) (m^2/N)		Density (ρ) (kg/m^3)		Thickness (m)	
Layers	Mean	STD	Mean	STD	Mean	STD	Mean	STD
1	4.2e-11	3.3 e-10	1.4 e-11	3.8 e-10	2346	100	84	100
2 (H4)	6.1 e-11	1 e-11	4.4 e-11	1 e-11	1880	20	6	1
3	4.7 e-11	3.6 e-10	1.9 e-11	4.4 e-10	2282	100	143	100
4 (H5)	6.1 e-11	1 e-11	4.4 e-11	1 e-11	1880	20	7	2
5	4.8 e-11	2.5 e-10	1.8 e-11	5.9 e-10	2284	100	166	100
6 (H3)	6.1 e-11	1 e-11	4.4 e-11	1 e-11	1880	20	5	3
7	4.6 e-11	4.5 e-11	1.8 e-11	5.9 e-10	2298	100	108	100

Table 4.3: Interpreted seven-layer model for W3 with the mean and standard deviation for the different properties. H4, H5 and H6 are horizons corresponding to thin coal seams.

Well 3 (W3)	Kappa (κ) (m^2/N)		M (M) (m^2/N)		Density (ρ) (kg/m^3)		Thickness (m)	
Layers	Mean	STD	Mean	STD	Mean	STD	Mean	STD
1	4.2e-11	3.3 e-10	1.4 e-11	3.8 e-10	2346	100	59.6	100
2 (H6)	6.1 e-11	1 e-11	4.4 e-11	1 e-11	1880	20	10	1
3	4.7 e-11	3.6 e-10	1.9 e-11	4.4 e-10	2282	100	56	100

4 (H4)	6.1 e-11	1 e-11	4.4 e-11	1 e-11	1880	20	10	1
5	4.8 e-11	2.5 e-10	1.8 e-11	5.9 e-10	2284	100	96	100
6 (H5)	6.1 e-11	1 e-11	4.4 e-11	1 e-11	1880	20	5	2
7	4.6 e-11	4.5 e-11	1.8 e-11	5.9 e-10	2298	100	284	100

The blocked well logs are used to build a prior model at the well locations, which is subsequently interpolated for every CMP, guided by the picked horizons. These models now consist of a set of layer properties and layer thicknesses, with means and standard deviations, for every layer and every lateral location. The next step is to translate the prior layer model to a prior model defined on a equidistant vertical depth grid, according to equations (3.8) and (3.9).

For the determination of the weight matrix $\mathbf{W}$ in these equations we created an ensemble of models drawn from the layer property and thickness distributions, for which blocky trace representations in depth were made. In Figure 4.8 we show, at the location of W1, the true compressibility of the model, in black, a realisation consisting of the means of all layer properties, in red, and the mean of the ensemble in the grid domain, in blue.

Without any prior information the starting model for the first outer loop iteration in Figure 2.1 is the background model, i.e. zero contrast values (equations (2.1) to (2.3)). With the availability of a prior model, we can have either the mean realisation of the prior model as starting model for the inversion, or the mean of an ensemble of blocky trace realisations drawn from the prior model. In Figure 4.7 we show both the layer-based mean realisation and the mean of the grid-based realisations, for the whole section. As a starting model for inversion we prefer the mean of the gridded blocky trace realisation, over the mean realisation of the layer model, because there is more uncertainty in the grid-based mean, due to the uncertainty to what layer a certain grid-point belongs to, as expressed by the weight matrix $\mathbf{W}$. The prior model tells us there are coal seams in the section, but it doesn't prescribe exactly where the coal seams are, because the thicknesses of the overlying layers have wide standard deviations. Apart from providing a starting model for the inversion, the multi-grid-point prior probability density function is used in Bayes' rule to update the unconstrained inversion result (MLE) to a maximum a priori (MAP) prediction.
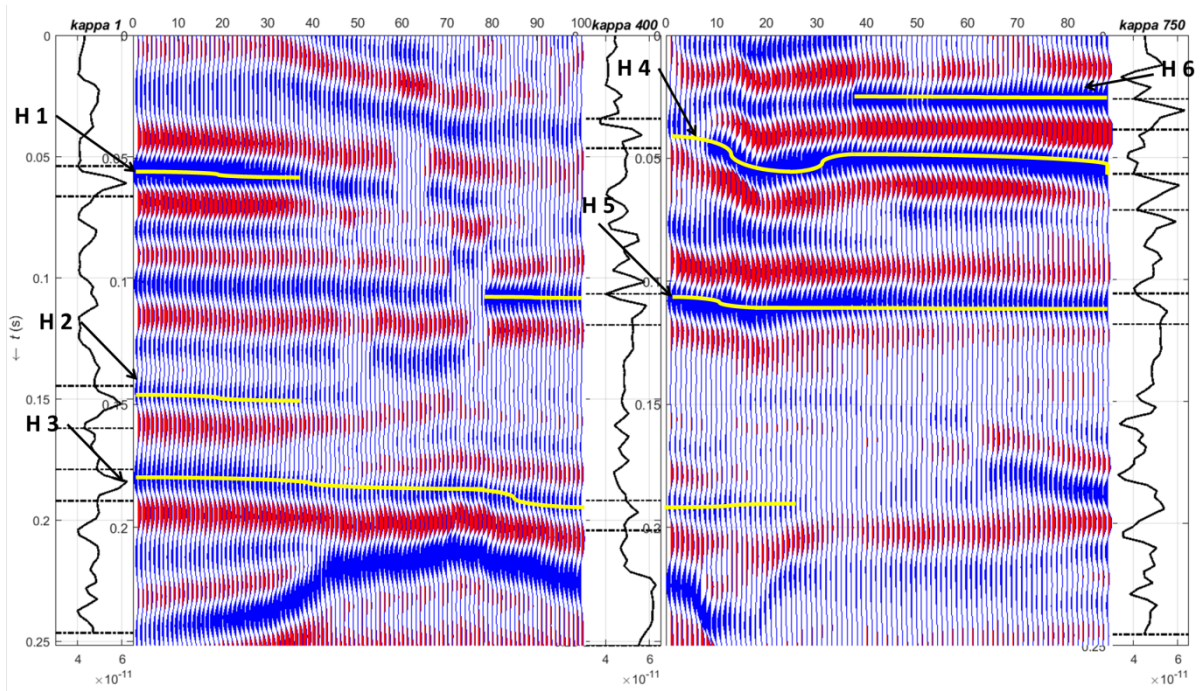
Figure 4.6: Zero-angle section for PP data showing the interpreted horizons with the corresponding κ (compressibility) log in the time domain. Horizons 1 and 2 pinch out in middle of the section between W1 and W2 while horizon 3 is can be mapped between W1 and W2. Horizons 4 and 5 can be mapped between W2 and W3 while horizon 6 is pinches out in middle of the section.

4.5 Results and Discussion

In this section we present the application of our method, first to the data at the location of W1 and then for the full Book Cliffs section as shown in Figure 4.4. We will show two results: one without any prior information except the background models, and one with prior information in the form of a starting model and a MAP update after every outer loop iteration in the WEB inversion. As mentioned before, we prefer to start from the mean of the gridded realisations of the ensemble drawn from the prior model as constructed for every lateral location. The prior model in the gridded domain, for all lateral locations, is constructed from well logs and seismic horizons, as explained in detail in the previous sections.
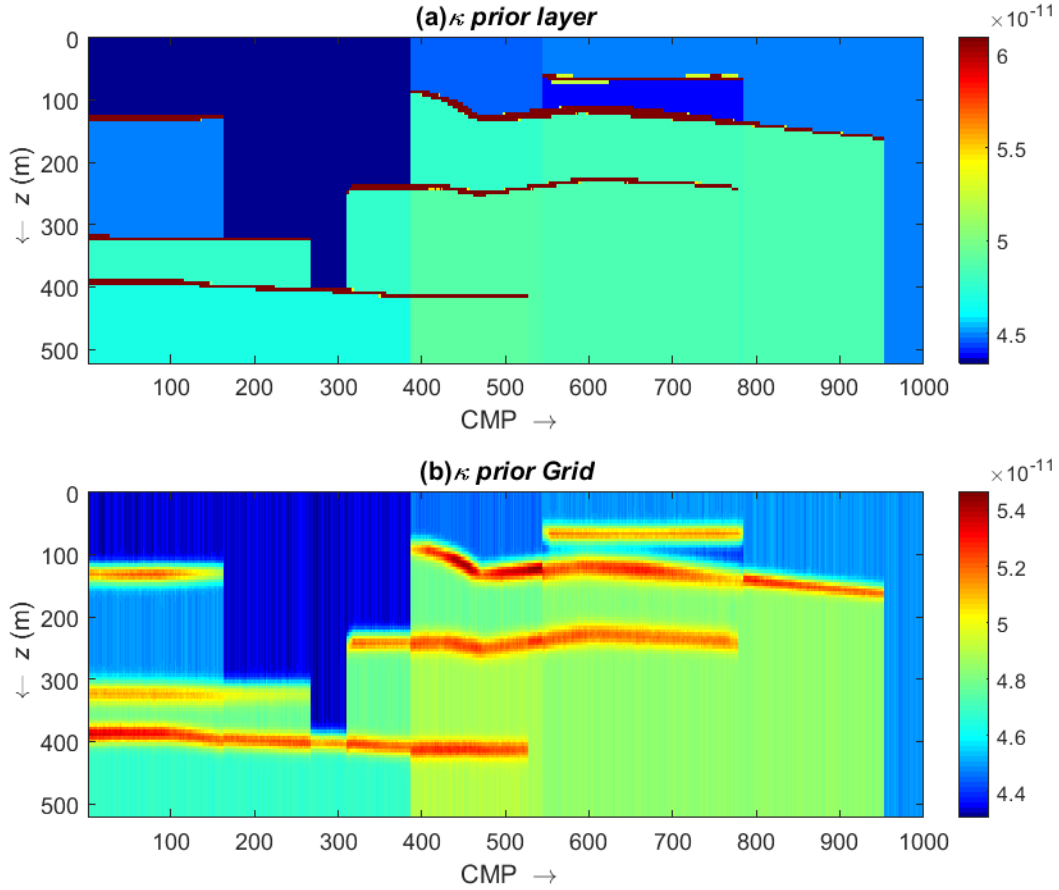
Application to the Book Cliffs Model

Figure 4.7: (a) Mean realisation of the interpreted layer-based prior model for the Books Cliff section between W1, W2 and W3. (b) Mean of the gridded model for the interpreted layer-based model. The mean thickness of the layer and property is calculated from the well logs whereas the standard of the thickness changes away from the well.

First, we apply the method to a single location where we know the truth. We can do this because WEB-AVP inversion works in the 1.5D domain and all input image gathers from migration are inverted independently. We will carry out the inversion twice, once without any prior information and once with a prior model that serves the double purpose of providing a starting model for the inversion, as well as allowing performing a MAP update after every outer loop iteration of the inversion.

The true logs for the three properties κ, M, ρ for W1 are shown in black in Figure 4.8. The mean realisation of the seven-layer prior model is shown in red. The mean of an ensemble of gridded realisations drawn from the prior model is shown in blue. The background models for the three properties κ, M, ρ for W1 are shown in Figure 4.5, in red.

The results for the two different inversion trials are shown in Figure 4.9. In Figure 4.9(a) the inversion results for κ, M, ρ are shown for the case when we start from the background model and no prior information is used while carrying out the inversion. In Figure 4.9 (b) we see the results for κ, M, ρ

when we start from the mean of the gridded prior model realisations and apply the MAP update after every outer loop iteration of the inversion. It is clear that without prior knowledge on the presence or absence of thin coal seams the inversion fails to resolve them and shows a tuning effect (Widess, 1973) in the final results (Figure 4.9 (a)). On the other hand, if we bring in a geological concept that allows the presence or absence of these coal seams, we are able to resolve them fully. In addition, the density, which is always hard to get from seismic data, is greatly helped by the prior information (Figure 4.9 (b)).
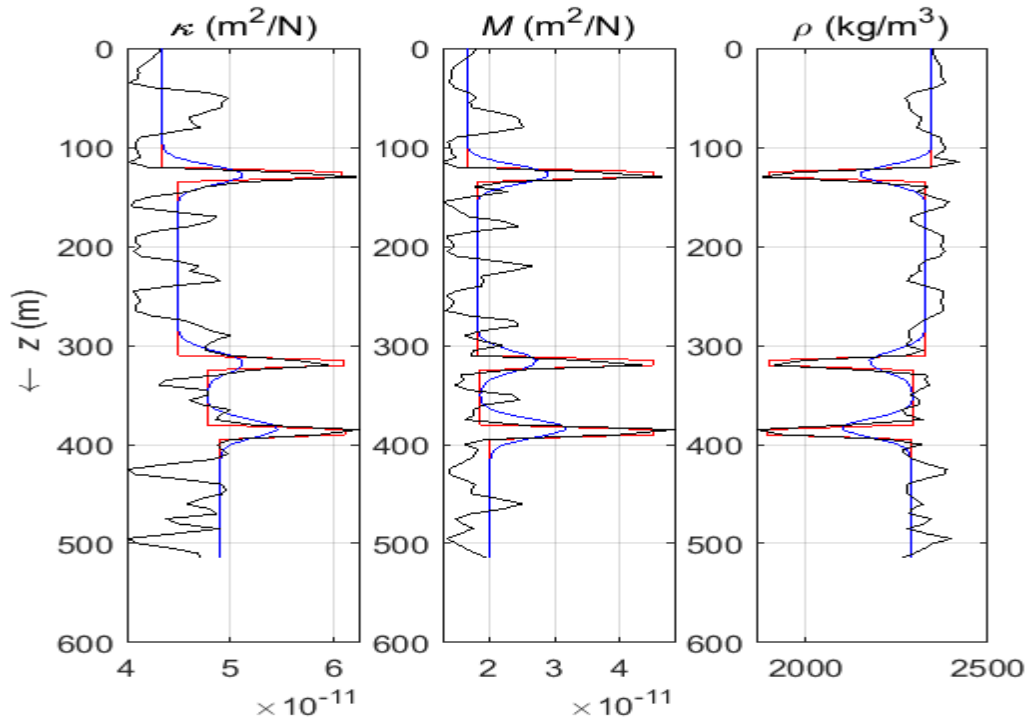

Figure 4.8: The black curves are the real properties. The red curves show the blocky trace representations of a model where all layer properties have their mean value. The blue curves show the mean of an ensemble of gridded blocky traces, where the layer properties have been drawn from the prior layer distributions.
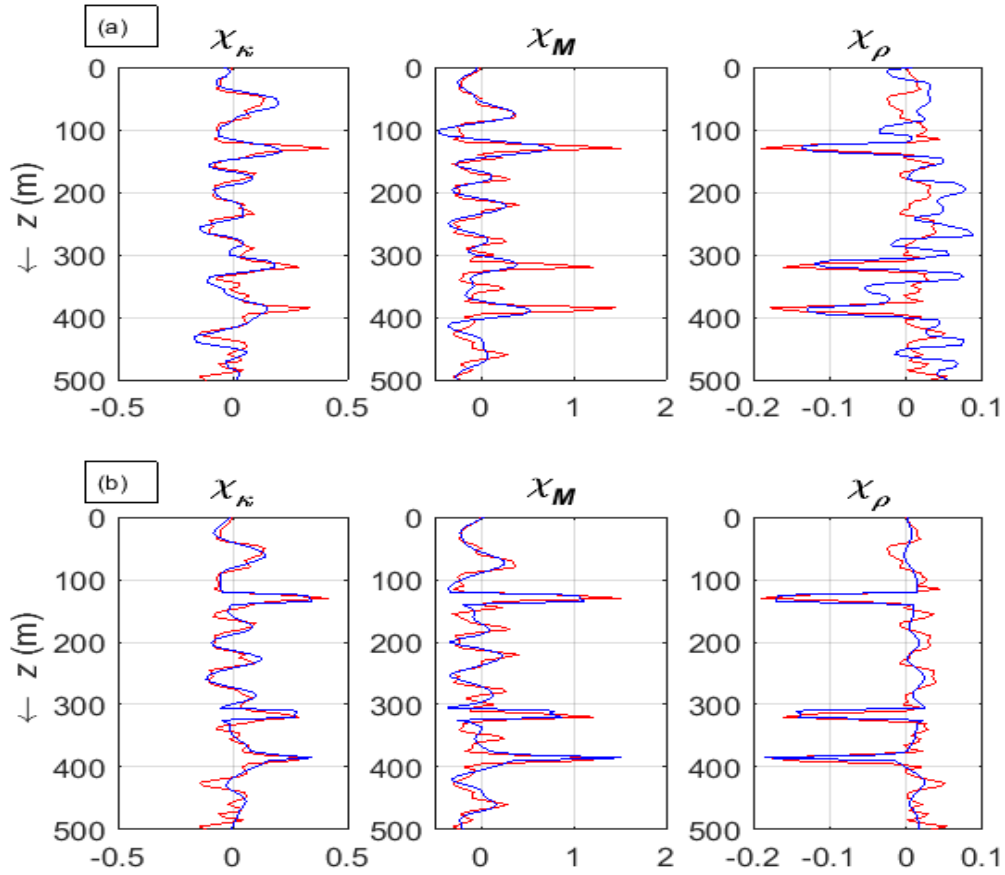
Application to the Book Cliffs Model

Figure 4.9: The inverted results for well W1. (a): Without prior model , (b): With prior model. The inverted results are shown in blue and the red curve are the real properties.

Next, the inversion trial described above is carried out for every CMP location in the Book Cliffs model. Figure 4.10(a) shows the true compressibility contrast of the model, as χ_κ (equations (2.1) through (2.3)). Figure 4.10 (b) shows the inversion results for χ_κ without any prior information. Figure 4.10 (c) shows the starting model for the inversion with prior information. It should be borne in mind, though, that the prior model is also used for the MAP update after every outer loop iteration in the inversion. Finally, in Figure 4.10 (d) we see the final MAP predictions for the χ_κ contrasts. Similarly, in Figure 4.11 and Figure 4.12 we show the final results for shear compliance χ_M and density χ_ρ respectively.
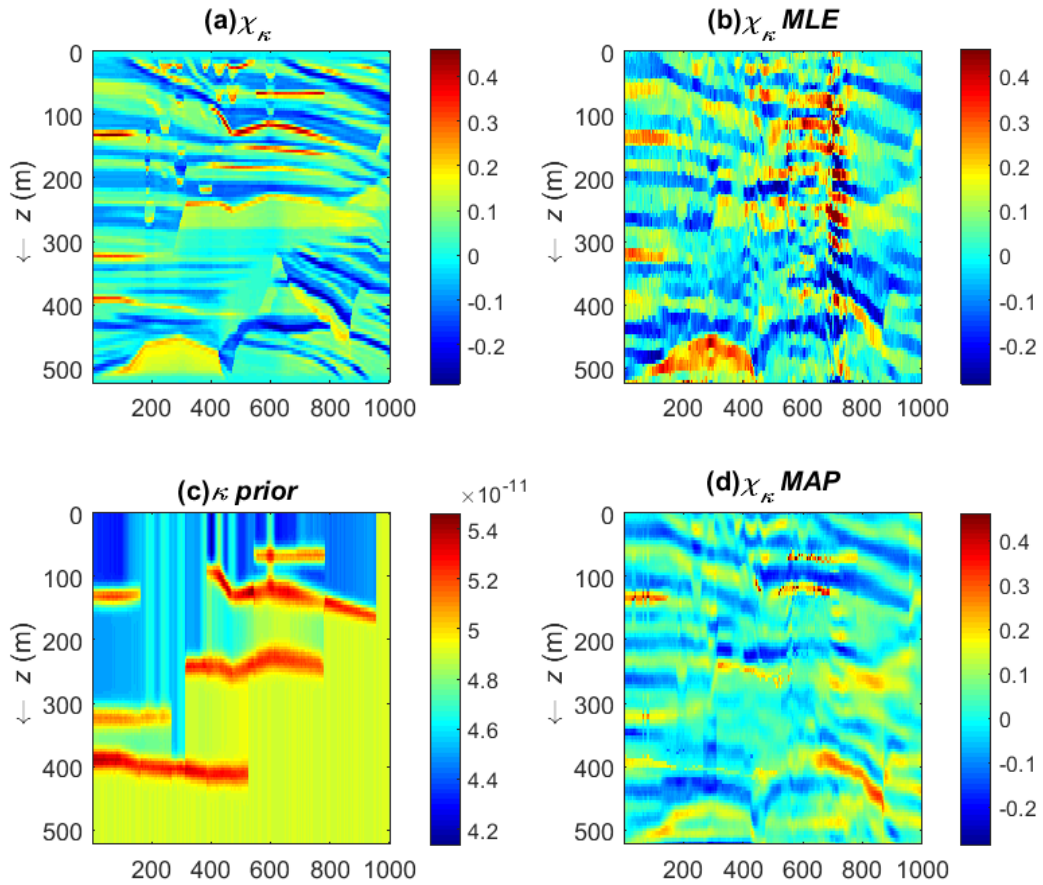
Figure 4.10: (a) The true compressibility contrast for Book Cliffs model. (b) The WEB-AVP inversion results for compressibility contrast without prior Information (MLE) for the Book Cliffs model. (c) The prior model for compressibility. (d) The MAP estimate for compressibility contrast for the Books Cliffs model.

The inversion starting with the background model only, i.e. zero contrasts and no MAP updates, provided us already with a good estimate of the properties (Figure 4.10, Figure 4.11, Figure 4.12 (b)), while using a minimal amount of prior information in the form of the smooth background models only. However, it failed to resolve the thin coal seams, which could be important for the geological interpretation of the inversion result. In addition, in some places the lateral continuity is missing because the inversion is carried out on individual CMPs independently. Both these shortcomings are addressed when we provide a prior model that contains the information about these coal seams and brings in some lateral continuity. The mean of the prior model is not smooth in nature and lateral continuity is not apparent either, because it is only one realisation of the whole prior model and it changes from location to location. In order to appreciate the lateral continuity in the prior model we should be looking at distributions, rather than the means only for every single location, but that information is difficult to render in 2D displays.
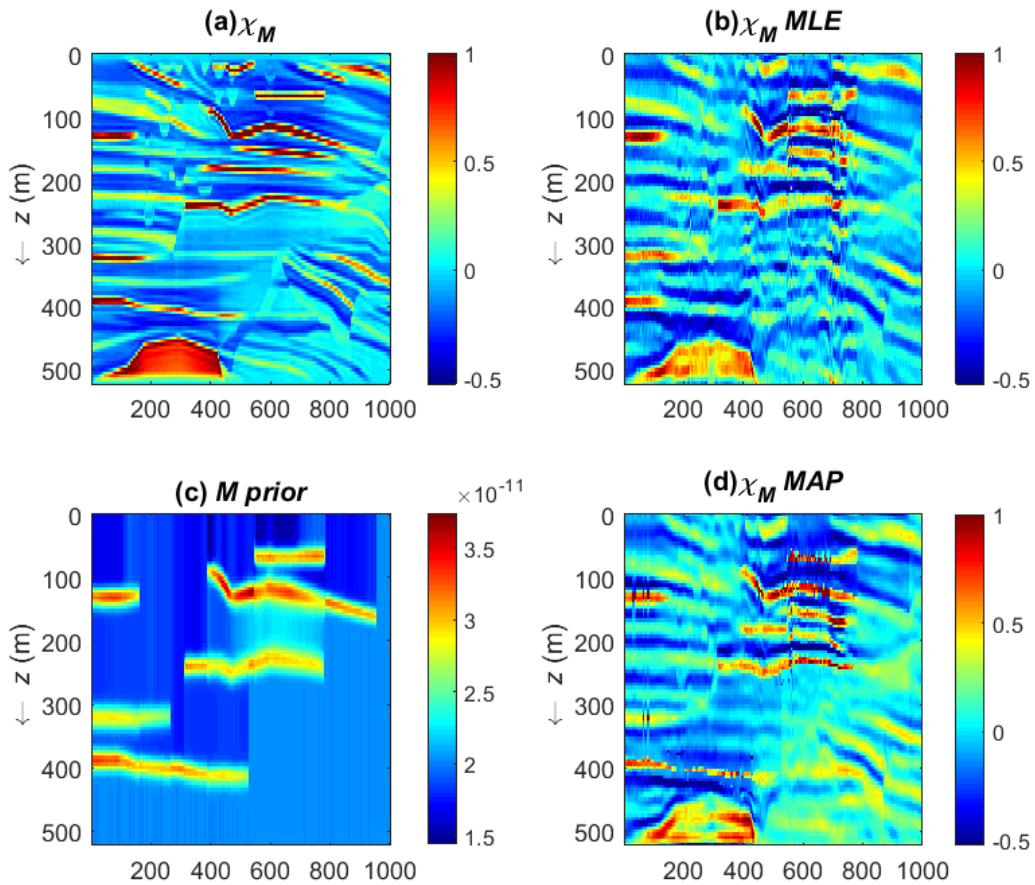
Application to the Book Cliffs Model

Figure 4.11: (a) The true shear compliance contrast for Book Cliffs model. (b) The WEB-AVP inversion results for shear compliance contrast without prior Information (MLE) for the Book Cliffs model. (c) The prior model for shear compliance. (d) The MAP estimate for shear compliance contrast for the Books Cliffs model.

Using a different starting model that contains more information than the smooth background model, will already provide a better estimate in the inner loop in Figure 2.1. On top of that, having a MAP update after every outer loop iteration will keep the inversion results close to the prior model which displays lateral continuity and subsequently will bring in lateral coherency in final MAP estimate. The imprint of the prior model is very evident in the MAP estimates in Figure 4.10, Figure 4.11 and Figure 4.12 (d). In the posterior estimate we can locate some of the coal seams corresponding to horizon 4 and 5, which were earlier not resolvable by unconstrained WEB-AVP. Also the lateral continuity is much better, especially between wells W2 and W3.
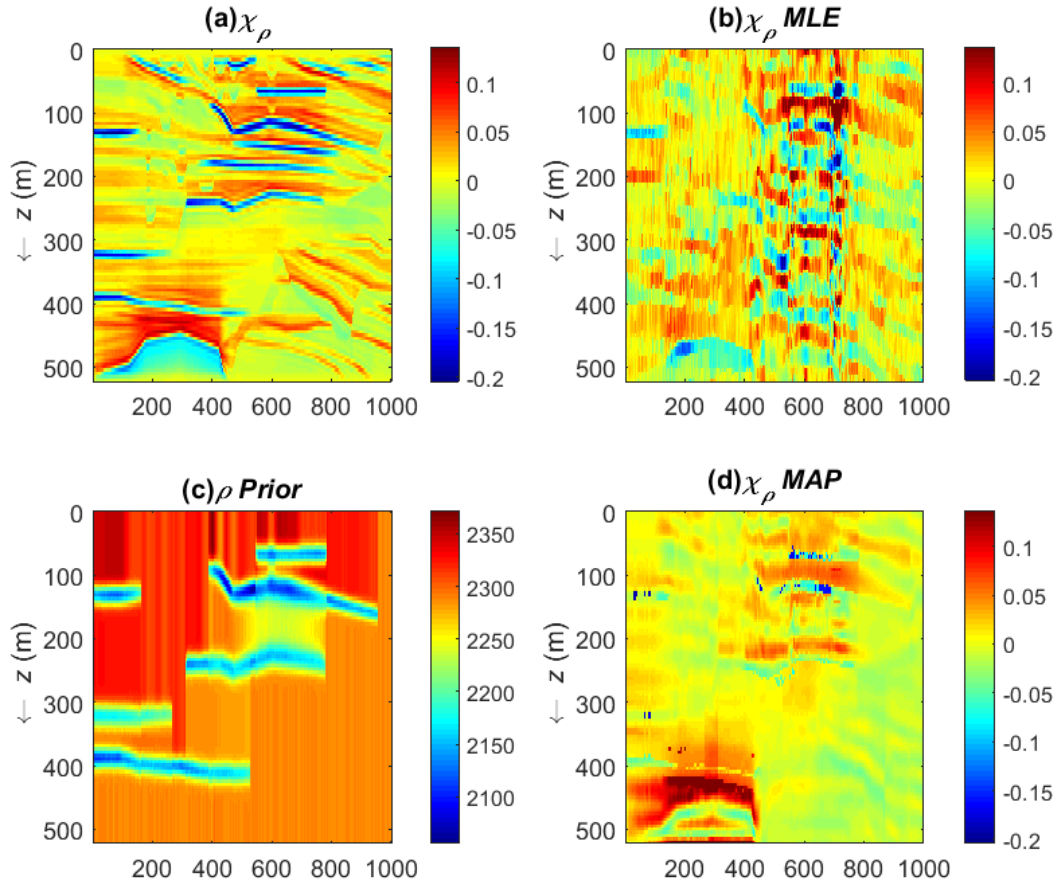
Figure 4.12: (a) The true density contrast for Book Cliffs model. (b) The WEB-AVP inversion results for density contrast without prior Information (MLE) for the Book Cliffs model. (c) The prior model for density. (d) The MAP estimate for density contrast for the Books Cliffs model.

The methodology also provides an estimate of the standard deviation for the MAP estimate, which is associated with the second derivative of our objective function in equation 3.13. We have assumed the grid points to be statistically independent, which enables us to calculate a localised estimate of the standard deviation in the neighbourhood of the MAP estimate, for every grid point. The standard deviations are calculated for absolute values of compressibility, shear compliance and density and are shown in Figure 4.13. The standard deviations are about 100 times smaller than the mean MAP estimate for all three properties. The standard deviations for the MAP estimates are always smaller than the standard deviations of the gridded prior model and the standard deviations of the Likelihood function.
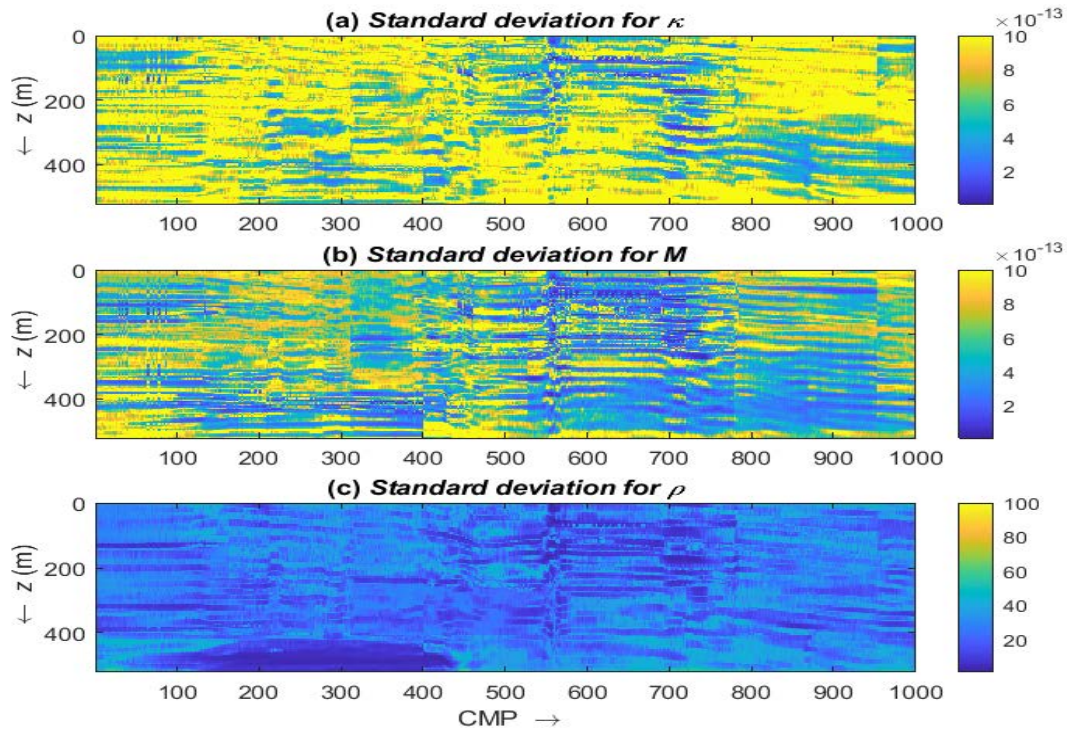
Figure 4.13: Standard deviations for the MAP estimates for compressibility, shear compliance and density for the Books Cliffs model.

4.6 Conclusions

In the present study it is shown how to incorporate geological prior knowledge into the WEB-AVP inversion. The methodology presented deals with acquiring prior information in terms of layered models and how to translate this prior information to prior information for a gridded model, which is subsequently used in non-linear wave-equation-based inversion. This gives a simple Bayesian formulation of incorporating prior information into the inversion. The translated prior model in the gridded domain can be used as a starting model for the WEB-AVP inversion, as well as being used in the inversion to update the unconstrained inversion result (MLE) to a posterior result (MAP) after every outer loop iteration. The methodology provides a MAP estimate after every iteration as well as an estimate of the standard deviation in the vicinity of the MAP estimate. The results shown suggests that the approach is justified and they give insight into how to incorporate the geological knowledge provided by geologists into WEB-AVP inversion.

Chapter 4

Chapter 5
Scenario Testing

In the previous chapters we presented a new Bayesian methodology to incorporate geological information in WEB-AVP inversion. However, geological information from well logs is subject to analysis by experts (geologists) to build scenarios that are based on geological concepts. As the geological information required resides in higher dimensional parameter space, interpretations from an experts cannot explain the variability in the subsurface in a single scenario. This leads to a new aspect of the Bayesian approach: the quantification of the probability of different scenarios, given the seismic data. We extend the Bayesian methodology presented in Chapter 3 to quantify different scenarios in terms of probabilities on the basis of how much they overlap with the seismic inversion results.

Chapter 5

5.1 Introduction

In Chapter 3 a new methodology for incorporating the geological prior information into WEB-AVP inversion was introduced. The geological prior information in terms of layer-based model is translated to grid-based models that are used to build prior probability distribution. These prior probability distribution are used to update the maximum likelihood estimate (MLE) from unconstrained WEB-AVP inversion to maximum a posterior (MAP) estimate. The layer-based models are built using interpretation of the well-logs and other geological data available to the experts. As the methodology presented in Chapter 3 starts with an interpretation of well logs in terms of layers, one needs to address the issue of multiple interpretations of the same well log(s) in terms of number of layers, property distributions and thickness distributions. In this chapter we extend the methodology presented in Chapter 3 to estimate the probabilities of different interpretations (scenarios) with the help of WEB-AVP inversion results.

In the present chapter we build a Bayesian framework to incorporate geological uncertainties in terms of geological scenarios and quantify the probabilities of the scenarios on the basis of the output of the seismic inversion. The positive aspects of this kind of formulation are two-fold, firstly we do not need to run seismic inversion for every geological scenario, and secondly we decrease the computational cost of sampling from the whole model space.

5.2 Methodology

We follow a Bayesian methodology for the purpose of integrating geological scenarios and seismic data. Bayes' rule states that combining the prior probability density function $P(\mathbf{m}|S)$ for the scenario S, with the likelihood function $P(\mathbf{d}|\mathbf{m})$, which is the probability density function of the data $\mathbf{d}$, given a model $\mathbf{m}$, we get the posterior probability density function $P(\mathbf{m}|\mathbf{d}, S)$, which is the probability density of the model vector $\mathbf{m}$ given the data $\mathbf{d}$

$$P(\mathbf{m}|\mathbf{d}, S) = \frac{P(\mathbf{d}|\mathbf{m})P(\mathbf{m}|S)}{P(\mathbf{d}|S)},$$

(5.1)

where $P(\mathbf{d}|S)$ is the probability distribution of the data, acting as a normalisation factor to make $P(\mathbf{m}|\mathbf{d}, S)$ a valid probability density function. It can easily be seen that we should have :

$$P(\mathbf{d}|S) = \int_{\mathbf{M}} P(\mathbf{d}|\mathbf{m})P(\mathbf{m}|S)d\mathbf{m},$$

(5.2)

Scenario Testing

which makes $P(\mathbf{d}|S)$ a functional of the scenario S. When a number of scenarios are available such as $\{S_1, S_2, S_3, ... S_n\}$ (Figure 5.1), we can renormalize the probability of the data, given the scenario, to the probability of the scenario given the data.

The methodology begins with defining a geological concept that captures information regarding the regional geology, the local environment of deposition and facies observed in the well. These interpreted data are used to build layer-based models that are location dependent, guided by the structural interpretation of seismic data. The layer-based models should be populated with property and thickness distributions, derived from the well data, depth-below-mudline trends and other information specific for the scenario. All this information is captured in the multi-variate probability density function $P(\mathbf{m}|S)$.
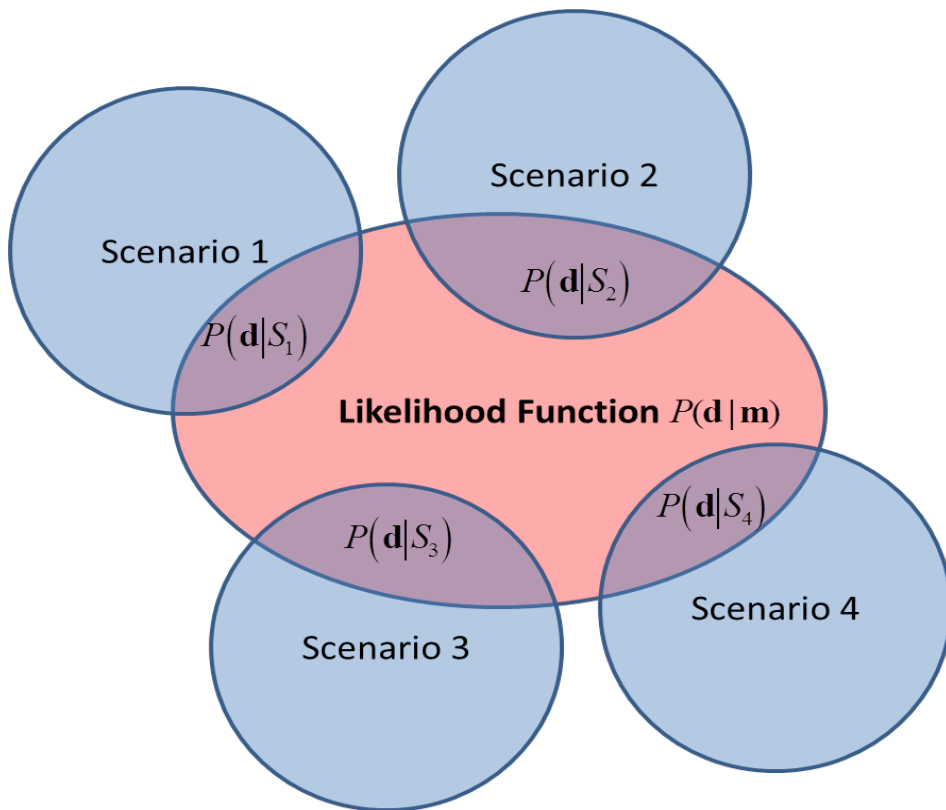
Figure 5.1: Schematic representation of scenario testing. An ensemble of grid-based models is created using a Gaussian distribution for the likelihood function $P(\mathbf{d}|\mathbf{m})$. The probability of the data $P(\mathbf{d}|S)$ is calculated individually for all scenarios, given an ensemble of realisation drawn from the likelihood function, which is the overlap between the likelihood function and prior scenario distribution. $P(\mathbf{S}|\mathbf{d})$ is calculated by re-normalising the probability of data, to add up to one, when summed over all scenarios.

Chapter 5

The probability of the data $P(\mathbf{d}|S)$, as defined by equation (5.2), is the overlap between the likelihood function and prior probability distribution, and can be calculated by evaluating the integral in equation (5.2). There are several problems in evaluating this integral. Firstly, the likelihood function is defined on the gridded model space where the seismic forward problem is evaluated, whereas the scenarios are defined by prior probability density functions defined in the layer-parameter domain. Secondly, numerical evaluation of this integral is not straightforward and we need to use sampling methods to make an approximation of this integral.

To address the first issue, we have to bring the prior probability density function from the layer-parameter domain to the gridded domain. This step has already been presented in Chapter 3, where an ensemble of blocky trace realisation was drawn from the layer-based prior distributions, from which histograms can be made for the number of times a grid point is found in a certain layer. From these histograms the weight matrix for the Gaussian mixture model for every grid point is constructed.

For the purpose of approximating the integral in equation (5.2), we create an ensemble of model realisations in the gridded domain drawn from the Gaussian likelihood function. For this ensemble we calculate the grid-based prior probability density for every realisation and add them all up. The integral in equation (5.2) is then approximated by:

$$P(\mathbf{d}|S) \approx \frac{1}{N}\sum_{i=1}^{N} P(\mathbf{m} = \mathbf{m}_i | S),\tag{5.3}$$

where N is the number of realisations in the ensemble drawn from Gaussian likelihood function $P(\mathbf{d}|\mathbf{m})$ and $\mathbf{m}_i$ is a single realisation from that ensemble.

Once we have $P(\mathbf{d}|S)$ for a number of scenarios S, one can calculate $P(S|\mathbf{d})$ using:

$$P(S|\mathbf{d}) = \frac{P(\mathbf{d}|S)P(S)}{\int_{\mathbf{S}} P(\mathbf{d}|S)P(S)}.\tag{5.4}$$

If all the scenarios are equiprobable, $P(S|\mathbf{d})$ are simply normalised with respect to $P(\mathbf{d}|S)$ summed over all scenarios. If scenarios are not equiprobable, one need to consider the probability of scenario $P(S)$ in equation 5.4. For the sake of thesis, only equiprobable scenarios are considered.

5.3 Synthetic Example

The new method was tested on a very detailed model based on a real outcrop, which was even further downscaled based on a realistic geological scenario (Feng et al., 2017). For the purpose of this study we select a section of about 8 km from the Book Cliffs model with well logs on either side.

5.3.1 Seismic Modelling and Inversion

We use the same data as in Chapter 4. The maximum frequency in the data is 60 Hz. This data is considered to be observed data, with some white noise added. We are going to invert this data to retrieve the elastic properties of the subsurface. We use the WEB-AVP seismic inversion to invert seismic data simulated using the Kennett method (Kennett, 1983).

The inversion was carried out on the selected part of the Book Cliffs model and inversion results for the κ, M and ρ property contrasts against the background, as shown in Figure 5.2, represent a good approximation of the true model. The estimates for κ and M are better compared to the one for ρ. Apparently, the angle range in the seismic data was insufficient to retrieve a better estimate of density. In the final results we are missing some lateral continuity, because the inversion is performed on all locations independently along the section. The lateral continuity is very important to delineate geological layering in the subsurface.

If we focus on the most prominent feature in the section: the coal seams, which are very thin in nature but produce a high contrasts for all three properties, we see that they are not very well resolved. This is because they are beyond seismic resolution, even for WEB-AVP. Also CMP's between 550 and 750 a new thin coal is present in the true model that hampers the lateral continuity in the MLE estimates.
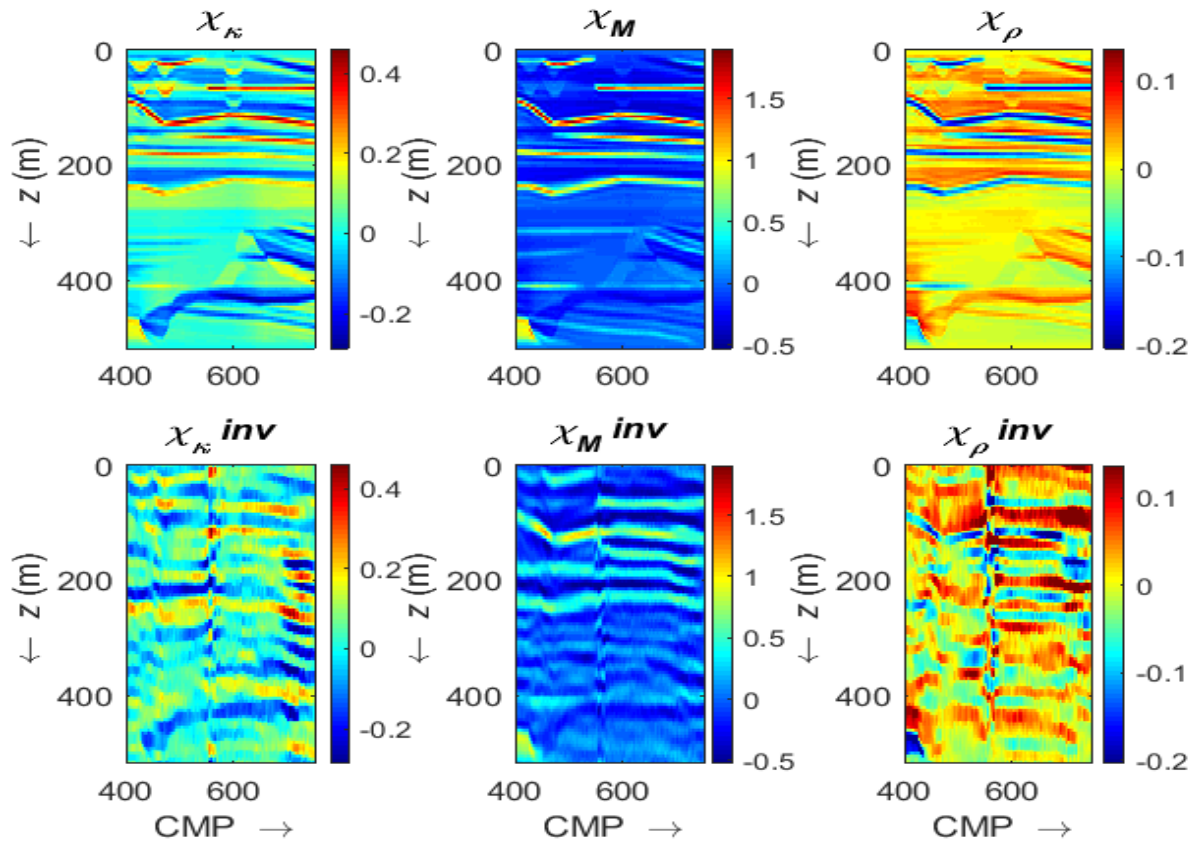
Figure 5.2: WEB AVP inversion results for the selected part of Book Cliffs Model without any prior information except the background model. Top row: True contrasts for compressibility, shear compliance and density. Bottom row: Unconstrained inversion results for the same contrasts, with only the background model as prior information being used.

5.3.2 Creating Prior Scenarios

To address the issues with the inversion results shown in Figure 5.2 that were pointed out in the previous section, we make use of other information available to us. In Chapter 4 creating the prior scenarios using the well logs is explained in detail.

In Figure 5.3 we also see the used V_p logs, in the time domain, on either side of the zero-angle seismic section. We can interpret two horizons that are continuous between the two wells. These are interpreted as thin coal seams. A six-layer model is interpreted from the two wells and interpolated across the section with the help of the two horizons. The thicknesses of these layers are based on the interpretation (blocking) of the well logs at the well location, but the most important aspect in this example is to estimate the thickness of the reservoir layer away from well, which is difficult based on the bandlimited inversion result.
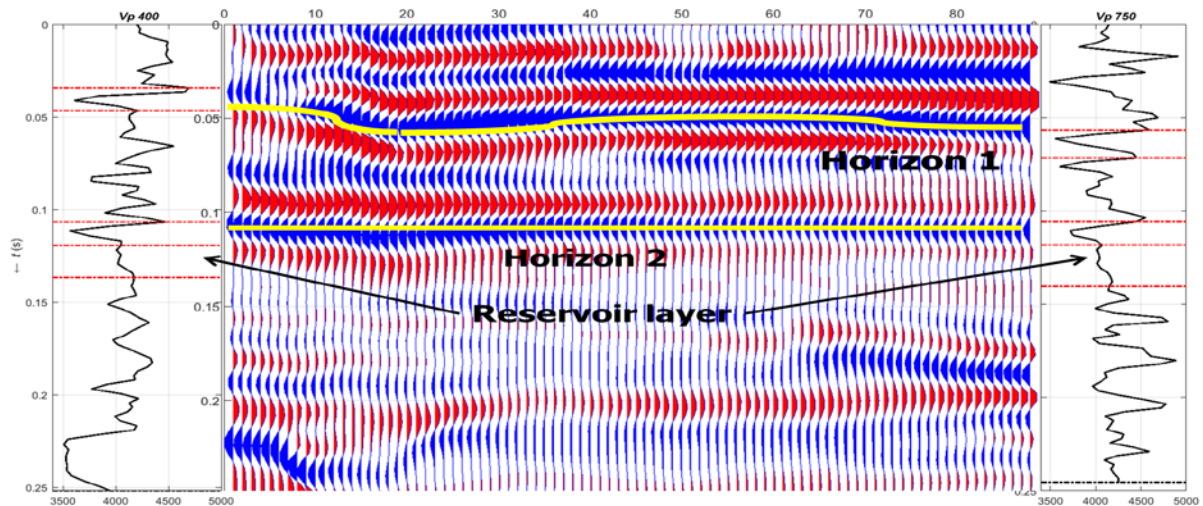
Scenario Testing

Figure 5.3: Zero-angle section of the synthetic data. Also shown are two interpreted horizons that represent the coal seams, used for building of the prior model. A six layer model is interpreted between the well logs with layer 2 and 4 representing the horizon 1 and 2 respectively, whereas layer 5 corresponds to a potential reservoir layer.

The three scenarios that were built differ in the mean of the thickness distribution of the reservoir layer and are organised in increasing values for that thickness (Table 5.1). For the first scenario, the mean thickness of the reservoir layer is 0 m, which means that the reservoir layer is absent. For the second scenario, the true mean thickness of the reservoir layer (35 m) is used and for the third scenario a mean reservoir thickness of 70 m is assumed. We first carry out the posterior estimates for all these scenarios and posterior results are shown for the scenarios 1, 2 and 3 in Figure 5.4, Figure 5.5 and Figure 5.6 respectively.

Table 5.1: Three different scenarios with different mean value of thickness distribution of reservoir layer.

Scenario	Mean thickness of reservoir layer (m)
Scenario 1 (Reservoir layer absent)	0
Scenario 2 (True mean thickness of reservoir layer)	35
Scenario 3 (Thicker reservoir layer)	70

5.4 Results

5.4.1 Scenario 1

In Scenario 1 a mean thickness of 0 m is assigned to the reservoir layer. Firstly, the unconstrained inversion is carried out and the results for the compressibility, shear compliance and density contrasts are shown Figure 5.2. These results can be interpreted as the maximum likelihood estimates. Now we bring in the prior information as interpreted from the well logs, as prior distributions, and we build different scenarios. The mean of an ensemble of gridded realisations of these prior models for the compressibility, shear compliance and density contrast are shown in the top panel of Figure 5.4. After the Bayesian update we have the posterior probability density function, from which we pick the maximum that is the nearest to the unconstrained inversion result (MLE), for compressibility, shear compliance and density contrasts. These results are shown in bottom panel of Figure 5.4.

It is evident from the posterior inversion result that the prior information significantly improves the continuity that is lacking in the unconstrained inversion results and also improves the resolution. But because the reservoir layer is absent in the prior model, we do not expect to find a significant improvement in the resolution of the reservoir layer in the MAP estimate.

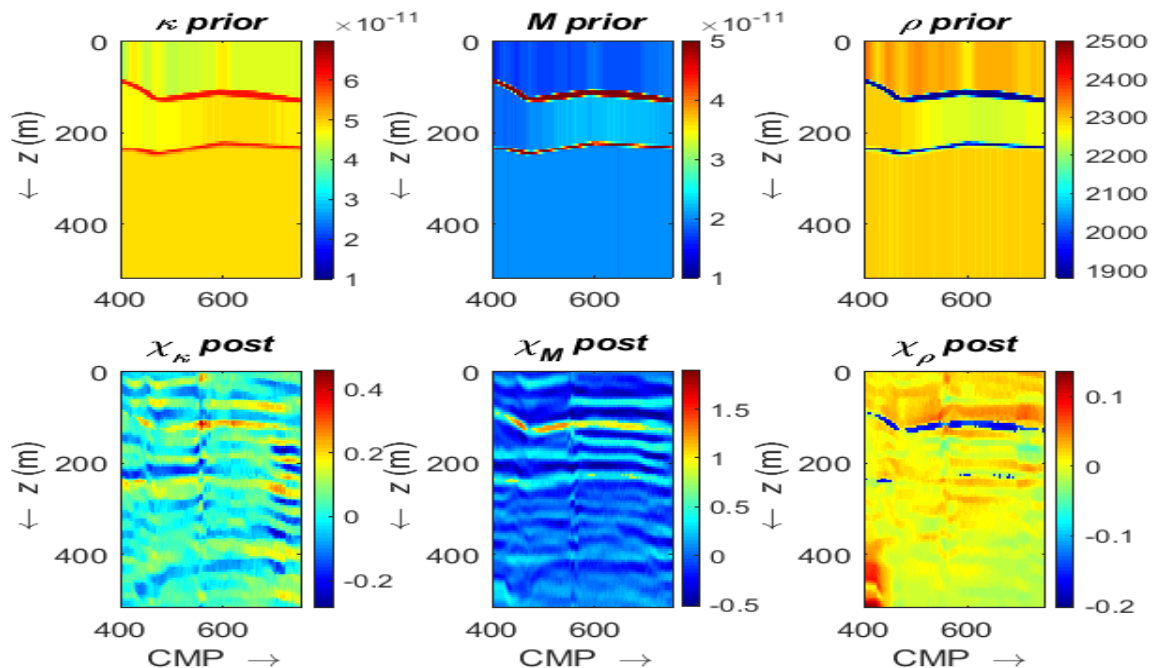*Figure 5.4: (Top row) Mean of translated prior model for Scenario 1. Layer 5 that represents the reservoir layer has 0 m thickness so it is not visible in the mean of the translated prior model. (Bottom row) Posterior estimate of elastic properties for Scenario 1. It is a big improvement over the unconstrained inversion results (MLE Figure 5.2), with much better lateral continuity and a better resolution of the coal seams.*

5.4.2 Scenario 2

In the next Scenario a mean thickness of 35 m is assigned to the reservoir layer, which represents the true mean thickness of the reservoir layer for the section we are considering. It is evident from the top panel of Figure 5.5 that in the mean of the ensemble of gridded realisations, the reservoir layer is present and is quite close to its true thickness. The unconstrained inversion results are, of course, the same. The posterior estimates shown in the bottom panel of Figure 5.5 now show a significant improvement over the unconstrained inversion result, but not very different from the posterior estimate of Scenario 1, except that we are able to resolve some aspects of the reservoir layer.
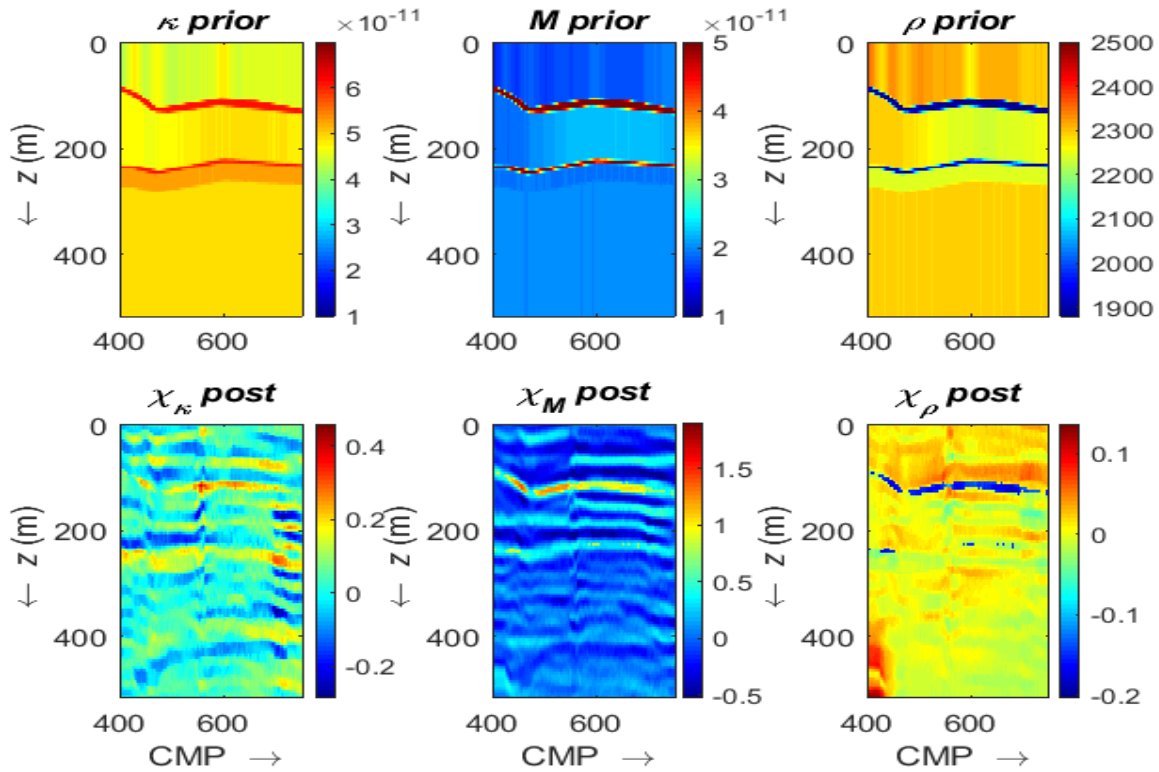

Figure 5.5: (Top row) Mean of the grid-based version of the prior model for Scenario 2. Layer 5, which represents the reservoir layer, has 35m thickness and is very clearly visible in the mean of the grid-based prior model. (Bottom row) Posterior estimate of elastic properties for the Scenario 2. It is a big improvement over the unconstrained inversion results (MLE, Figure 5.2), with much better lateral continuity and a better resolution of the coal seams and also a vague hint of the reservoir layer.

5.4.3 Scenario 3

In Scenario 3 mean thickness of 70 m is assigned to the reservoir layer. It can be seen from the top panel of Figure 5.6 that in the mean of the ensemble of gridded realisations, the reservoir layer is present and is much thicker than in the Scenarios 1 and 2. The unconstrained inversion results are, of course, the same. The posterior estimates shown in bottom panel of Figure 5.6 now shows a significant

improvement over the unconstrained inversion result, but not very different from posterior estimate of Scenarios 1 and 2.
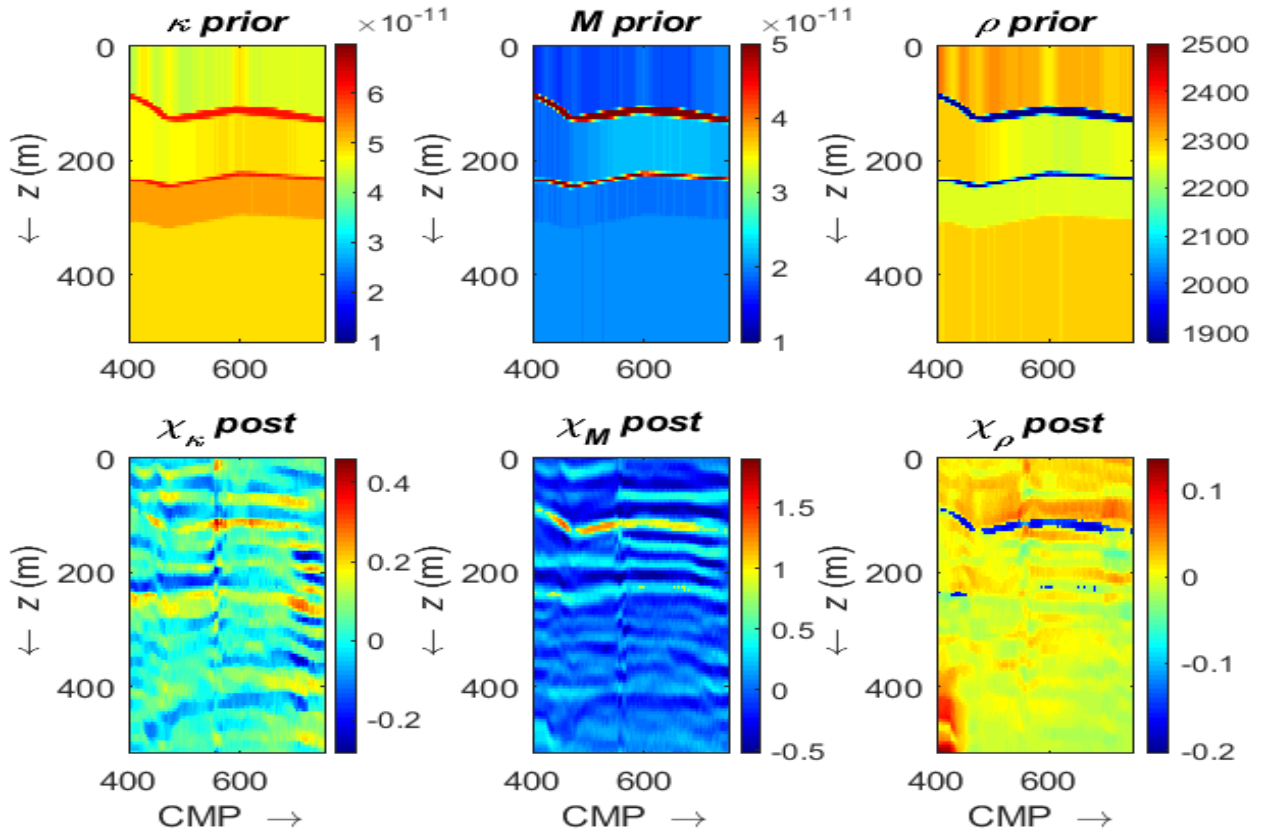

Figure 5.6: (Top row) Mean of grid-based prior model for Scenario 3. Layer 5, which represents the reservoir layer, has 70 m thickness, so it is much more thicker than the mean of the grid-based prior model of Scenario 2 . (Bottom row) Posterior estimate of the elastic properties for Scenario 3. It is a big improvement over the unconstrained inversion results (MLE, Figure 5.2), with much better lateral continuity and a better resolution of the coal seams but not much different from the results of Scenarios 1 and 2.

5.4.4 Scenario Probabilities

We have shown in the previous section that having a large variability in the mean of the thickness distribution of the reservoir layer for different scenarios does not mean that there will be a significant difference in the posterior estimates. This may be due to the fact that the prior probability distribution are very similar for all three scenarios. The question now arises which scenario best fits the data. To answer that question we have to analyse the scenario probabilities for all three scenarios. The scenario probability is calculated by evaluating equation 5.3, discussed in detail in the previous section. These scenario probabilities are shown in Figure 5.7. We can see from Figure 5.7 that the scenario probability estimate for Scenario 2, which represents the presence of a reservoir layer having the mean thickness of 35 m, is higher than scenario probabilities for the other two scenarios. The average

thickness of the reservoir layer is 38 m along this section and the scenario probabilities confirm that all along the section Scenario 2 is more probable compared to other two scenarios. There are some instances along the section where the Scenario 2 has lower probability than Scenarios 1 and 3, which can be explained by analysing the WEB-AVP inversion result (Figure 5.2). At these locations the reservoir layer was not resolved properly.
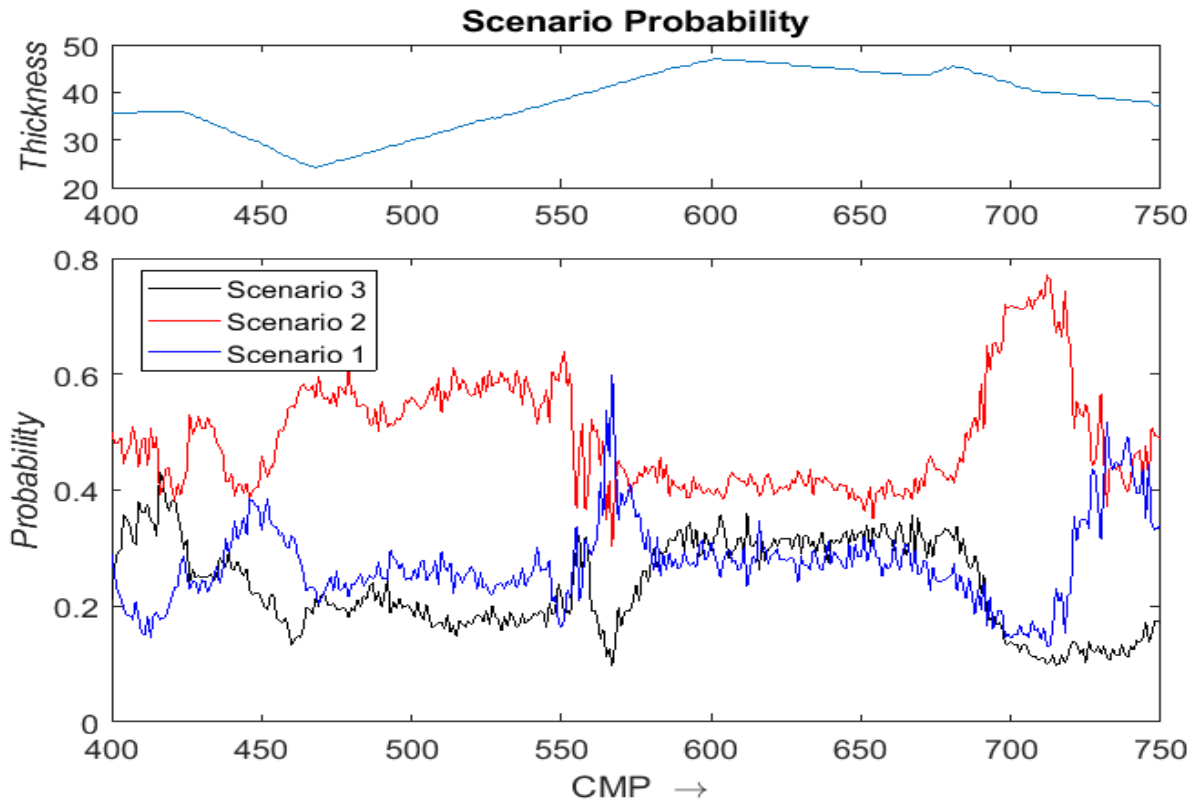

Figure 5.7: Scenario probability for all different scenarios. (Top panel) The true thickness along the section is shown which has a mean value of 38m. (Bottom panel) The relative scenario probabilities of the scenarios. Scenario 2 with 35 m thickness has the highest probability along the section except at some locations which can be attributed to the presence of a new coal seam around CMP 550.

5.5 Conclusion

In the present study it is shown that using geological prior information in seismic AVP inversion not only provides a better starting model, but also leads to more laterally continuous posterior predictions. In addition, it provides an integrated framework to build different scenarios based on the information available prior to the inversion. These scenarios, in the form of grid-based prior distributions, can be used, in conjunction with the likelihood estimate obtained from unconstrained WEB-AVP inversion using Bayes rule, to yield the probability of the data, given the scenario. These probabilities of the data, given the scenarios can easily be renormalised to provide the probability of the scenarios, given the data.

Chapter 5

71

Chapter 6
Field Data Example

Chapter 6

6.1 Introduction

In the previous chapters we have developed a Bayesian methodology for honouring geological prior information in a reservoir-oriented WEB-AVP inversion. The methodology provides a simple but very efficient way of including a parametric layer model derived from petrophysical and geological information (blocking of well logs and regional geological information) into a grid-based WEB-AVP inversion. In Chapter 4 and Chapter 5 the methodology was illustrated with the help of a very detailed geological model based on outcrops from the Book Cliffs (Utah, USA). The results showed an improvement over unconstrained WEB-AVP inversions, by bringing in lateral continuity, more detailed starting models and considerable improvement in the resolution of thin layers. A new scheme for quantifying the probability of different prior model scenarios was also developed in Chapter 5, which provided a probabilistic comparison of different scenarios. In the present chapter, the methodology will be illustrated on real data provided by the E&P company OMV (Vienna, Austria).

6.2 Data and Pre-Processing

The data was Pre-Stack-Depth-Migrated (PSDM) to create migrated image gathers in depth and subsequently the migration velocities were used to convert the gathers in time domain. These image gathers in time were put at our disposal, to be used as input to the WEB-AVP inversion. The full suite of logged data such as P-sonic , S-sonic, density log, gamma ray, resistivity log, neutron log for a single well in the survey area were also provided. The logged data is used for three different purposes: to calibrate the seismic and extract the wavelet from seismic-to-well match, to extract a low wavenumber background model for the inversion from the logged properties, and to build prior model scenarios. In this study we follow the de-migration procedure, where the migrated image gathers over a target window, are converted (de-migrated) to τ/p gathers that represent the time-domain plane-wave response acquired at the top of the local 1D target interval using ray tracing. This will be the input for the reservoir oriented WEB-AVP inversion. In the pre-processing step the target interval (Figure 6.1) was identified on the PSDM image gathers. This data is still referenced to surface offsets. The surface offsets are converted to ray-parameters (horizontal slowness) of plane waves incident on the target interval, by ray-tracing through a locally stratified overburden. Subsequently, the image gathers as a function of ray parameters are de-migrated to the τ/p domain, by assigning ray-parameter dependent two-way travel-times to the migrated samples in vertical two-way travel-time. For this data-set there were 10 ray-parameters chosen, such that the smallest and largest ray-parameters are associated with surface offsets fully contained within the real surface offsets. However, in this dataset the usable ray-parameter range was very small and the average angle on the inner trace is 18°, whereas the average angle on the outer trace was only 21.5°, so that there is very little angle

Field Data Example

variation in the de-migrated gathers. The final data is shown in Figure 6.2. Given the fact that only a very narrow range of ray-parameters was selected, there is very little elliptic move-out visible on the de-migrated gathers.
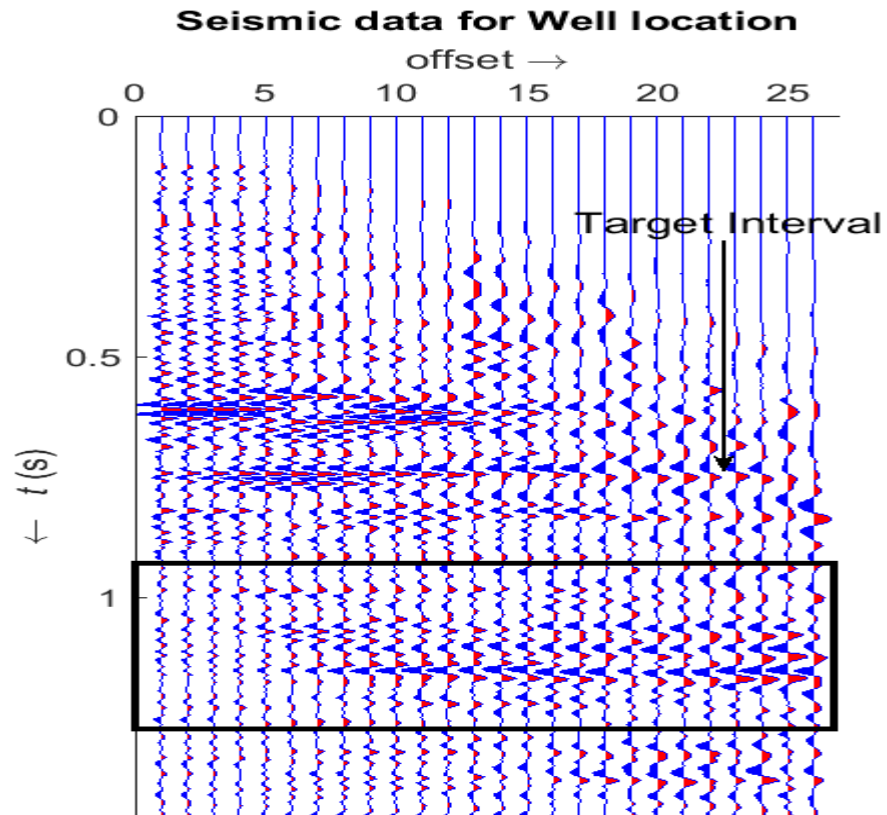

Figure 6.1: PSDM image gathers for the well location in the time domain with the target interval shown in the box. The data from the surface is de-migrated to the top of the target interval using ray tracing.
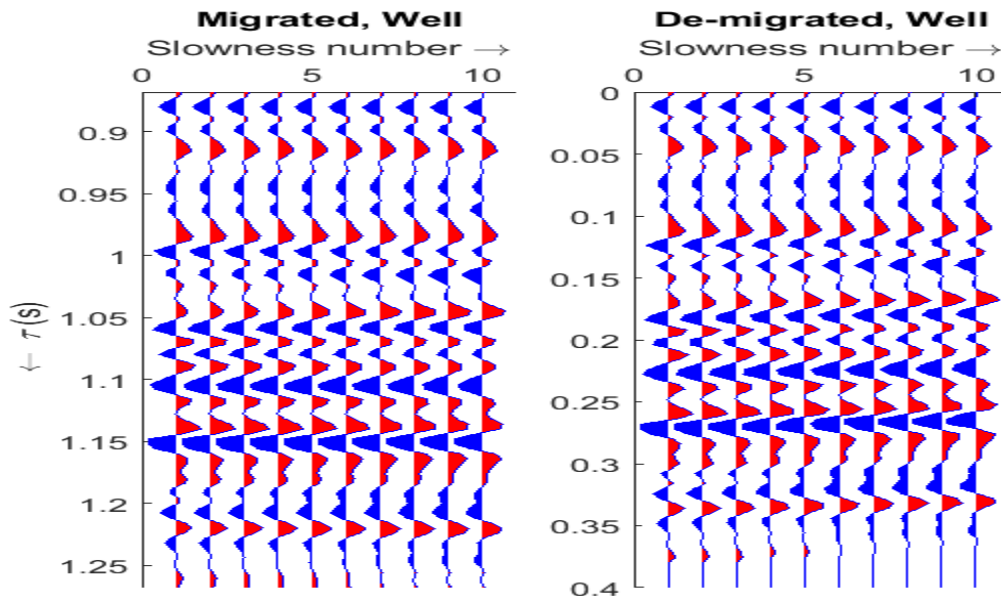
Figure 6.2: A gather for a CMP location close to the well location (left) before and (right) after de-migration. There is not much elliptic move-out in the de-migrated data because the angle range considered was very small.

6.3 Wavelet Extraction

Inversion is a feed-back loop of forward modelling and back-projection of the error. In WEB-AVP the forward modelling is based on the integral representation of the full elastic wave-equation (see Chapter 2). It requires a wavelet for calculating the synthetic data. Wavelet estimation and calibration of data to account for the transmission effect of the overburden is based on matching the real data gather at the well location to the well synthetic gather. As the well logs corresponding to V_p, V_s and ρ were also provided, we made use of them to forward-model broadband 0-5-90-100 Hz synthetic data. For generating the synthetic data, the Kennett algorithm (Kennett, 2009), which is also an exact method in a heterogeneous elastic layered medium, is used. A wavelet is estimated by least-squares matching of the broadband synthetics and the de-migrated data at the well location. In Figure 6.3, the broadband synthetics and the seismic data, both in the de-migrated domain, are shown. The matched synthetics, where the wavelet extracted from the match was applied to the broad-band synthetic, shows the match that has been obtained. The seismic-to-well match was carried out for all ray-parameters (horizontal slowness) in the data individually, resulting in ray-parameter dependent wavelets. The wavelets are shown in Figure 6.4. It can be seen that the wavelets looks quite acceptable, but they contain some ringing effects, which apparently were introduced into the data by propagation through the overburden and are captured in the wavelets.

Field Data Example
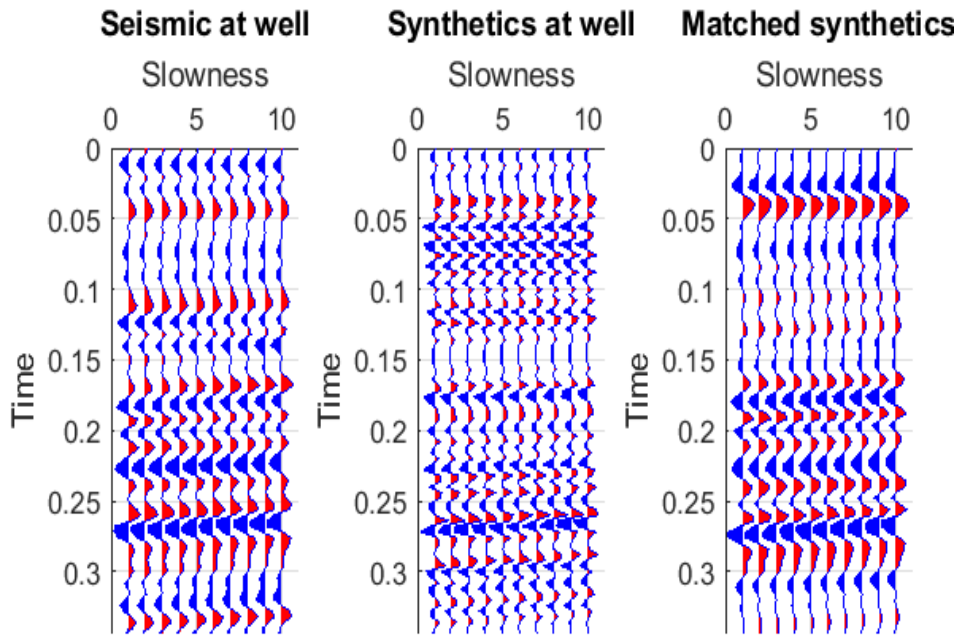
Figure 6.3: Left: Seismic at the well. The de-migrated data on the top of the target interval. Middle: Synthetics at the well. Broadband synthetics from Kennett modelling using the well log. Right: Matched Synthetics at the well, by least-squares matching the broadband synthetics with the de-migrated data.
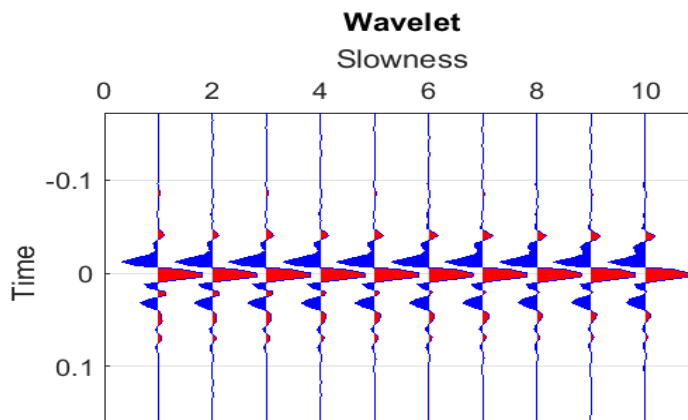
Figure 6.4: Angle dependent wavelets as a result of the seismic-to-well match. The wavelets look quite acceptable, but contain some ringing effects, which apparently was introduced into the data in the overburden and is captured here.

6.4 WEB-AVP Inversion

After data preparation and wavelet extraction, we are almost ready to carry out the inversion, but first the background model for κ, M and ρ need to be extracted from the well logs. The background models are used to calculate the Green's functions and the incident wave-fields. The well logs are smoothed as if they are going to be resampled to the seismic inversion grid, which in this case is 3 m.

However, after smoothing the logs are not resampled but kept at their original sampling in order to keep the Kennett method accurate, which is based on property differencing. The backgrounds are created by severe smoothing of the well logs, equivalent to a 4 Hz low-pass filter (red curve in Figure 6.5). The properties κ and M are calculated from V_p, V_s and ρ according to equations (2.4) and (2.5).

Figure 6.5: Since the inversion is carried out on a 3m grid we apply high-cut filter to the logged data to allow for a fair comparison. The red curves are background models which are very smooth versions of the black curves.
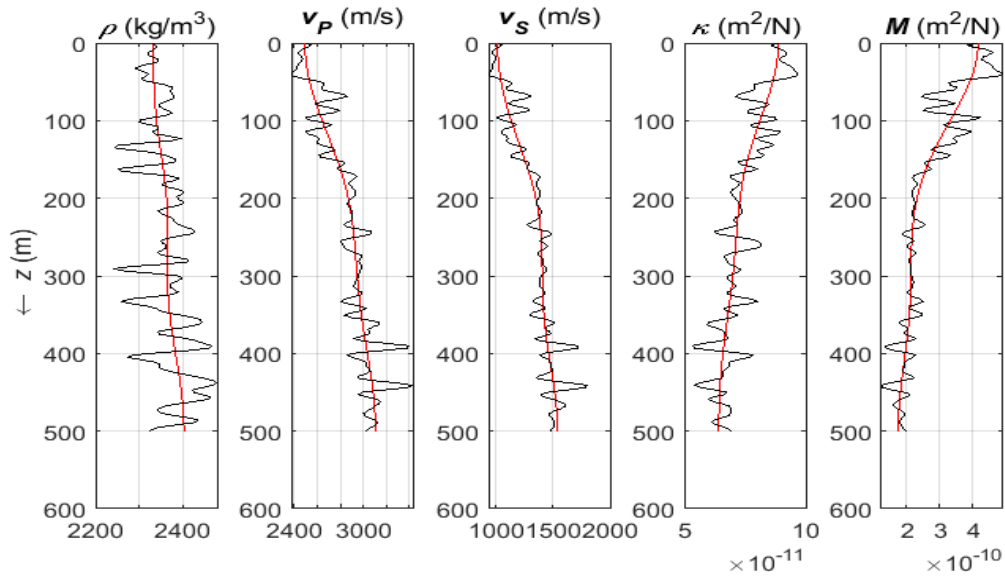
The WEB-AVP inverts for the property contrast for κ, M and ρ against the backgrounds, shown in Figure 6.6.
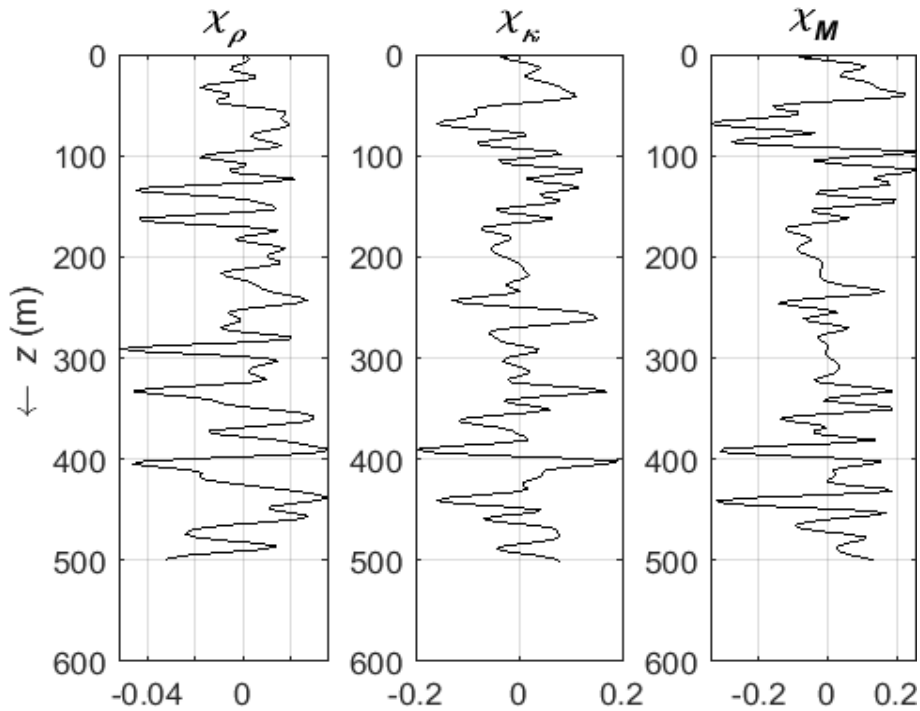
Figure 6.6: The property contrast χ_κ, χ_M and χ_ρ against their backgrounds, as calculated from the well logs. The WEB-AVP inversion inverts for the property contrasts against the background.

6.4.1 WEB-AVP with Background Model

Initially we carry out the inversion with only the smooth background models as a starting point. As a benchmark we first invert the matched synthetics, using the wavelet that was extracted from the seismic-to-well match. The result is shown in Figure 6.7.

We get a good result for χ_κ and a rather poor result for χ_M. Because of the narrow angle range in the data we did not attempt to invert for χ_ρ, which was left equal to zero. The fact that χ_M was poorly resolved from the synthetic data with only 3% noise, can be understood when we look at the contributions to the synthetic data made by χ_κ, χ_M and χ_ρ in case we use the true properties for the synthetic data. This is shown in Figure 6.8, where it can be seen that in this example the synthetic data is almost exclusively determined by the κ contrast.
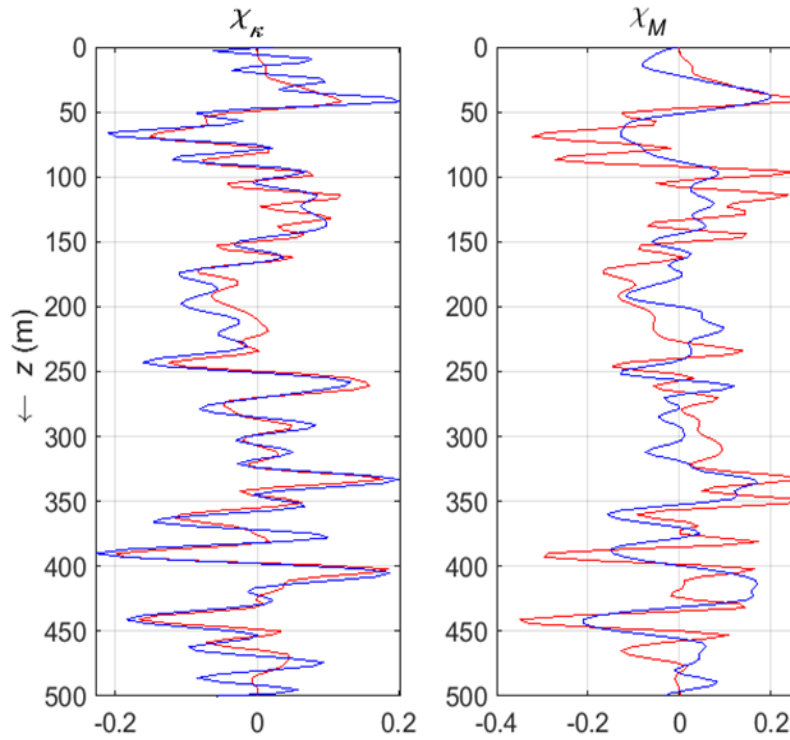
Figure 6.7: Results from the inversion of the matched synthetic data, for compressibility contrast (left) and shear compliance contrast (right). Red is true property contrast and blue is inverted property contrast. This serves as the benchmark for the subsequent inversion.
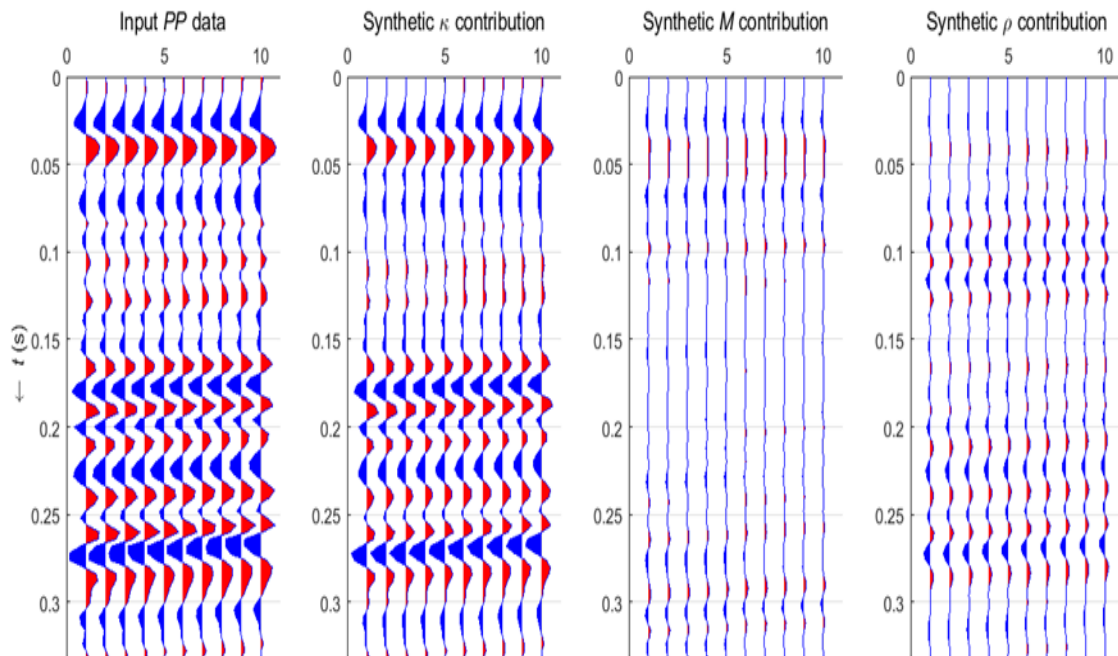
Figure 6.8: Synthetic contributions made by χ_κ, χ_M and χ_ρ to the synthetic data. The contribution from χ_M and χ_ρ is negligible compared to χ_κ.

Field Data Example

The results for the inversion of the real data gathers at the well location are shown in Figure 6.9. Inversion of the real data gives a relatively good estimate for κ and a poor result for M, in line with the synthetic benchmark.
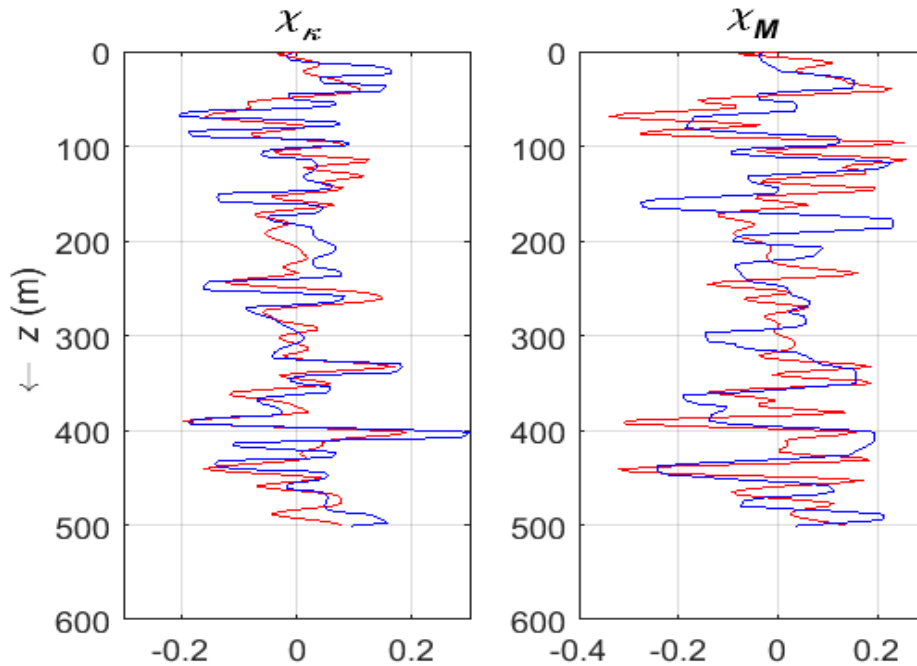
Figure 6.9: The WEB-AVP inversion for compressibility contrast χ_κ (left), and shear compliance contrast χ_M (right) without using any prior information.

6.5 Scenario Building from Well logs

For the building of a prior model we go back to the full suite of unsmoothed well-logs that were provided (Figure 6.10). From these logs a seven-layer prior model was built. The property distribution for each layer was extracted from the well-logs by fitting Gaussian distributions to the original unsmoothed data within a layer, giving us means and standard deviation $\boldsymbol{\mu}_p$ and $\boldsymbol{\sigma}_p$ respectively, where p is any property. The thickness distributions are also assigned Gaussian distributions, with means $\boldsymbol{\mu}_D$ and standard deviation $\boldsymbol{\sigma}_D$ obtained by blocking the well logs. The thickness distribution should reflect the geological understanding of the environment of deposition.
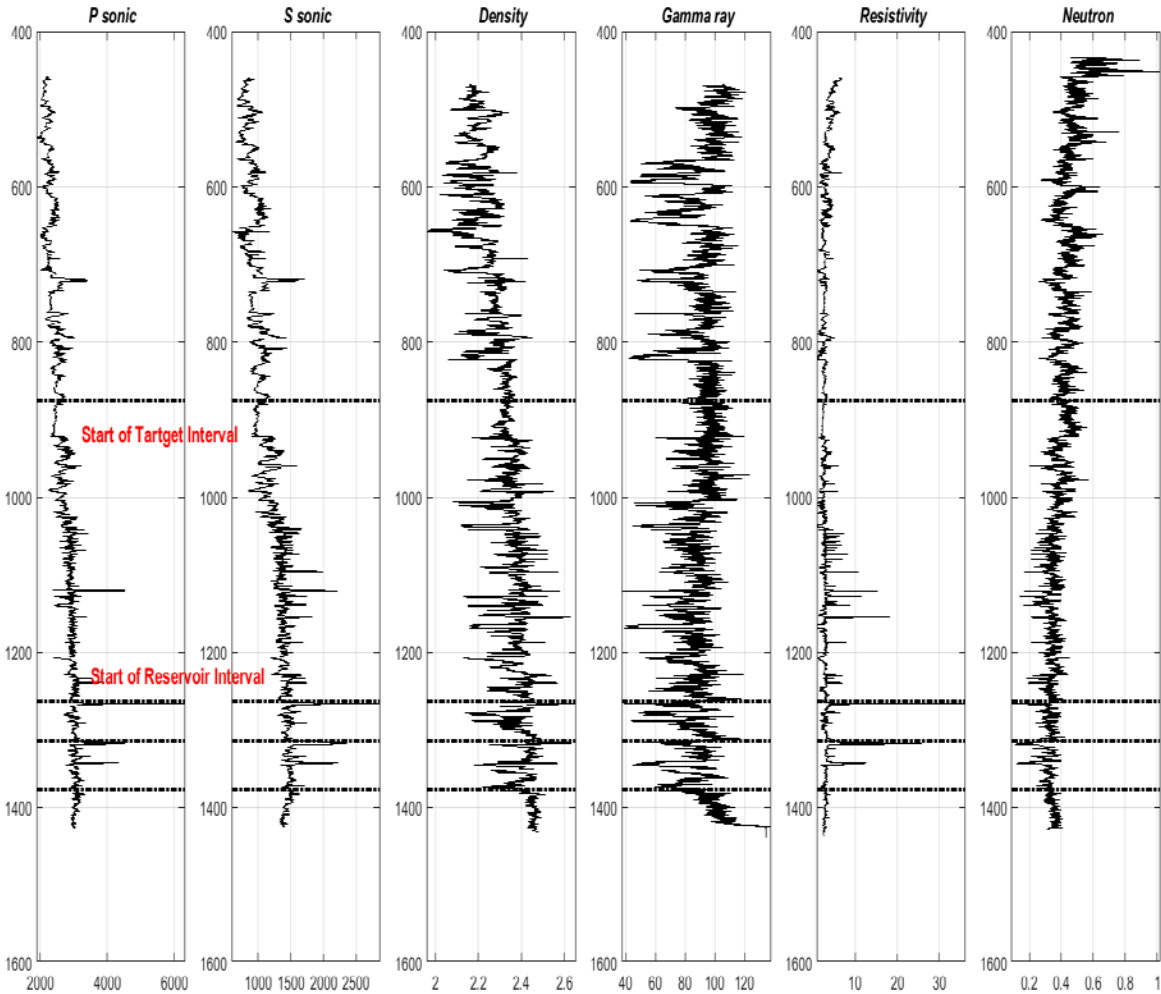
Figure 6.10: The whole suite of logged data with the target interval and the reservoir being highlighted. This logging data is used to infer the scenarios used in the next section.

A layer model built with the mean values for all layer parameters is shown in Figure 6.11 (blue curves). After transforming the layer-based distributions to grid-based distributions, we can calculate the mean values for all gridded properties. This is also shown in Figure 6.11 (black curve). Although it is hard to visualize, all parameters, layer-based as well as grid-based, have distributions functions associated with them. For the layer-based properties these distributions are Gaussian, and truncated Gaussian for the layer thicknesses; for the grid-based properties these distributions are Gaussian mixtures, with weights determined from the layer-based truncated Gaussian layer thickness distributions.

6.5.1 WEB-AVP inversion with starting model from Scenario 1

In this experiment we only use the prior information as starting model for the WEB-AVP inversion and we do not perform Bayesian updates. This starting model contains more prior information than the background model that is otherwise used as starting model. The starting model is the mean of the grid-

based prior parameter distribution built in the previous section and shown in Figure 6.11 (black curve). The inversion results for this experiment are shown in Figure 6.12. The results does not show much improvement over the initial results with the smooth background only as starting model, except that it stabilises the overshooting to some extent. The reason the WEB-AVP result is not very sensitive to the starting model is that WEB-AVP loses the effect of the starting model in subsequent outer loop iterations (Figure 2.1) and is known to be robust against local minima.
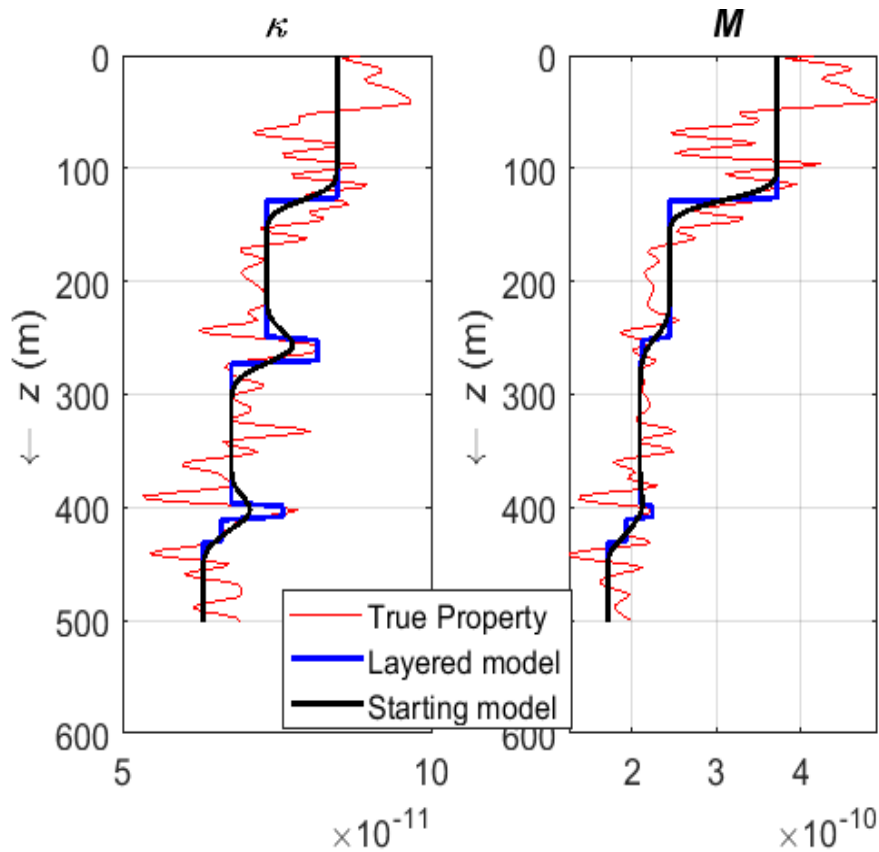
Figure 6.11: A seven-layer scenario inferred from logging data for the compressibility κ (left) and shear compliance M (right). The true model is shown in red, the mean of the layer-based interpretation is shown in blue and the mean of the grid-based model is shown in black.
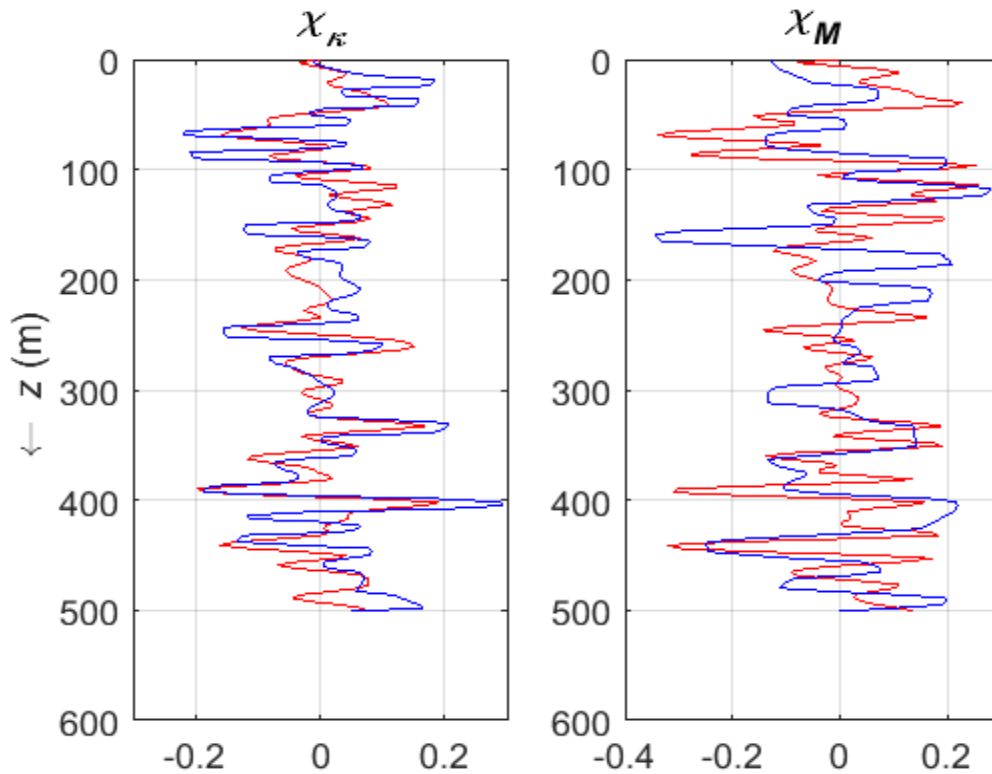
Figure 6.12: The WEB-AVP inversion for the compressibility contrast χ_κ (left), and the shear compliance contrast χ_M (right) using the mean of the scenario as the starting model for the inversion. The true properties are shown in red and inverted properties are shown in blue.

6.5.2 WEB-AVP inversion with MAP updates

In the third experiment we want to update the maximum likelihood estimate (MLE), after every outer loop iteration (Figure 2.1), to a maximum a posteriori (MAP) estimate by making use of the prior distributions. In this experiment we again use the grid-based mean of the properties as starting model for the inversion. The results are a big improvement over the earlier experiments, as shown in Figure 6.13. The reservoir is fully resolved in κ, while in M it is much better than from earlier experiments. The posterior update steers the inversion results towards the prior distribution while ensuring that seismic data is also explained properly. There is a trade-off parameter, for which we use the residual energy of the MLE estimate, which is determined by the amount of faith we have in either the MLE, or the prior scenario. This parameter was set in such a way that for the well determined parameter κ we do not see much influence from the prior in the final result, but for the relatively poorly determined parameter M, we clearly see the blocky nature of the model come through.
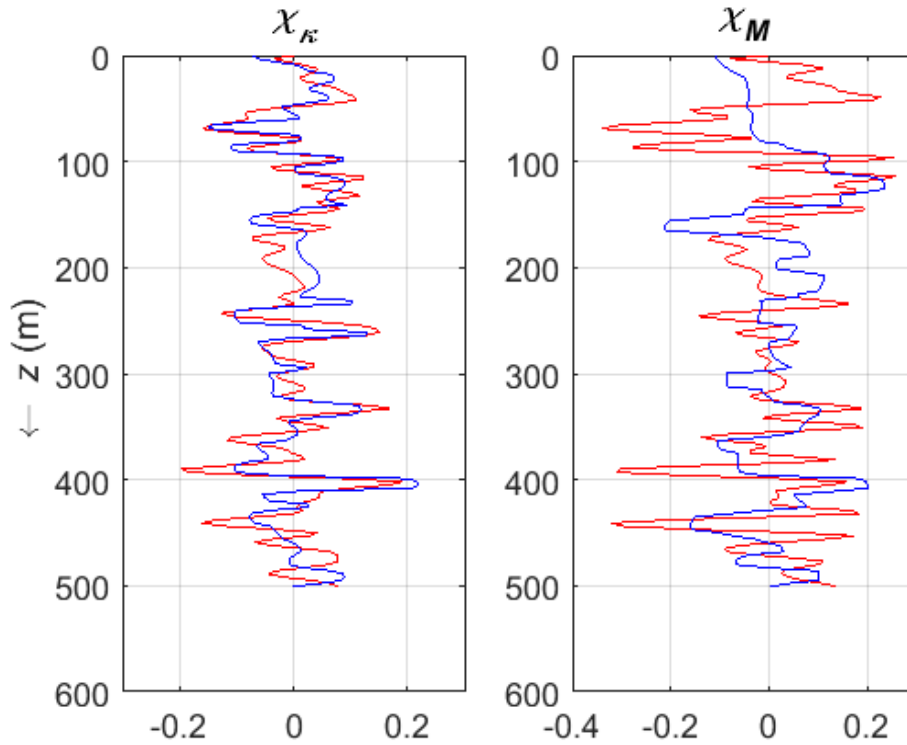
Figure 6.13 The MAP estimate for the compressibility contrast χ_κ,(left) and the shear compliance contrast χ_M (right) using scenario as prior information to update the WEB-AVP inversion result after every outer loop iteration. The result shows a big improvement over the previous two experiments. The true properties are shown in red and inverted properties are shown in blue.

6.6 Scenario Testing

In this section two different prior scenarios are built, which will only differ in the presence or absence of the reservoir layer and we are going to assign probabilities to these scenarios based on the WEB-AVP likelihood function results together with the grid-based prior distributions. The scenario probability is then calculated from the probability of the data obtained from the sampling method described (equation (5.3)) in Chapter 5.

In Figure 6.14 the layer based realisation of all mean values for two different scenarios are shown, which differ in the presence of the reservoir layer (layer 5). Scenario 1 contains seven layers with layer 5 being the reservoir, whereas in Scenario 2 the reservoir layer is absent, making it a six layer model. The probabilities of these scenarios are quantified from the MLE inversion result shown in Figure 6.14 by calculating the two probabilities of the data given by equation (5.3) for both scenarios and then re-normalizing them to add up to 1. The probability of Scenario 1 is 0.52 whereas for Scenario 2 it comes out to be 0.48, which suggests that the scenario containing the reservoir layer is slightly more probable than the one without. A source of inaccuracy is the sampling of the model spaces to calculate the probability of the data (equation (5.3)) as there is repetition of model realisations and it is expected that these predictions can be made more robust by better sampling of the model space using Monte

Carlo methods such as Monte Carlo Markov Chain (MCMC) (Mosegaard and Tarantola, 1995; Sen and Stoffa, 1995; Maliverno, 2000, 2002).
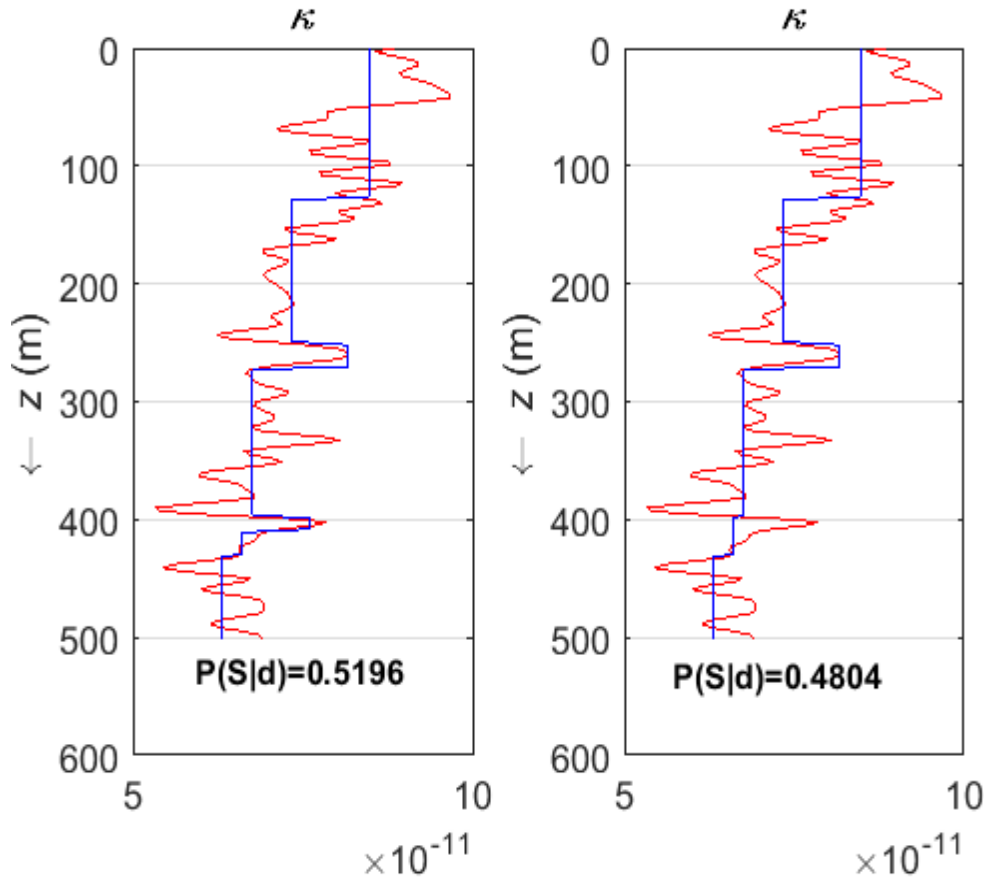
Figure 6.14: The scenario probability for two scenarios with 7 and 6 layers. Scenario 1 (7 layers, left) contains the reservoir layer, whereas Scenario 2 (6 layers, right) does not.

6.7 Conclusion

In the present study it is shown how to incorporate geological prior knowledge into the WEB-AVP for a field data example. Even though we did not have a particularly good seismic-to-well match and the usable ray-parameter was very small, the WEB-AVP inversion still provided a reasonable estimate, at least for κ. It was also demonstrated that for the shear compliance M a good result should not be expected, even when inverting synthetic data based on the true properties. After bringing in prior knowledge in the form of a seven-layer prior model scenario, the MAP estimate from the field data showed a significant improvement over the MLE inversion result. Scenario testing was also demonstrated with two scenarios which only differ in the presence, or absence of the reservoir layer. The probability of scenario, given the data, shows a marginally higher probability for the scenario that contains the reservoir layer compared to the other scenario that does not contain the reservoir layer. It is expected that this narrow margin can be widened by using better sampling techniques for the calculation of the probability of the data.

Chapter 7

Conclusions and

Recommendations

Chapter 7

7.1 Conclusions

In Chapter 2 of this thesis, a recently developed methodology for reservoir-oriented full waveform inversion (Gisolf and van den Berg, 2010a; Gisolf and van den Berg, 2010b) was introduced and illustrated by its application to a three-layer wedge model. The method is a full elastic wave-equation based pre-stack amplitude vs. offset (AVO) inversion, or rather amplitude versus ray-parameter (WEB-AVP) inversion, in which the 1.5D full elastic wave-equation is solved locally, in conjunction with inverting for density ρ, the elastic parameters compressibility κ and shear-compliance M, or their inverses: the bulk modulus K and the shear modulus μ. The methodology has proved to yield good quantitative results on both synthetic and field data. This method accounts for the entire complex wave-propagation field over the target interval, including local internal multiples (peg-legging), transmission effects and multiple mode-conversions. For this reason we have adopted this inversion method to see what prior geological knowledge can still add to this state-of-the-art method. Like any other full waveform scheme, WEB-AVP inversion suffers from the problem of non-uniqueness of the solution meaning that many models can describe the same data. This problem has been addressed in the past, mostly using regularisation methods. We summarise the advantages of WEB-AVP inversion over conventional reflectivity-based inversion methods as follows:

- Due to the non-linear character of the relationship between the data to be inverted and the parameters to invert for, quantitative broadband properties can be estimated from band-limited seismic data.

- Therefore, the WEB-AVP inversion has the ability to resolve subsurface features that cannot be resolved by linear inversion schemes.

- Non-linear effects like multiple scattering, transmission effects, multiple mode-conversions and travel-time differences between the background medium and the real medium are fully taken into account.

- The target-oriented character of the inversion, together with an efficient iterative solutions of the non-linear inversion scheme, reduces the computational demand and make it a feasible alternative for conventional AVO inversion.

Having adopted WEB-AVP as our inversion technology of choice, we investigate the use of geological prior information scenarios, derived from well logs and regional geological information before the inversion is carried out, to reduce the null-space of the inversion and increase further the power to resolve thin layers. The geological prior information considered in this thesis consists of layer interpretations of the target interval of the Earth's subsurface where different lithologies or facies are stacked on top of each other. This interpretation is made on well logs, using regional geology and taking the assumed environment of deposition into account. The basic premise of the work was not to constrain the inversion process on the basis of a parametric model but to use geological scenarios to

Conclusions and Recommendations

update the model-free inversion result on a regular subsurface grid in the Bayesian sense. Bayes' rule provides a simple framework to update the probability of a model from prior to posterior, when data becomes available. In this thesis, geological prior models with uncertainties, called scenarios, are considered hypotheses describing the subsurface in terms of a layer model that can be updated to more realistic grid-based model distributions, when new data becomes available in the form of seismic inversion results.

In the Chapter 3, a Bayesian formulation for updating the WEB-AVP inversion results with the help of geological prior scenarios was presented. The methodology starts with a parametric layer model interpreted from well logs with layers properties having been assigned Gaussian distributions and truncated Gaussian distributions for the layer thicknesses. The parametric layer model represents the prior knowledge that is going to be updated by the WEB-AVP inversion results. Since the prior information is in parametric layer form and the inversion result is on a regular depth grid, we first have to translate the prior model from layer parameters to gridded properties. The whole procedure can be summarised as follows:

- Prior information in the form of Gaussian distributions for layers properties is translated into highly non-Gaussian grid-based prior distributions, analytically represented by Gaussian mixtures.
- The weights for the Gaussian mixtures model are obtained from an ensemble of blocky property realisations in depth, drawn from the prior layer parameter distributions. For every grid point we count the number of times it is found in a certain layer.
- From the unconstrained seismic inversion a Gaussian likelihood function can be created, also analytically. The mean of this Gaussian is the actual solution vector in grid-space and the standard deviation is constructed from the Hessian of the inversion problem and the residual energy after the current outer loop iteration. This unconstrained inversion result is termed the maximum likelihood estimate (MLE).
- The Bayesian posterior is the product of the Gaussian likelihood functions and the highly non-Gaussian, multimodal grid-based prior in analytic form. The multi-variate posterior distribution can be optimized to find the maximum nearest to unconstrained seismic inversion result (MLE). This new estimate is termed the maximum a posteriori estimate (MAP). To start the search for the MAP estimate from the MLE is a choice that expresses the belief that the unconstrained seismic inversion result will always be a good guess that only needs minor adjustment to become better.
- The point-wise uncertainty around the MAP estimate can also be determined by calculating the second derivative of the posterior analytically.

Chapter 7

Obviously, there will be ambiguity in the construction of prior model scenarios from the geological and petrophysical data available. There could be different concepts that a priori seem equally likely. We can assign probabilities to different scenarios by calculating the probability of data for a given scenario. This was presented in Chapter 5. Equation 5.3 is used to approximate the denominator in equation 3.1. The denominator provides an estimate of the overlap between the likelihood function and the prior distributions and can be approximated by sampling an ensemble of grid-based models from the Gaussian likelihood function and calculate prior probability density for all models in the ensemble and sum all of them up. When a number of different scenarios is available, the probability of the data, given the scenario, can be re-normalised to give the probability of the scenario, given the data. The calculation of the scenario probability can be summarised as follows:

- The denominator in equation 3.1 can be approximated by creating an ensemble of grid-based models drawn from the Gaussian likelihood function over the gridded model space.
- When different scenarios are available, the different probabilities of the data, given the scenario, can be re-normalised to give the probability of the scenario, given the data.
- The MAP estimate with associated uncertainty estimate can also be calculated for all scenarios.

In the Chapters 4 and 5, the methodology was demonstrated for a very realistic, detailed geological model based on the Book Cliffs, (Utah, USA) outcrops. The Bayesian methodology was demonstrated on the full model which is 52 km long with 2099 equally spaced lateral locations. The geological scenario was built by selecting three locations as well-logs, of which the true properties were derived for each of the seven layers. Also seismic horizons were used to guide the interpolation of this layer-model between the wells. For the purpose of scenario testing in chapter 5, part of the full model is used with only two well logs on either side of this model, with three different interpretations in terms of the mean value of the thickness distribution of the layers. The results are shown in the respective chapters but the summarising conclusions are as follows:

- The geological scenarios provide a choice for starting model, which contains more prior information than is present in the previously used smooth background models.
- The Bayesian update of unconstrained WEB-AVP inversion provides a better resolution for some layers that were not fully resolved using seismic data only.
- The MAP estimate has better lateral continuity than the MLE, which can be attributed to the lateral continuity present in the prior model.
- When using different scenarios the MAP estimate does not show a significant difference for the different scenarios which is due to the fact that the Bayesian update always favours the seismic data more than the prior.

- The probability of a scenario, given the data, provides a simple framework for comparing a number of equally likely *a-priori* scenarios.

In Chapter 6, the methodology was demonstrated on a field dataset provided by OMV. The full suite of logging data were also provided, which were used to build two different scenarios differing only in the presence and absence of the reservoir layer. These scenarios were used to carry out three different experiments. Firstly, to use the mean of an ensemble of grid-based realisations as starting model for the inversion. In the second experiment, the MLE from the WEB-AVP inversion is updated to the MAP estimate using the prior model information. In the last experiment, we quantified the probability of both scenarios, given the data. By data in this case we mean the unconstrained seismic inversion result, from which a likelihood function could be constructed. The final conclusions for Chapter 6 are summarised below:

- The unconstrained WEB-AVP inversion provided a good estimate of the compressibility κ but a lesser estimate of the shear compliance M. This might be due to the fact that the angle range considered in the data was very small and the low contrasts in M gave an almost negligible contribution to the data.
- When using the mean of the grid-based prior distributions as the starting model, the result did not improve significantly, because the effect of the starting model is to a large extent lost during the subsequent outer loop iterations.
- The update to the MAP after every outer loop iteration steers the inversion results towards the prior when the uncertainty in the MLE is large. Conversely, if the MLE has a low uncertainty, the MAP stays very close to the MLE.
- The reservoir layer, which is almost beyond seismic resolution, was better resolved after the MAP updates.
- The scenario testing estimated a marginally higher probability for the prior scenario with the reservoir layer than for the one without.

7.2 Recommendations

7.2.1 Geological Modelling

During this study we make a big leap towards incorporating geological knowledge in seismic full-waveform inversion. Geological information is an abstract word for the interpretation made by geologists on the basis of a detailed analysis of data from different sources, such as well logs, cores or seismic interpretation, available to them. The interpretation always has geological reasoning behind it in terms of the regional geology, the environment of deposition and other parameters that might have influenced the depositional patterns and architecture of the basin. This information has a very high

Chapter 7

dimensionality in terms of parameters controlling the geological process, and depending on the scale at which the interpretation is made, it may take a large amount of computational power to carry out forward modelling and inversion in that environment. To use prior geological information in conjunction with seismic inversion, we have to up-scale the Earth model so that it can be parametrized by a number of stratified units that are stacked on top of each other. But in order to accommodate the maximum amount of variability in the subsurface without making the integration with seismic data very complicated, layer-based modelling proves to be very useful and generally compatible with stratigraphic interpretations. While constructing layer-based models as prior models for seismic inversions, some points should be kept in mind:

- The number of layer (N_L) for a scenario is the most important parameter. It gives a blocky representation of the subsurface in terms of interfaces separating different lithologies and facies. This number of layers should be chosen in such a way that the interfaces it represents should be visible on both well logs and seismic data. We should try to use as few as possible layers in prior modelling, because we want to explain the seismic data through inversion and use prior information only to guide the inversion and not to override information coming from seismic data with prior information.

- The thickness distributions are described as truncated Gaussian distributions, where the part of the Gaussian curve extending over the negative thicknesses represents the probability that the layer is absent. While we could easily estimate those distributions at well locations, we could use the amplitude information from seismic data to estimate the means of these distributions away from the wells, because for thin reservoirs in the tuning range the amplitude of a reflector is directly proportional to the thickness of the layer it represents.

- The mapping of the layer-based model space to a grid-based model space is carried out by means of creating an ensemble of model realisations by sampling from thickness distributions and counting the number of times a particular layer is present on a single grid point and then normalising it for every grid point to get the weight matrix for the Gaussian mixture model. Depending on the size of the ensemble this procedure gives an approximate estimate of the weight matrix, but it could also be handled analytically to save computational cost and gain accuracy.

- For the work in this thesis, we did not make use of rock-physics models or petro-physical relationships when creating layer-based prior model scenarios. Rock-physics models provide relationships between elastic parameter such as velocity, density and reservoir parameters such as porosity, saturation, permeability, net/gross, etc. which can be established from well-logs. We could bring in rock-physics models as an integral part of the prior model building process, to connect these layer-based scenarios directly to reservoir properties that can be

measured at well locations. This should be one of the important aspect of future research to be carried out regarding this topic.

7.2.2 Posterior distribution

We use Bayes' rule to integrate prior geological concepts as prior information, with the likelihood function provided by seismic inversion, to get a posterior distribution in the grid-based model space. The posterior distribution is multi-model and contains all information regarding the grid-based model, given the seismic data and the prior scenario. In the context of this thesis, we minimise the negative of the logarithm of the posterior distribution to search for the maximum a posteriori (MAP) estimate. As the posterior distribution, like the grid-based prior distributions, is multi-modal in nature, it contains a number of local maxima. To arrive at the global maximum we need to have a starting model close to the global maximum. We chose to use the maximum likelihood estimate (MLE) as a starting model in the search for the MAP estimate and look for the nearest maximum. This approach assures that seismic data is given more weight and that only a relatively small update is affected by the prior model. This process makes sense if one is interested in finding a deterministic solution to the problem, but Bayes' rule could provide more solutions, given the data, and a more thorough search of the model space could be carried out to find solutions further away from MLE. Some of the recommendation for future research in terms of optimising the posterior distribution are as follows:

- As we already have an analytical expression for the posterior distribution in the gridded model space, we should make use of sophisticated sampling methods such as Monte Carlo Markov Chain (MCMC) to provide the full posterior distribution for each and every grid point.
- Equally, we do not translate the posterior model vector in the gridded model space back to the layer-based model space, which is a very non-linear process. We can use inference algorithms such as expectation maximization or MCMC to get a posterior estimate in layer-based model space. The comparison of the prior estimate and the posterior estimate of layer-model space will provide us with more quantitative information regarding the presence and absence of some layers away from the well location.

7.2.3 Scenario Testing

In scenario testing we deal with the problem of quantification of the probabilities of different scenarios available as result of different interpretations provided by experts. We follow the Bayesian formulation, but we are interested in calculating the probability of a scenario, which is related to the denominator of equation 3.1. The denominator is only a number which normalises the posterior

distribution, but physically it provides an estimate of overlap between the likelihood function and the prior scenario distribution. We provided an innovative way of approximating the denominator or probability of the data given the scenario $P(\underline{d}\,|\,S)$ and with different scenarios available we calculate the $P(\underline{d}\,|\,S_i)$ individually for all the scenarios available and renormalize them so that they add up to 1 when summed over all scenarios. This method provides a quantitative way of comparing scenario probabilities but it has some limitations and further research related to issues mentioned below should be carried out.

- We propose a simple multivariate sampling method to create an ensemble of grid-based models drawn from the Gaussian likelihood function and calculate the respective grid-based prior density estimate for the whole ensemble and sum up the outcomes. This sum is an approximation of the denominator in equation 3.1 or the probability of data for a given scenario. We use a simple sampling method that creates an ensemble with a lot of repetitions of the model and thereby, overestimate the denominator. It is not stable in terms of a repetition of the experiments, meaning that it provides a different value with every experiment with the same scenario. This issue can be attributed to the naïve sampling method, which creates a different ensemble of models every time it is repeated, thus making it unstable.

- The Monte Carlo Markov Chains (MCMC) method has proved to provide a good estimate of the denominator in Bayes' rule, which then should become stable.

Appendix

A. Appendix.

The objective function is given by (equation 3.16):

$$F_{Post}\left(\mathbf{m}\right) = \tfrac{1}{2}\left(\mathbf{m}\text{-}\mathbf{m}_{mle}\right)^{T}\mathbf{V}^{-1}\left(\mathbf{m}\text{-}\mathbf{m}_{mle}\right) - \sum_{j=1}^{Nz}\ln P_{j}\left(\mathbf{m}_{j}\right), \tag{A.1}$$

where $\mathbf{m}_{j}$ is the model vector for a single grid point and is given by :

$$\mathbf{m}_{j} = \left(\kappa_{j}, M_{j}, \rho_{j}\right). \tag{A.2}$$

The gradient of the objective function with respect to the model parameters is given by :

$$\frac{\partial F_{post}\left(\mathbf{m}\right)}{\partial\mathbf{m}} = \mathbf{V}^{-1}\left(\mathbf{m} - \mathbf{m}_{mle}\right) - \sum_{j=1}^{Nz}\frac{\partial\ln P\left(\mathbf{m}_{j}\right)}{\partial\mathbf{m}_{k}}, \tag{A.3}$$

$$\frac{\partial\ln P_{j}(\mathbf{m}_{j})}{\partial\mathbf{m}_{j}} = \frac{1}{P_{j}(\mathbf{m}_{j})}\frac{\partial P_{j}(\mathbf{m}_{j})}{\partial\mathbf{m}_{j}}, \tag{A.3}$$

$$\frac{\partial P_{j}\left(\mathbf{m}_{j}\right)}{\partial\mathbf{m}_{j}} = \sum_{i=1}^{N}w_{ji}\frac{\partial N_{i}\left(\mathbf{m}_{j}, \mu_{i}, \sigma_{i}\right)}{\partial\mathbf{m}_{j}}, \tag{A.4}$$

$$\frac{\partial P_{j}\left(\mathbf{m}_{j}\right)}{\partial\mathbf{m}_{j}} = \sum_{i=1}^{N} -w_{ji}N_{i}\left(\mathbf{m}_{j}, \mu_{j}, \sigma_{i}\right)\frac{\left(\mathbf{m}_{j} - \mu_{i}\right)}{\sigma_{i}^{2}}, \tag{A.5}$$

$$\mu_{i} = \left(\mu_{\kappa_{i}}, \mu_{M_{i}}, \mu_{\rho_{i}}\right) \quad , \quad \sigma_{i} = \left(\sigma_{\kappa_{i}}, \sigma_{M_{i}}, \sigma_{\rho_{i}}\right).$$

$$\frac{\partial F_{post}\left(\mathbf{m}\right)}{\partial\mathbf{m}} = \mathbf{V}^{-1}\left(\mathbf{m} - \mathbf{m}_{mle}\right) + \sum_{j=1}^{Nz}\frac{1}{P_{j}(\mathbf{m}_{j})}\sum_{i=1}^{N}w_{ji}N_{i}\left(\mathbf{m}_{j}, \mu_{i}, \sigma_{i}\right)\frac{\left(\mathbf{m}_{j} - \mu_{i}\right)}{\sigma_{i}^{2}}. \tag{A.6}$$

The second derivative of equation (3.16) is given by:

$$\frac{\partial^{2}F_{post}\left(\mathbf{m}\right)}{\partial\mathbf{m}_{j}^{2}} = V_{j}^{-1} - \sum_{i=1}^{N_{L}}\frac{\partial^{2}\ln P\left(\mathbf{m}_{j}\right)}{\partial\mathbf{m}_{j}^{2}}, \tag{A.7}$$

As $\mathbf{V}_{j}^{-1}$ is diagonal, one can write $\Sigma_{\kappa_{j}}^{-1} = \left(\mathbf{V}_{\kappa}^{-1}\right)_{jj}$ for compressibility (κ) at a jth grid point. The equation A.7 is further simplified and shown for compressibility (κ),

Appendix

$$\frac{\partial^2 F_{post}(\mathbf{m})}{\partial \kappa_j^2} = \Sigma_{\kappa_j}^{-1} + \left[\frac{1}{\left(P_j(\mathbf{m}_j)\right)^2} \left(\frac{\partial P_j(\mathbf{m}_j)}{\partial \kappa_j}\right)^2 - \frac{1}{P_j(\mathbf{m}_j)}\frac{\partial^2 P_j(\mathbf{m}_j)}{\partial \kappa_j^2} \right], \quad (A.8)$$

The gradient in equation A.6 vanishes at extrema (MAP estimate) of equation A.1:

$$\Sigma_{\kappa_j}^{-1}\left(\kappa_{map} - \kappa_{mle}\right) = \frac{1}{P_j\left(\mathbf{m}_j^{map}\right)}\left(\frac{\partial P_j(\mathbf{m}_j)}{\partial \mathbf{m}_j}\right)_{\mathbf{m}=map}, \quad (A.9)$$

Using equation A.9 and A.8 and after rearranging, the local standard deviation $\left(\sigma_{\kappa_j}\right)_{\mathbf{m}=map}$ at the extrema is given by:

$$\left(\frac{1}{\sigma_{\kappa_j}^2}\right)_{\mathbf{m}=map} = \frac{1}{\Sigma_{\kappa_j}}\left(1 + \frac{\left(\kappa_{map}-\kappa_{mle}\right)^2}{\Sigma_{\kappa_j}}\right) - \frac{1}{P_j\left(\mathbf{m}_j^{map}\right)}\left(\frac{\partial^2 P_j(\mathbf{m}_j)}{\partial \kappa_j^2}\right)_{\mathbf{m}=map}, \quad (A.10)$$

Where:

$$\frac{\partial^2 \ln P(\mathbf{m}_j)}{\partial \kappa_j^2} = -\sum_{i=1}^{N_L}\frac{w_{ji}N_i\left(\mathbf{m}_j, \boldsymbol{\mu}_i, \boldsymbol{\sigma}_i\right)}{\sigma_{\kappa_i}^2}\left[1 - \left(\frac{\kappa_j - \mu_{\kappa_i}}{\sigma_{\kappa_i}}\right)^2\right]. \quad (A.11)$$

Bibliography

Abubakar, A., van den Berg, P.M., Habashy, T.M., and Braunisch, H., 2004, A multiplicative regularization approach for deblurring problems. *IEEE trans. Image processing*, **13**, 1524-1532

Agunwoke, G. O., Egbele, E., Onyekonwu, M., et al., 2004. A statistical approach to reservoir zonation. *In: Nigeria Annual International Conference and Exhibition, 2004*.

Al-Adani N., 2012. Data blocking or zoning: Well-log data application. *Journal of Canadian Petroleum Technology*, **51**(1), 66-73.

Aster, R. C., Borchers, B., Thurber, C. H., 2018. *Parameter estimation and inverse problems*. Elsevier.

Avseth, P., Mukerji, T., Mavko, G., 2005. *Quantitative seismic interpretation*. Cambridge University Press.

Azevedo, L., Nunes, R., Soares, A., Mundin, E. C., Neto, G. S., 2015. Integration of well data into geostatistical seismic amplitude variation with angle inversion for facies estimation. *Geophysics*, **80**(6), 113-128.

Bachrach, R., 2006. Joint estimation of porosity and saturation using stochastic rock physics modelling. *Geophysics*, **71**(5), 53-63.

Bayes, T., 1763. An essay towards solving a problem in the doctrine of chances. by the late rev. Mr. Bayes, communicated by Mr. Price, in a letter to john canton. *Philosophical Transactions of the Royal Society of London*, **53**, 370-418.

Bednar, J. B., 1999. A theoretical comparison of equivalent-offset migration and dip move-out pre-stack imaging. *Geophysics*, **64**(1), 191-196.

Berkhout, A.J., 1982. Seismic migration, imaging of acoustic energy by wavefield extrapolation, a: theoretical aspects: Elsevier.

Berkhout, A.J., 2014a. Review paper: An outlook on the future seismic imaging, Part I: forward and reverse modelling. Geophysical Prospecting, 62(5), 911–930.

Berkhout, A.J., 2014b. Review paper: An outlook on the future seismic imaging, Part III: Joint Migration Inversion. Geophysical Prospecting, 62(5), 950–971.

Berryhill, J. R., 1984, Wave-equation datuming before stack. *Geophysics*, 49, 2064-2066.

Bibliography

Bornard, R., Allo, F., Coléou, T., Freudenreich, Y., Caldwell, D., Hamman, J., 2005. Petrophysical seismic inversion to determine more accurate and precise reservoir properties. *In: 67th EAGE Conference & Exhibition 2005.*

Bosch, M., Mukerji, T., Gonzalez, E. F., 2010. Seismic inversion for reservoir properties combining statistical rock physics and geostatistics: A review. *Geophysics*, **75**(5), 165-176.

Bremmer, H., 1951. The WKB approximation as a first term of a geometric-optical series. *In: The Theory of Electromagnetic Waves: A symposium*, 169-179.

Brossier, R., Operto, S., Virieux, J., 2009. Seismic imaging of complex onshore structures by 2D elastic frequency-domain full-waveform inversion. *Geophysics*, **74**(6),105-118.

Buland, A., Kolbjørnsen, O., 2012. Bayesian inversion of CSEM and magneto-telluric data. *Geophysics*, **77**(1), 33-42.

Buland, A., Kolbjørnsen, O., Carter, A. J., 2011. Bayesian dix inversion. *Geophysics*, **76**(2), 15-22.

Buland, A., Omre, H., 2003. Bayesian linearized AVO inversion. *Geophysics*, **68**(1), 185-198.

Buland, A., Ouair, Y. E., 2006. Bayesian time-lapse inversion. *Geophysics*, **71**(3), 43-48.

Bunks, C., Saleck, F. M., Zaleski, S., Chavent, G., 1995. Multiscale seismic waveform inversion. *Geophysics*, **60**(5), 1457-1473.

Chopra, S., Marfurt, K. J., 2007. *Seismic Attributes for Prospect Identification and Reservoir Characterization*. SEG Books.

Chunduru, R. K., Sen, M. K., Stoffa, P. L., 1997. Hybrid optimization methods for geophysical inversion. *Geophysics*, **62**(4), 1196-1207.

Claerbout, J. F., 1971. Toward a unified theory of reflector mapping. *Geophysics*, **36**(3), 467-481.

Coléou, T., Allo, F., Bornard, R., Hamman, J., Caldwell, D., 2005. Petrophysical seismic inversion. *In: SEG Technical Program Expanded Abstracts 2005.*

Connolly P. A., Hughes, M. J., 2016. Stochastic inversion by matching to large numbers of pseudo-wells. *Geophysics*, **81**(2), 7-22.

Datta D., Sen, M. K., 2016. Estimating a starting model for full-waveform inversion using a global optimization method. *Geophysics*, **81**(2), 211-223.

Bibliography

Dessa, J.X., Pascal, G., 2003. Combined travel-time and frequency-domain seismic waveform inversion: a case study on multi-offset ultrasonic data. *Geophysical Journal International*, **154**(1), 117-133.

Douma, J., Naeini, E. Z., 2014. Application of image-guided interpolation to build low frequency background model prior to inversion. *In: 76th EAGE Conference and Exhibition 2014.*

Doyen, P., 2007. *Seismic Reservoir Characterization: An Earth Modelling Perspective.* EAGE Publications bv.

Duijndam, A. J. W., 1988. Bayesian estimation in seismic inversion. part I: Principles. *Geophysical Prospecting*, **36**(8), 878-898.

Duijndam, A. J. W., 1988. Bayesian estimation in seismic inversion. Part II: Uncertainty analysis. *Geophysical Prospecting*, **36**(8), 899-918.

Dvorkin, J., Gutierrez, M. A., Grana, D., 2014. *Seismic Reflections of Rock Properties.* Cambridge university Press.

Eidsvik, J., Mukerji, T., Switzer, P., 2004. Estimation of geological attributes from a well log: An application of hidden Markov chains. *Mathematical Geology*, **36**(3), 379-397.

Fanchi, J. R., 2002. *Shared Earth Modeling*, Elsevier, 170–181.

Feng, R., Luthi, S. M., Gisolf, A., Angerer, E., 2018. Reservoir lithology classification based on seismic inversion results by hidden Markov models: Applying prior geological information. *Marine and Petroleum Geology*, **93**, 218-229.

Feng, R., Luthi, S. M., Gisolf, A., 2018. Simulating reservoir lithologies by an actively conditioned Markov chain model. *Journal of Geophysics and Engineering*, **15**(3), 800-815.

Feng, R., Luthi, S. M., Gisolf, A., Sharma, S., 2017. Obtaining a high-resolution geological and petrophysical model from the results of reservoir-orientated elastic wave-equation based seismic inversion. *Petroleum Geoscience*, **23**(3), 376-385.

Fichtner, A., Kennett, B. L. N., Igel, H., and Bunge H.P., 2008. Theoretical background for continental and global-scale full-waveform inversion in the time-frequency domain. *Geophysical Journal International*, **175**(2), 665-685.

Fichtner, A., Trampert, J., Cupillard, P., Saygin, E., Taymaz, T., Capdeville, Y., Villaseñor, A., 2013. Multiscale full waveform inversion. *Geophysical Journal International*, **194**(1), 534-556.

Bibliography

Fjeldstad T., Grana, D., 2017. Joint probabilistic petrophysics-seismic inversion based on Gaussian mixture and Markov chain prior models. *Geophysics*, **83**(1), 31-42.

Garg, A. and Verschuur, D.J., 2016. Reservoir impulse response estimation using Joint Migration Inversion. EAGE, Eur. Ass. of Geosc. and Eng., Expanded abstracts, Vienna, 4pp.

Garg, A. and Verschuur, D.J., 2017. Elastic reflectivity preserving full waveform inversion. SEG, Soc. Expl. Geophys., Expanded abstracts, Houston, 5pp.

Gisolf, D., & Verschuur, E., 2010. *The principles of quantitative acoustical imaging*. EAGE publications bv.

Gisolf, A., Haffinger, P. R., Doulgeris, P., 2017. Reservoir-oriented wave-equation-based seismic amplitude variation with offset inversion. *Interpretation*, **5**(3), 43-56.

Gisolf, A., In't Veld, R. H., Haffinger, P., Hanitzsch, C., Doulgeris, P., Veeken, P., 2014. Non-linear full wavefield inversion applied to carboniferous reservoirs in the Wingate gas field (SNS, offshore UK). *In: 76th EAGE Conference and Exhibition 2014*.

Gisolf, A., van den Berg, P.M., 2010a. Target oriented non-linear inversion of seismic data. *In 72nd EAGE Conference and Exhibition incorporating SPE EUROPEC 2010*.

Gisolf, A., van den Berg, P.M., 2010b. Target-oriented non-linear inversion of time-lapse seismic data. *In: SEG Technical program Expanded Abstracts, 2010*.

González, E. F., Mukerji, T., Mavko, G., 2008. Seismic inversion combining rock physics and multiple-point geostatistics. *Geophysics*, **73**(1), 11-21.

Grana, D., Rossa, E. D., 2010. Probabilistic petrophysical properties estimation integrating statistical rock physics with seismic inversion. *Geophysics*, **75**(3), 21-37.

Gunning, J., Glinsky, M. E., 2007. Detection of reservoir quality using Bayesian seismic inversion. *Geophysics*, **72**(3), 37-49.

Haffinger, P.R., 2013. Seismic broadband full waveform inversion by shot/receiver refocusing.

Haffinger, P., Von Wussow, P., Doulgeris, P., Henke, C., Gisolf, A., 2015. Reservoir delineation by applying a nonlinear AVO technique - a case study in the Nile delta. *In: 77th EAGE Conference and Exhibition 2015*.

Hampson, D. P., Schuelke, J. S., Quirein, J. A., 2001. Use of multi-attribute transforms to predict log properties from seismic data. *Geophysics*, **66**(1), 220-236.

Bibliography

Hansen, T. M., Journel, A. G., Tarantola, A., Mosegaard, K., 2006. Linear inverse Gaussian theory and geostatistics. *Geophysics*, **71**(6), 101-111.

Hansen, T. M., Mosegaard, K., Pedersen-Tatalovic, R., Uldall, A., Jacobsen, N. L., 2008. Attribute-guided well-log interpolation applied to low-frequency impedance estimation. *Geophysics*, **73**(6), 83-95.

Jeffreys, H., 1939, *Theory of probability*, Clarendon Press, (3rd edition 1983).

Kennett, B., 2009. *Seismic wave propagation in stratified media*. ANU Press.

Klienman, R. E., and van den Berg, P. M., 1991. Iterative methods for solving integral equations. *Radio Science*, **26**(1), 175-181.

Kim, Y., Shin, C., Calandra, H., Min, D.J., 2013. An algorithm for 3D acoustic time laplace- fourier-domain hybrid full waveform inversion. *Geophysics*, **78**(4), 151-166.

Kukreja, N. , Louboutin, M. , Lange, M. , Luporini, F., Gorman, G., 2017. Rapid development of seismic imaging applications using symbolic math. *In: Third EAGE Workshop on High Performance Computing for Upstream 2017*.

Larsen, A. L., Ulvmoen, M., Omre, H., Buland, A., 2006. Bayesian lithology/fluid prediction and simulation on the basis of a Markov chain prior model. *Geophysics*, **71(5)**, 69-78.

Malinverno, A., 2000. A Bayesian criterion for simplicity in inverse problem parametrization. *Geophysical Journal International*, 140, 267–285.

Malinverno, A., 2002. Parsimonious Bayesian Markov chain Monte Carlo inversion in a nonlinear geophysical problem. *Geophysical Journal International*, 151, 675–688.

Mavko, G., Mukerji, T., Dvorkin, J., 2009. *The Rock Physics Handbook*. Cambridge University Press.

Mazzotti A., Zamboni, E., 2003. Petrophysical inversion of AVA data. *Geophysical Prospecting* **51**(6), 517-530.

Mora, P., 1987. Nonlinear two-dimensional elastic inversion of multi-offset seismic data, *Geophysics*, **52**(9), 1211-1228.

Mosegaard, K. and Tarantola, A. (1995). Monte Carlo sampling of solutions to inverse problems. *Journal of Geophysical Research: Solid Earth*, 100, 12431–12447

Bibliography

Mukerji, T., Avseth, P., Mavko, G., Takahashi, I., González, E. F., 2001. Statistical rock physics: Combining rock physics, information theory, and geostatistics to reduce uncertainty in seismic reservoir characterization. *The Leading Edge*, **20**(3), 313-319.

Mukerji, T., Jørstad, A., Avseth, P., Mavko, G., Granli, J. R., 2001. Mapping lithofacies and pore-fluid probabilities in a North sea reservoir: Seismic inversions and statistical rock physics. *Geophysics*, **66**(4), 988-1001.

Nivlet, P., 2004. Low-frequency constrain in a priori model building for stratigraphic inversion. *In: SEG Technical Program Expanded Abstracts 2004*.

Plessix, R. E., 2006. A review of the adjoint-state method for computing the gradient of a functional with geophysical applications. *Geophysical Journal International*, **167**(2), 495-503.

Plessix, R.E., Perkins, C., 2010. Thematic set: Full waveform inversion of a deep water ocean bottom seismometer dataset. *First Break*, **28**(4), 71-78.

Pratt, G., Shin, C., Hicks, 1998. Gauss-newton and full newton methods in frequency-space seismic waveform inversion. *Geophysical Journal International* **133**(2), 341-362.

Pratt, R. G., 1990. Inverse theory applied to multi-source crosshole tomography. Part 2 : Elastic wave equation method. *Geophysical Prospecting*, **38**(3), 311-329.

Pratt, R. G., 1999. Seismic waveform inversion in the frequency domain, part 1: Theory and verification in a physical scale model. *Geophysics*, **64**(3), 888-901.

Prieux, V., Operto, S., Brossier, R., Virieux, J., 2009. Application of acoustic full waveform inversion to the synthetic Valhall velocity model. *In: SEG Technical Program Expanded Abstracts 2009*.

Rimstad, K., Avseth, P., Omre, H., 2012. Hierarchical Bayesian lithology/fluid prediction: A North sea case study. *Geophysics* **77**(2), 69-85.

Robinson, E., 1982. Migration of seismic data as W.K.B. approximation, *Geoexploration* **20**(1-2), 7-30.

Rosenbaum, M. S., Culshaw, M. G., 2003. Communicating the risks arising from geohazards. *Journal of the Royal Statistical Society. Series A (Statistics in Society)*, **166**(2), 261-270.

Sams, M., Carter, D., 2017. Stuck between a rock and a reflection: A tutorial on low frequency models for seismic inversion. *Interpretation*, **5**(2), 17-27.

Schneider, W.A., 1978. Integral formulation for migration in two and three dimensions. *Geophysics*, **43**(1), 49-76.

Bibliography

Schön, J. H., 2015. *Physical properties of rocks: Fundamentals and principles of petrophysics*. Elsevier.

Schuster, G. T., Yu, J., Sheng, J., Rickett, J., 2004. Interferometric/daylight seismic imaging. *Geophysical Journal International*, **157**(2), 838-852.

Sen, M. K., Stoffa, P. L., 1995. *Global Optimization Methods in Geophysical Inversion*. Cambridge University Press.

Sharma, S., Gisolf, D., Luthi, S., 2018. Bayesian update of wave equation based seismic inversion using geological prior information and scenario testing. *In: 80th EAGE Conference and Exhibition 2018*.

Shen P., Symes, W. W., 2008. Automatic velocity analysis via shot profile migration. *Geophysics*, **73**(5), 49-59.

Shewchuk, J. R., 1994. An Introduction to the Conjugate Gradient Method without the agonizing pain. *Tech. Rep. Carnegie Melon University, Pittsburgh, PA, USA.*

Shin C., Min, D.J., 2006. Waveform inversion using a logarithmic wave-field. *Geophysics*, **71**(3), 31-42.

Sirgue L., Pratt, R. G., 2004. Efficient waveform inversion and imaging: A strategy for selecting temporal frequencies. *Geophysics*, **69**(1), 231-248.

Staal, X.R. [2015] Combined imaging and velocity estimation by Joint Migration Inversion. Ph.D. thesis, Delft University of Technology.

Stolt, R. H., 1978. Migration by Fourier transform. *Geophysics*, **43**(1), 23-48.

Symes, W. W., Carazzone, J. J., 1991. Velocity inversion by differential semblance optimisation. *Geophysics*, **56**(5), 654-663.

Tarantola, A., 2005. *Inverse Problem Theory and Methods for Model Parameter Estimation*. Society for Industrial and Applied Mathematics.

Tetyukhina, D., Luthi, S. M., Gisolf, A., 2014. Acoustic nonlinear full-waveform inversion on an outcrop-based detailed geological and petrophysical model (Book Cliffs, Utah). *AAPG Bulletin*, **98**(1), 119-134.

Van den Berg, P.M., Abubakar, A., Fokkema, J.T., 2003. Multiplicative regularization for contrast profile inversion. *Radio Sci.*, **38**(2), 23-1-23-10.

Bibliography

Varela, C. L., Stoffa, P. L., Sen, M. K., 1998. Background velocity estimation using non-linear optimisation for reflection tomography and migration misfit. *Geophysical Prospecting*, **46**(1), 51-78.

Virieux J., Operto, S., 2009. An overview of full-waveform inversion in exploration geophysics. *Geophysics*, **74**(6), 1-26.

Wagoner, J. C. V., 1995. "Sequence Stratigraphy and Marine to Non-marine Facies Architecture of Foreland Basin Strata, Book Cliffs, Utah, U.S.A." *In Sequence Stratigraphy of Foreland Basin Deposits: Outcrop and Subsurface Examples from the Cretaceous of North America. American Association of Petroleum Geologists.*

Widess, M. B., 1973. How thin is a thin bed? *Geophysics*, **38**(6), 1176-1180.

Wood, R., Curtis, A., 2004. Geological prior information and its applications to geoscientific problems. *Geological Society, London, Special Publications*, **239**(1), 12-14 (2004).

Xia, G., Sen, M. K., Stoffa, P. L., 1998. 1D elastic waveform inversion: A divide-and conquer approach. *Geophysics*, **63**(5), 1670-1684.

Acknowledgements

During the course of my PhD journey, I met some of the best minds in the world directly or indirectly related to my work or people from other departments with whom I had hour-long discussions about work, life, and many abstract topics. As I am in the last phase of my PhD, it gives me a great pleasure to reminiscence all those who contributed not only to my scientific work but also to my personal development.

Foremost, I would like to express my sincere gratitude to my promoter Prof. Stefan M. Luthi and my daily supervisor Prof. Dries A. Gisolf. It was a pleasure to work with you and I highly appreciate all those meeting we had on Fridays mornings. Prof. Luthi has always shown a keen interest in my work and kept encouraging me. I highly appreciate your patience that you have shown towards me all these years. I appreciate your efforts for managing my project so well.

I am indebted to my daily supervisor Prof. Dries A. Gisolf for giving overall guidance throughout my PhD, whether it was work-related or personal life, you have always listened to me and helped me. Especially, I can never forget all those hour-long brainstorming sessions I had with you on Friday mornings about non-linearity of the problems, Gaussian distributions and Bayes' theorem. I shall cherish those times all my life and I hope your guidance keeps motivating me after my PhD is completed.

I would like to express my sincere gratitude to Dr Eric Verschuur for being a great motivator during my PhD and also presenting on my behalf on some occasions in Delphi meetings. Being a part of the Delphi consortium has its perks and I fully enjoyed all the Delphi meetings in the Houston as well in Den Haag with friends: Mikhail, Apostolos, Abdulrahman, Bouchaib, Hussain, Aparajita, Shogo, Jan-Willem, Özkan, Shan, Aayush, Prabu, Ewoud, Sixue, Matteo, Nick, Alok, Tomohide, Gabriel. I enjoyed my time with you all and I wish you very good luck in your future endeavours.

I thank people of Delft Inversion: Panos, Peter, Stefan, Gabrio for your expert comments during dry runs for Delphi meetings.

I would like to thank my fellow colleagues from The Applied Geology and Geophysics sections Remi, Max, Koen, Kevin, Helena, Cees, Andrea, Niels, Asiya, Pawan, Ayush, Santosh, Youwei, Rahul, Navid, Quinten, Gil, Boris, Joeri, Lissane, Iris, Ranjaini, Myrna, Lele, Rueben, Carlos, for all the good times we had together in the last five years. I worked with Runhai Feng and always got amazed by his dedication towards his work. We have shared rooms during conferences and Delphi meetings and you have introduced me to one of the best food places all around the world while we were travelling.

Acknowledgement

I would like to thank support staff Ralf, Lydia, Marlijn, Margaret, Marijke for providing me with your assistance all this time.

Special thanks to my housemate and a very good friend Prashant Srinivasan (PP). First thing you told me was 'Patience is a virtue ' and I hope in the future I might be able to apply this in my life.

My journey in the Netherlands started with Sudhanshu Pandey, a former friend from India. We enjoyed the Netherlands so much together and I hope we keep doing this for the rest of our life.

A very heartfelt thanks to one of my closest friends in the Netherlands, Wilco Zuidema and Danillo de Koning for introducing me to the Dutch lifestyle. I hope we stay in touch all our life.

I would like to mention Locus Publicus, where I had some of the best times with friends outside the office. Special thanks to Vikram, Ashwath, Walter, Bert, Aditi, Paulina, Robert, Jimmy, Nico, Peter, Martin, Adarsha, Rishab, Peter, Nicole, Luc for being a great company all these years. I think without you people it would have been really boring in Delft.

Last but not the least, I would like show my gratefulness to Jinyu Tang, for being with me in last six months of my PhD while I was writing my thesis.

Siddharth Sharma

Curriculum Vitae

Siddharth Sharma

28-11-1989   Born in Shahajahanpur, Uttar Pradesh, India

Education

2004 - 2006   High School, New Delhi, India

2007 - 2012   Integrated BS-MS, Geosciences,

                     Indian Institute of Science Education and Research, Kolkata,(IISER-K), India

2012 - 2013   Master of Research, Exploration Geophysics

                     Institute de Physique du Globe De Paris, (IPGP),Paris, France

2013 - 2019   PhD Applied Geology, Delphi Consortium,

                     Technical University of Delft, Delft, The Netherlands.